

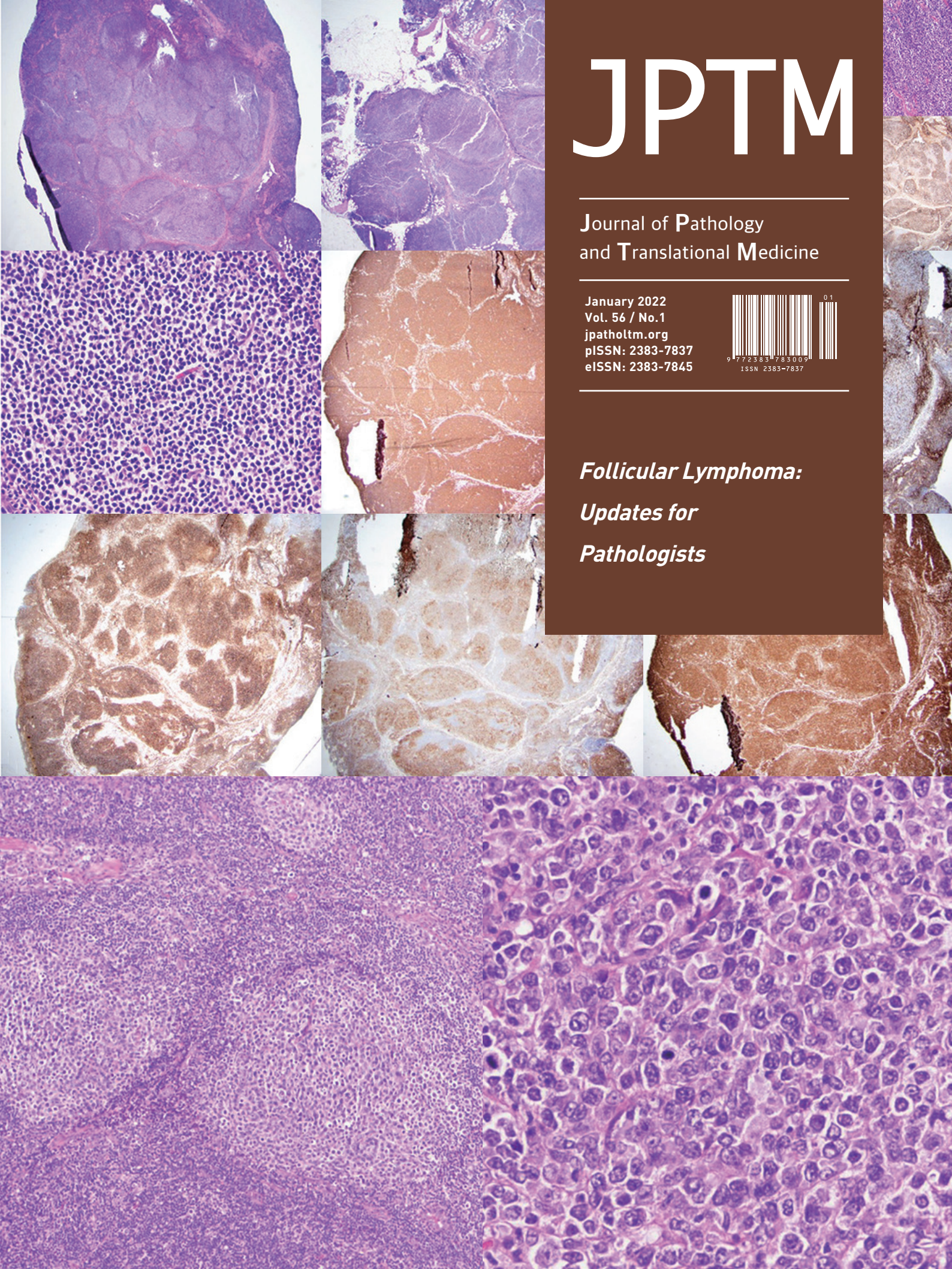
JPTM

Journal of Pathology
and Translational Medicine

January 2022
Vol. 56 / No.1
jpatholm.org
pISSN: 2383-7837
eISSN: 2383-7845



*Follicular Lymphoma:
Updates for
Pathologists*



Aims & Scope

The *Journal of Pathology and Translational Medicine* is an open venue for the rapid publication of major achievements in various fields of pathology, cytopathology, and biomedical and translational research. The Journal aims to share new insights into the molecular and cellular mechanisms of human diseases and to report major advances in both experimental and clinical medicine, with a particular emphasis on translational research. The investigations of human cells and tissues using high-dimensional biology techniques such as genomics and proteomics will be given a high priority. Articles on stem cell biology are also welcome. The categories of manuscript include original articles, review and perspective articles, case studies, brief case reports, and letters to the editor.

Subscription Information

To subscribe to this journal, please contact the Korean Society of Pathologists/the Korean Society for Cytopathology. Full text PDF files are also available at the official website (<https://jpathol.tnm.org>). *Journal of Pathology and Translational Medicine* is indexed by Emerging Sources Citation Index (ESCI), PubMed, PubMed Central, Scopus, KoreaMed, KoMCI, WPRIM, Directory of Open Access Journals (DOAJ), and CrossRef. Circulation number per issue is 50.

Editors-in-Chief

Jung, Chan Kwon, MD (*The Catholic University of Korea, Korea*) <https://orcid.org/0000-0001-6843-3708>

Park, So Yeon, MD (*Seoul National University, Korea*) <https://orcid.org/0000-0002-0299-7268>

Associate Editors

Shin, Eunah, MD (*Yongin Severance Hospital, Yonsei University, Korea*) <https://orcid.org/0000-0001-5961-3563>

Kim, Haeryoung, MD (*Seoul National University, Korea*) <https://orcid.org/0000-0002-4205-9081>

Bychkov, Andrey, MD (*Kameda Medical Center, Japan; Nagasaki University Hospital, Japan*) <https://orcid.org/0000-0002-4203-5696>

Editorial Board

Avila-Casado, Maria del Carmen, MD (*University of Toronto, Toronto General Hospital UHN, Canada*)

Bae, Young Kyung, MD (*Yeungnam University, Korea*)

Bongiovanni, Massimo, MD (*Lausanne University Hospital, Switzerland*)

Bova, G. Steven, MD (*University of Tampere, Finland*)

Choi, Joon Hyuk, MD (*Yeungnam University, Korea*)

Chong, Yo Sep, MD (*The Catholic University of Korea, Korea*)

Chung, Jin-Haeng, MD (*Seoul National University, Korea*)

Fadda, Guido, MD (*Catholic University of Rome-Foundation Agostino Gemelli University Hospital, Italy*)

Fukushima, Noriyoshi, MD (*Jichi Medical University, Japan*)

Go, Heounjeong, MD (*University of Ulsan, Korea*)

Hong, Soon Won, MD (*Yonsei University, Korea*)

Jain, Deepali, MD (*All India Institute of Medical Sciences, India*)

Kakudo, Kennichi, MD (*Izumi City General Hospital, Japan*)

Kim, Jang-Hee, MD (*Ajou University, Korea*)

Kim, Jung Ho, MD (*Seoul National University, Korea*)

Kim, Se Hoon, MD (*Yonsei University, Korea*)

Komuta, Mina, MD (*Keio University, Tokyo, Japan*)

Kwon, Ji Eun, MD (*Ajou University, Korea*)

Lai, Chiung-Ru, MD (*Taipei Veterans General Hospital, Taiwan*)

Lee, C. Soon, MD (*University of Western Sydney, Australia*)

Lee, Hye Seung, MD (*Seoul National University, Korea*)

Lee, Sung Hak, MD (*The Catholic University, Korea*)

Liu, Zhiyan, MD (*Shanghai Jiao Tong University, China*)

Lkhagvadorj, Sayamaa, MD (*Mongolian National University of Medical Sciences, Mongolia*)

Moran, Cesar, MD (*MD Anderson Cancer Center, U.S.A.*)

Paik, Jin Ho, MD (*Seoul National University, Korea*)

Park, Jeong Hwan, MD (*Seoul National University, Korea*)

Ro, Jae Y., MD (*Cornell University, The Methodist Hospital, U.S.A.*)

Sakhuja, Puja, MD (*Govind Ballabh Pant Hospital, India*)

Shahid, Pervez, MD (*Aga Khan University, Pakistan*)

Song, Joon Seon, MD (*University of Ulsan, Korea*)

Tan, Puay Hoon, MD (*National University of Singapore, Singapore*)

Than, Nandor Gabor, MD (*Semmelweis University, Hungary*)

Tse, Gary M., MD (*The Chinese University of Hong Kong, Hong Kong*)

Yatabe, Yasushi, MD (*Aichi Cancer Center, Japan*)

Zhu, Yun, MD (*Jiangsu Institution of Nuclear Medicine, China*)

Ethic Editor

Choi, In-Hong, MD (*Yonsei University, Korea*)

Huh, Sun, MD (*Hallym University, Korea*)

Statistics Editors

Kim, Dong Wook, MD (*National Health Insurance Service Ilsan Hospital, Korea*)

Lee, Hye Sun, MD (*Yonsei University, Korea*)

Manuscript Editor

Chang, Soo-Hee, MD (*InfoLumi Co., Korea*)

Layout Editor

Kim, Haeja, MD (*iMiS Company Co., Ltd., Korea*)

Website and JATS XML File Producers

Cho, Yoonsang, MD (*M2Community Co., Korea*)

Im, Jeonghee, MD (*M2Community Co., Korea*)

Administrative Assistants

Kim, Da Jeong, MD (*The Korean Society of Pathologists*)

Jeon, Anmi, MD (*The Korean Society for Cytopathology*)

Contact the Korean Society of Pathologists/the Korean Society for Cytopathology

Publishers: Nam, Jong Hee, MD, Gong, Gyungyub, MD

Editors-in-Chief: Jung, Chan Kwon, MD, Park, So Yeon, MD

Published by the Korean Society of Pathologists/the Korean Society for Cytopathology

Editorial Office

Room 1209 Gwanghwamun Officia, 92 Saemunan-ro, Jongno-gu, Seoul 03186, Korea

Tel: +82-2-795-3094 Fax: +82-2-790-6635 E-mail: office@jpathol.tnm.org

#1508 Renaissancetower, 14 Mallijae-ro, Mapo-gu, Seoul 04195, Korea

Tel: +82-2-593-6943 Fax: +82-2-593-6944 E-mail: office@jpathol.tnm.org

Printed by iMiS Company Co., Ltd. (JMC)

Jungang Bldg. 18-8 Wonhyo-ro 89-gil, Yongsan-gu, Seoul 04314, Korea

Tel: +82-2-717-5511 Fax: +82-2-717-5515 E-mail: ml@smileml.com

Manuscript Editing by InfoLumi Co.

210-202, 421 Pangyo-ro, Bundang-gu, Seongnam 13522, Korea

Tel: +82-70-8839-8800 E-mail: infolumi.chang@gmail.com

Front cover image: Representative histologic and immunohistochemical features of follicular lymphoma (p3, 4).

© Copyright 2022 by the Korean Society of Pathologists/the Korean Society for Cytopathology

© Journal of Pathology and Translational Medicine is an Open Access journal under the terms of the Creative Commons Attribution Non-Commercial License (<https://creativecommons.org/licenses/by-nc/4.0>).

© This paper meets the requirements of KS X ISO 9706, ISO 9706-1994 and ANSI/NISO Z.39.48-1992 (Permanence of Paper).

CONTENTS

REVIEW

- 1 Follicular lymphoma: updates for pathologists

Mahsa Khanlari, Jennifer R. Chapman

ORIGINAL ARTICLES

- 16 Clinicopathological differences in radiation-induced organizing hematomas of the brain based on type of radiation treatment and primary lesions

Myung Sun Kim, Se Hoon Kim, Jong-Hee Chang, Mina Park, Yoon Jin Cha

- 22 Association of PTTG1 expression with invasiveness of non-functioning pituitary adenomas

Su Jung Kum, Hye Won Lee, Soon Gu Kim, Hyungsik Park, Ilseon Hwang, Sang Pyo Kim

- 32 Clinicopathologic implication of PD-L1 gene alteration in primary adrenal diffuse large B cell lymphoma

Ki Rim Lee, Jiwon Koh, Yoon Kyung Jeon, Hyun Jung Kwon, Jeong-Ok Lee, Jin Ho Paik

- 40 Polo-like kinase 4 as a potential predictive biomarker of chemoradioresistance in locally advanced rectal cancer

Hyunseung Oh, Soon Gu Kim, Sung Uk Bae, Sang Jun Byun, Shin Kim, Jae-Ho Lee, Ilseon Hwang, Sun Young Kwon, Hye Won Lee

CASE REPORTS

- 48 Chronic lymphocytic leukemia and concurrent seminoma in the same testis

Kosuke Miyai, Fumihisa Kumazawa, Kimiya Sato, Hitoshi Tsuda

- 53 TTF1-positive SMARCA4/BRG1 deficient lung adenocarcinoma

Anurag Mehta, Himanshi Diwan, Divya Bansal, Manoj Gupta

- 57 Composite follicular lymphoma and classic Hodgkin lymphoma

Han-Na Kim, Min Ji Jeon, Eun Sang Yu, Dae Sik Kim, Chul-Won Choi, Young Hyeoh Ko

Follicular lymphoma: updates for pathologists

Mahsa Khanlari¹, Jennifer R. Chapman²

¹Department of Pathology and Hematopathology, St. Jude Children's Research Hospital, Memphis, TN;

²Department of Pathology, Division of Hematopathology, University of Miami, Sylvester Comprehensive Cancer Center, and Jackson Memorial Hospitals, Miami, FL, USA

Follicular lymphoma (FL) is the most common indolent B-cell lymphoma and originates from germinal center B-cells (centrocytes and centroblasts) of the lymphoid follicle. Tumorigenesis is believed to initiate early in precursor B-cells in the bone marrow (BM) that acquire the t(14;18)(q32;q21). These cells later migrate to lymph nodes to continue their maturation through the germinal center reaction, at which time they acquire additional genetic and epigenetic abnormalities that promote lymphomagenesis. FLs are heterogeneous in terms of their clinicopathologic features. Most FLs are indolent and clinically characterized by peripheral lymphadenopathy with involvement of the spleen, BM, and peripheral blood in a substantial subset of patients, sometimes accompanied by constitutional symptoms and laboratory abnormalities. Diagnosis is established by the histopathologic identification of a B-cell proliferation usually distributed in an at least partially follicular pattern, typically, but not always, in a lymph node biopsy. The B-cell proliferation is biologically of germinal center cell origin, thus shows an expression of germinal center-associated antigens as detected by immunophenotyping. Although many cases of FLs are typical and histopathologic features are straightforward, the biologic and histopathologic variability of FL is wide, and an accurate diagnosis of FL over this disease spectrum requires knowledge of morphologic variants that can mimic other lymphomas, and rarely non-hematologic malignancies, clinically unique variants, and pitfalls in the interpretation of ancillary studies. The overall survival for most patients is prolonged, but relapses are frequent. The treatment landscape in FL now includes the application of immunotherapy and targeted therapy in addition to chemotherapy.

Key Words: Follicular lymphoma; Immunohistochemistry; Molecular; Cytogenetics; Prognosis; Treatment

Received: September 6, 2021 **Revised:** September 27, 2021 **Accepted:** September 29, 2021

Corresponding Author: Mahsa Khanlari, MD, Department of Pathology and Hematopathology, St. Jude Children's Research Hospital, 262 Danny Thomas Place, Memphis, TN 38105, USA

Tel: +1-901-595-0394, Fax: +1-901-595-3100, E-mail: Mahsa.Khanlari@stjude.org

Corresponding Author: Jennifer R. Chapman, MD, Department of Pathology, University of Miami Hospital, 4th floor, room 4076, 1400 NW 12th Ave., Miami, FL 33138, USA
 Tel: +1-305-689-1332, E-mail: JChapman@med.miami.edu

This article has been published jointly, with consent, in both *Journal of Pathology and Translational Medicine* and *PathologyOutlines.com*.

Follicular lymphoma (FL) is an indolent B-cell malignancy usually involving a lymph node with a morphologic appearance resembling follicular lymphoid structures. FL cells arise from germinal center B-cells of the lymphoid follicle (centrocytes and centroblasts) [1]. The biologic and histopathologic spectrum of FL is broad. In most cases, at least partial follicular (nodular) distribution is identified with varying degrees of diffuse neoplastic growth [2].

In 2017 World Health Organization (WHO) classification, grading of FL is based on the cytologic composition of neoplastic follicles and the number of centroblasts identified, on average, in at least 10 high power fields. FLs express germinal center B-cell markers by immunohistochemistry (IHC) [1].

Obsolete names for FL are Brill-Symmers disease, nodular lymphoma (in Rappaport classification), centroblastic/centrocytic lymphoma (Kiel classification), and follicular center lymphoma (in REAL classification) [2-5].

FL is the second most common non-Hodgkin lymphoma, comprising about 20%–25% of all new non-Hodgkin lymphoma diagnoses in Western countries, and about 5% of all hematologic neoplasms. The incidence of FL differs among geographic regions and ethnic groups. Age-standardized incidence is about 2–4 per 100,000 person-years, and male to female ratio is variable (1:1.7 in most series). The median age ranges 60–65 years [6].

About 80% of all FLs are systemic nodal tumors. Peripheral cervical and inguinal lymph nodes are the more frequently affected

sites, although central lymph nodes, including abdominal and thoracic, can also be involved. Extranodal sites that are commonly involved include bone marrow (BM), spleen, liver, and peripheral blood [7].

ETIOPATHOGENESIS

Biologic abnormalities that promote the development of FL can be broadly summarized as occurring in three stages of B-cell development: (1) BM events, (2) germinal center events, and (3) post-germinal center events.

BM events

BM precursor B-cells, usually in the pre- or pro-B-cell stage, acquire t(14;18)(q32;q21) *IGH/BCL2* because of repair failure during V(D)J recombination. The resulting overexpression of *BCL2*, an anti-apoptotic protein, promotes survival and discourages apoptosis of B-cells as they later mature during the germinal center reaction [8].

Germinal center events

B-cells harboring the t(14;18)(q32;q21) translocation retain germinal center functionality (e.g., *BCL6*-mediated pathways), and undergo somatic hypermutation and class switch recombination of immunoglobulin genes initiated by activation-induced cytidine deaminase with retention of IgM/IgD surface expression. This last phenomenon is known as the allelic paradox and promotes proliferation and survival pathways in malignant B-cells [9].

Post-germinal center events

Additional chromosomal alterations and mutational abnormalities occur, promoting the pre-lymphomatous t(14;18)+ cell into bonafide lymphoma cells. Reentry of a subset of *BCL2*+ memory B-cells to the germinal center also occurs [10].

In addition to the t(14;18)(q32;q21) translocation and *BCL2* mutation, FL is characterized by additional mutational abnormalities most commonly in chromatin modifiers, B-cell receptor signaling pathways, cell cycle regulation, transcription factors, and immune evasion genes [10-13]:

- Chromatin modification (*KMT2D*, *EZH2*, *CREBBP*, *ARID1A*, *MEF2B*, *EP300*): inactivating mutations of *KMT2D*, *CREBBP*, *ARID1A*, *MEF2B*, and *EP300* and gains of the function of *EZH2*.

- B-cell receptor signaling (*CARD11*, *IgHV*, *IgLV*, *TNFRSF14*): inactivating mutation of *TNFRSF14* and gain of function mu-

tation in *CARD11*, *IgHV*, *IgLV*.

- Cell cycle regulation (*RB1*, *CDK4*): deletion of *RB1* and gain of function mutation in *CDK4*.

- Transcription factors (*FOXO1*, *MEF2B*, *BCL6*): inactivating mutation of *MEF2B* and gain of function mutation of *FOXO1* and *BCL6*.

- Tumor suppressor and immune evasion (*EPHA7*, *TNRSF14*, *CREBBP*): deletion/inactivating mutation of *EPHA7*, *TNRSF14*, and *CREBBP*.

- Activation of *JAK-STAT* signaling (*STAT6*): gain of function mutation in *STAT6*.

The etiology of FL is mainly unknown. t(14;18)(q32;q21) *IGH/BCL2* alone is not sufficient to cause lymphoma [14]. Some essential factors which seem to play a contributing role are family history and inherited/genetic susceptibility (especially first-degree relatives) and environmental factors (such as exposure to pesticides and herbicides) [15,16].

Clinical features

The median age of patients with FL is the sixth decade [1]. Clinical presentation of FL is most commonly that of enlarged lymph nodes, frequently in the neck or abdomen. FL is a localized disease in about 10% to 20% of cases. The vast majority of FLs present with widespread nodal involvement (~80%) and advanced-stage disease (stages III–IV) at the time of diagnosis [7]. Some cases follow a chronic relapsing course. A subset progresses rapidly and transforms to aggressive lymphomas such as diffuse large B-cell lymphomas, double-hit large B-cell lymphomas, and lymphoblastic leukemia/lymphoma [17].

FL can also relapse as classic Hodgkin lymphoma, which is clonally related to the antecedent FL and with Hodgkin lymphoma cells also harboring the t(14;18) (q32;q21) translocation [18].

Most patients with FL are mainly asymptomatic. Symptomatic presentations may include fatigue, fever or night sweats, weight loss, or recurrent infections. Tissue biopsy (lymph node/extranodal sites), most frequently in the form of needle biopsy (both core needle biopsy and fine-needle aspiration biopsy), and occasionally as excisional biopsies, are the most frequent diagnostic materials. Peripheral blood and BM biopsy are usually performed for staging purposes [10].

Abnormal laboratory findings are uncommon. Leukemic phase FL is identified in < 5% of patients [19]. An increase in lactate dehydrogenase (LDH) and β 2-microglobulins are present in about 15% of patients [20].

Rarely, FL is found outside lymph nodes. Extranodal FL can cause a variety of symptoms depending on its location. For exam-

ple, in case of BM involvement, anemia is present (about 10% of patients with FL), while leukopenia/thrombocytopenia is rarely seen [19,21]. Involvement of mucosa-associated sites may be asymptomatic or present with symptomatology related to the involved disease site.

HISTOLOGIC FINDINGS

The diagnosis of FL is made histologically in tissue sections obtained from surgically excised lymph nodes or, more frequently, a needle biopsy (both core needle biopsy and fine-needle aspiration biopsy).

Gross examination of involved lymph nodes shows a vaguely nodular pattern in the cut section with bulging.

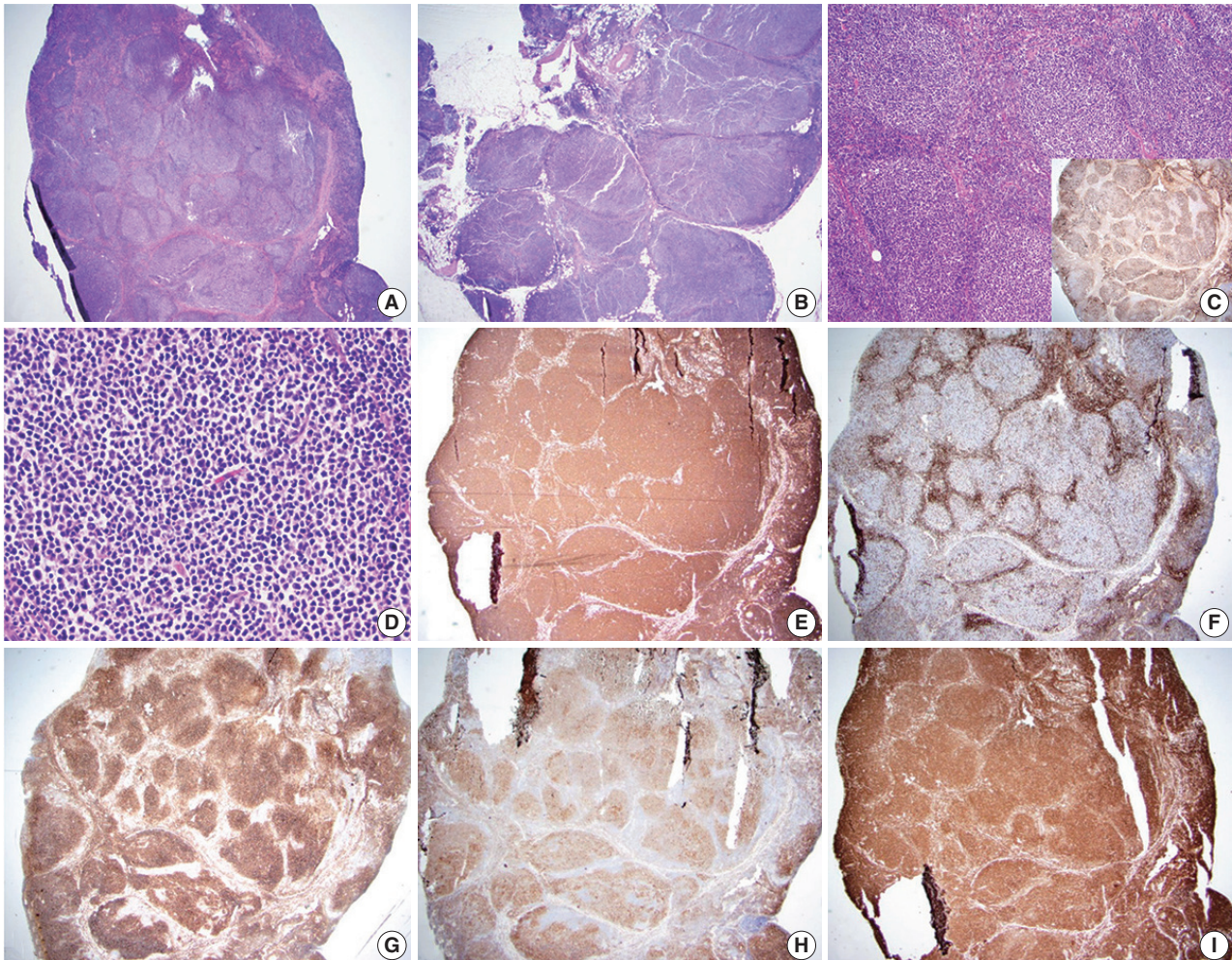


Fig. 1. Follicular lymphoma, low-grade. A representative case of follicular lymphoma, low-grade. H&E-stained excisional biopsy (A–D) and immunohistochemical stains (C inset, E–I) show classic morphology of follicular lymphoma cells, with increased, monotonous appearing neoplastic follicles in an excisional biopsy of the lymph node. The borders of the follicles are ill-defined and lack well-preserved mantle zones. Foci of sclerosis are identified (A). The neoplastic follicles are expansile and arranged in a back-to-back fashion. The neoplasm extends into perinodal fat (B) and has attenuated to absent mantle zones (C). Immunostain for CD21 highlights follicular dendritic cell meshworks within neoplastic follicles, which is useful in establishing the presence of lymphoid follicles (C, inset). The neoplastic follicle comprises numerous centrocytes and fewer centroblasts, compatible with grade 1–2 of 3 (D). Immunostain for CD20 highlights B lymphocytes in neoplastic follicles and interfollicular (diffuse) areas (E). Immunostain for CD3 highlights reactive T-cells in follicular lymphoma. The pattern of CD3, accumulating around neoplastic follicles, can be used to highlight the nodular distribution of lymphoma cells (F). Immunostain for CD10 confirms that the neoplastic cells are of germinal center origin (lymphoma cells are positive within neoplastic follicles). Scattered interfollicular neoplastic cells are weakly stained with CD10. The reactivity is stronger in germinal centers than in interfollicular regions (G). Immunostain for BCL-6 highlights neoplastic lymphoma cells of germinal center origin within neoplastic follicles (H). Immunostain for BCL2 is positive in neoplastic B-lymphocytes (I).

Microscopic examination shows partial or complete effacement of the lymph node architecture with numerous, similarly sized, nonpolarized neoplastic follicles with attenuated or absent mantle zones, typically present in a back-to-back fashion in involved sites (Fig. 1). The neoplastic follicles of FL may also contain many reactive T-cells and follicular dendritic cells (FDCs), but tingible body macrophages are usually few or absent. FL is typically composed of centrocytes (small and large cleaved B-cells) and larger centroblasts (large noncleaved B-cells).

Grading of FL is based on the number of centroblasts per

high-power microscopy field ($\times 40$ objective, 0.159 mm^2) [1]. Distinguishing between grades 1 and 2 (containing up to 15 centroblasts per field) is not recommended at this time. Grade 3 cases have > 15 centroblasts per field and are further subdivided to 3A (centrocytes present), 3B (solid aggregates of centroblasts with no or very rare intervening centrocytes) (Fig. 2). Grade 3A (or 3B) FL with diffuse growth containing > 15 centroblasts per high-power field should be classified as diffuse large B-cell lymphoma (DLBCL) according to the WHO system (Table 1) [1].

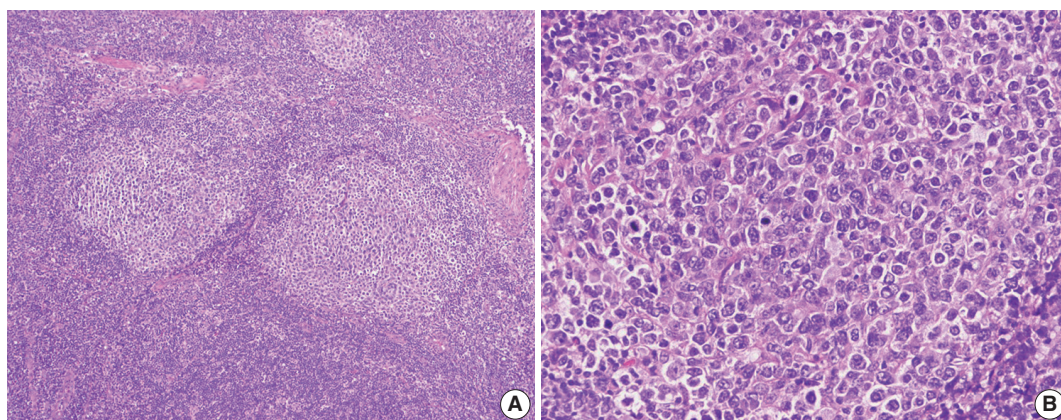


Fig. 2. Follicular lymphoma, high-grade morphology. A representative case of follicular lymphoma, high-grade (grade 3B). H&E-stained excisional biopsy (A, B). The neoplastic follicles are composed of a homogeneous population of large lymphoma cells. High power magnification shows a neoplastic follicle of FL, grade 3B. Most cells in this follicle are large centroblasts without intervening centrocytes.

Table 1. Follicular lymphoma grading, pattern, immunohistochemical and cytogenetic findings

World Health Organization grading of follicular lymphoma			
Grade	Definition	Pattern	Immunohistochemistry and cytogenetics
1	0–5 centroblasts/high power field	Follicular or diffuse	IHC: CD10: + (95%–100%)
2	6–15 centroblasts/high power field	Follicular or diffuse	BCL2: + (85%–90%) FISH: BCL2 translocation: + (80%–90%) BCL6 rearrangement: + (3–15%) Ki-67: $< 20\%$ ^a
3A	> 15 centroblasts/high power field Centrocytes present	Follicular If diffuse component: Reported as diffuse large B cell lymphoma and follicular lymphoma (% of each component is reported); correlate with clinical features and overall grade in cases with small	IHC: CD10: + (80%–95%) BCL2: + (50%–75%) FISH: BCL2 translocation: + (60%–70%) BCL6 rearrangement: + (30%–40%) Ki-67: $> 20\%$
3B	> 15 centroblasts/high power field Lack centrocytes	Follicular If diffuse component: Reported as diffuse large B-cell lymphoma and follicular lymphoma (% of each component is reported)	IHC: CD10: + (40%–85%) BCL2: + (45%–75%) FISH: BCL2 translocation: + (15%–30%) BCL6 rearrangement: + (40%–50%) CD10-IRF4/MUM1+: common Ki-67: $> 50\%$

High power field of 0.159 mm^2 ($\times 40$ objective).

Follicular: $> 75\%$ (proportion follicular %). Diffuse: 0% (proportion follicular %).

IHC, immunohistochemistry; FISH, fluorescence in situ hybridization.

^a~20% of low-grade follicular lymphomas have a high proliferation (Ki-67) rate.

WHO classification recommends documenting the proportion of the neoplasm that is present in a follicular versus diffuse distribution, as follows: follicular pattern (> 75% of the sample has a follicular pattern); follicular and diffuse pattern (25%–75% of the specimen has a follicular pattern); focally follicular/predominantly diffuse (< 25% of the specimen has a follicular pattern); and a diffuse pattern (absence of follicular areas) [1].

Based on these criteria, a neoplasm with a purely follicular pattern is considered FL, even if composed of centroblasts alone. For patients with low-grade FL, the tumor pattern of diffuse has no prognostic importance. Still, the possibility of sampling error in small biopsies should be considered or noted in the report. An area of increased subjectivity is when biopsies are small and show limited regions of diffuse pattern with grade 3A morphology. In these cases, especially if associated with low-grade FL in most specimens and clinical findings support low-grade FL, it is critical not to overcall that diffuse area as DLBCL [22].

FL of the usual type can show a wide range of morphologic variability, but are still classified as FL. Distinct from this, there are also WHO-defined FL variants which are also FL but have consistent clinicopathologic and biologic nuances that separate them from usual FL. In terms of morphologic variability in FL, some cases of FL, especially when neoplastic follicles invade beyond the lymph node capsule, particularly in retroperitoneal and mesenteric sites, can be associated with diffuse and prominent sclerosis, often associated with blood vessels. FL of the usual type may also show scattered Hodgkin-like cells, which must be distinguished from classic Hodgkin lymphoma and collision tumors with both FL and classic Hodgkin lymphoma, usually accomplished by careful and extensive immunophenotyping. FL can also have Castleman-like features, including concentric mantle zone cells, hyalinization and regression of follicles, and interfollicular vascular proliferation with penetrating vessels creating lollipop lesions. These cases may mimic hyaline vascular Castleman's disease to the point that the FL is not identified, creating a diagnostic pitfall [23]. In the floral variant of FL, neoplastic follicles are irregular in shape and surrounded by expanded, prominent mantle zone lymphocytes which penetrate neoplastic follicles. This variant FL resembles the non-neoplastic entity progressive transformation of germinal centers and may also mimic other lymphomas, including marginal zone lymphoma (with follicular colonization) or nodular lymphocyte-predominant Hodgkin lymphoma (NLPHL) [24,25]. Signet ring cell FL is a variant in which tumor cells have clear, vacuolated cytoplasm and an eccentric nucleus and should be distinguished from carcinoma cells. The vacuoles are composed of intracytoplasmic immunoglobulin

deposits [26].

FL variants include in situ follicular neoplasia, duodenal-type FL, diffuse variant FL, and testicular FL. In situ follicular neoplasia is diagnosed when lymph node biopsies show overall normal histologic findings with preservation of nodal architecture. Still, abnormal, bright BCL2-positive B-cells are identified within lymphoid follicles [1]. These BCL2-positive B-cells are confined to follicles and represent colonization of pre-existing germinal centers by monoclonal *BCL2*-rearranged B-cells [27,28]. Because a subset of these patients will have FL in other sites at the time of diagnosis of in situ follicular neoplasia, these patients should be staged. Approximately 5% of these patients will subsequently develop FL or DLBCL [29]. Further supporting that these lesions are biologically in situ neoplasms, sequencing studies performed in these selected cells show mutation abnormalities similar to those seen in FL but at lower variant allele frequency. Moreover, retrospective analysis of previously removed lymph nodes in patients diagnosed with FL can identify in situ FL in most of these patients [30,31].

As opposed to in situ follicular neoplasia, lymph nodes may show partial involvement by FL. Both neoplastic and reactive follicles are present in these cases, and lymph node architecture is partially effaced. These cases are still classified as FL, not in situ lesions, and the presence of only partial nodal involvement is associated with lower stage, and better prognosis, given adequate sampling [32].

Duodenal-type FL are FL that arise at extranodal, mucosal sites within the small bowel, usually the second portion of the duodenum (Fig. 3). These neoplasms do not typically pose diagnostic challenges since the histopathologic features are typical of low-grade FL. This variant is important to recognize clinically since it occurs in younger patients and remains localized in nature [33]. Therefore, it is amenable to localized radiation alone and generally does not require systemic therapy. Biologically this variant FL is intriguing in that it shows features overlapping between FL and extranodal marginal zone lymphoma. Like usual FL, duodenal-type FLs have *BCL2* translocations, somatically hypermutated immunoglobulin genes, and frequent mutations in *KMT2D*, *CREBBP*, and *TNFRSF14* [34]. However, these lesions additionally show features that overlap with those of extranodal marginal zone lymphoma, including restricted usage of immunoglobulin heavy chain variable region, suggesting development in the context of antigen stimulation [35].

The diffuse variant of FL has clinical, immunophenotypic, and molecular genetic differences from typical nodal FL. This variant FL typically presents at nodal sites, usually inguinal lymph nodes,

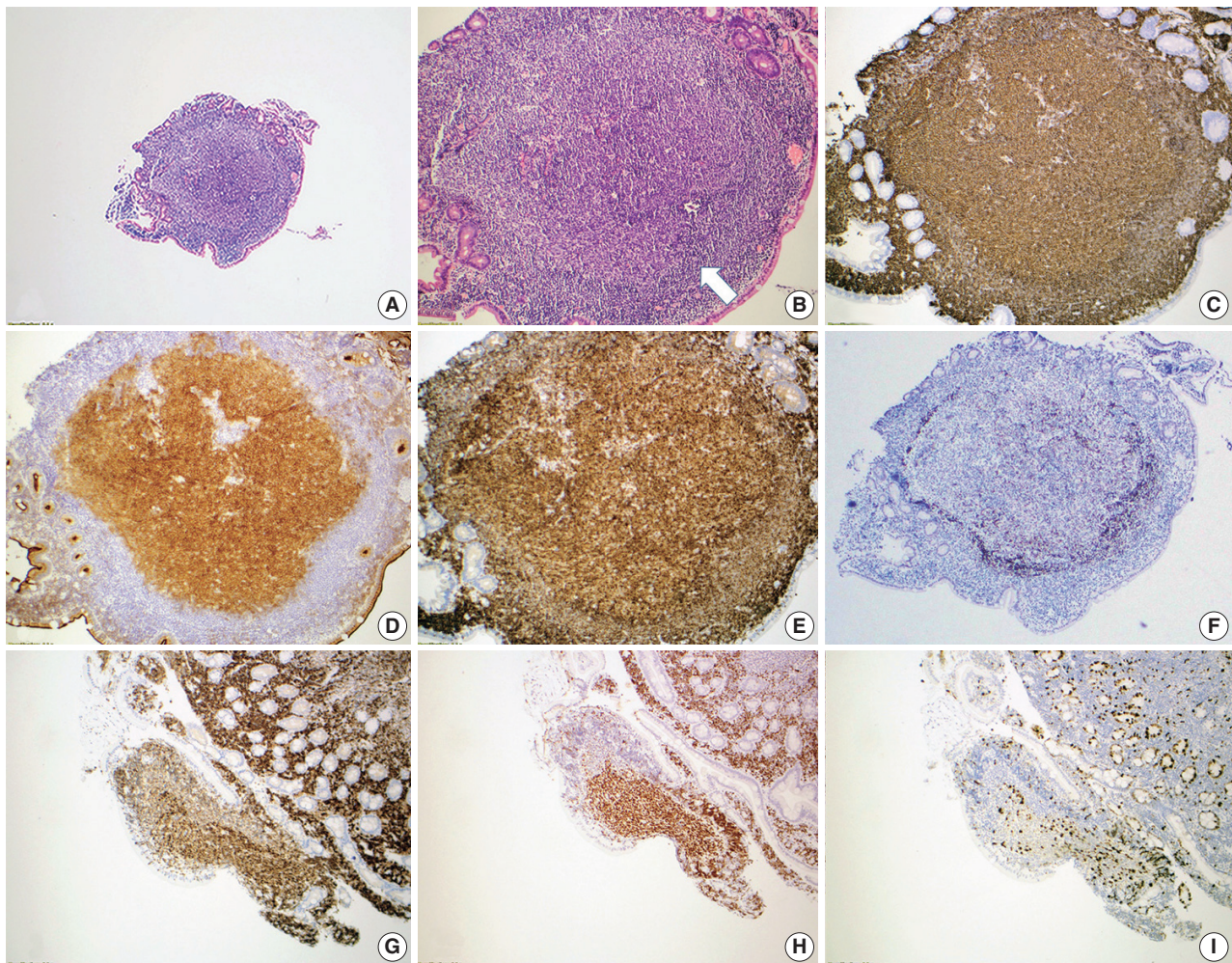


Fig. 3. Duodenal-type follicular lymphoma. A representative case of duodenal-type follicular lymphoma. H&E-stained biopsy (A, B) and immunohistochemical stains (C–I) show intramucosal follicular lymphoma, grade 1, forming polyps in the mucosa of the small intestine (A). The neoplastic follicles are partially surrounded by a thin layer of mantle cells (arrow) (B). Neoplastic lymphocytes are positive for CD20 (C) with the germinal center marker CD10 (D), and BCL6 (H) co-expression. CD10 also highlights the intestinal absorptive epithelium, which is internal control. The neoplastic lymphocytes co-express BCL2 (E, G), supporting follicular lymphoma diagnosis. CD21 confirms that the follicular dendritic meshwork is located at the periphery of the neoplastic follicle (F). Ki-67 proliferation index is not increased (I).

as a large mass [36,37]. However, as opposed to the usual FL, this variant is frequently localized without systemic involvement. Histologically, this variant may be challenging to recognize, given that the majority of the neoplasm is distributed in a diffuse pattern with only focal and usually small micronodular foci. Cytologically, lymphoma cells have typical centrocytic and centroblastic morphologic features and typically express CD10 and other germinal center B-cell markers. Diffuse expression of CD23 is consistently identified. Like usual FL, these neoplasms frequently show 1p36 chromosomal abnormalities and/or *TNFSRF14* and *CREBBP* mutations. However, unlike usual FL, these neoplasms lack the *BCL2* translocation harbor *STAT6* mutations.

The testicular variant of FL is rare. This neoplasm was initially

identified in children but has also rarely been reported in adults [38]. These neoplasms have several features similar to pediatric type FL. Histologically, these neoplasms have high-grade cytology (grade 3A or 3B histology), yet they are usually localized and associated with a good prognosis. Neoplastic cells in this variant do not express BCL2 protein and lack the *BCL2* translocation, similar to pediatric type FL.

Needle biopsy of BM is performed as part of staging procedures in patients with FL. In FL, focal or extensive BM involvement is found in most patients [39]. The most frequent pattern of involvement is paratrabeular aggregates of lymphoma cells, with or without interstitial or diffuse patterns. The pure follicular (nodular) pattern in BM is present in about 5% of cases with BM

involvement [40].

The liver and spleen are commonly involved in FL. In the liver, FL usually involves the portal tracts. However, large nodules in parenchyma are present when the spleen is extensively involved by lymphoma. In the spleen, the white pulp is preferentially involved with two predominant patterns: Expansion of the white pulp in most cases vs. relatively preserved white pulp architecture less frequently [41,42].

Fine-needle aspirations typically show variable mixtures of centrocytes and centroblasts. In comparison to reactive follicular hyperplasia, tingible body macrophages are rare or absent (Fig. 4). Centrocytes are small to large, have angulated nuclei, dense chromatin, and scant cytoplasm. Centroblasts are large cells with oval nuclei, vesicular chromatin, 1–3 nucleoli, moderate cytoplasm and are > three times the size of lymphocytes. Similar morphologic features might be seen in FDCs. However, FDCs have large round nuclei, dispersed and even nearly clear chromatin, single eosinophilic nucleolus, and indistinct cytoplasm [43].

IMMUNOHISTOCHEMICAL AND ANCILLARY STUDIES

By IHC, FL cells express pan-B-cell markers (CD19, CD20, CD22, CD79, PAX5) and monotypic surface Ig, most commonly IgM with or without IgD [1]. Germinal center markers, including CD10, BCL6, HGAL, LMO2, STMN1, GCET, MEF2B, etc., are variably expressed by FL cells [44–46]. BCL2 is positive in 85%–90% of FL grades 1 and 2 [46]. BCL2 and CD10 show decreased intensity and frequency of staining as the grade of FL increases (Table 1).

A subset of FL cases is truly negative for BCL2, especially in grade 3B [47–49]. These tumors also usually do not have the *BCL2* translocation of FL and may express MUM1 and cytoplasmic immunoglobulin, thus appearing to have biology more similar to post-germinal center B-cells. However, a subset of cases is falsely negative for BCL2 expression, which may be due to a point mutation in BCL2 that blocks binding of the BCL2 clone 124, which is used commonly in clinical IHC. Other anti-BCL2 antibodies such as clone E17 or SP66 will be positive [50].

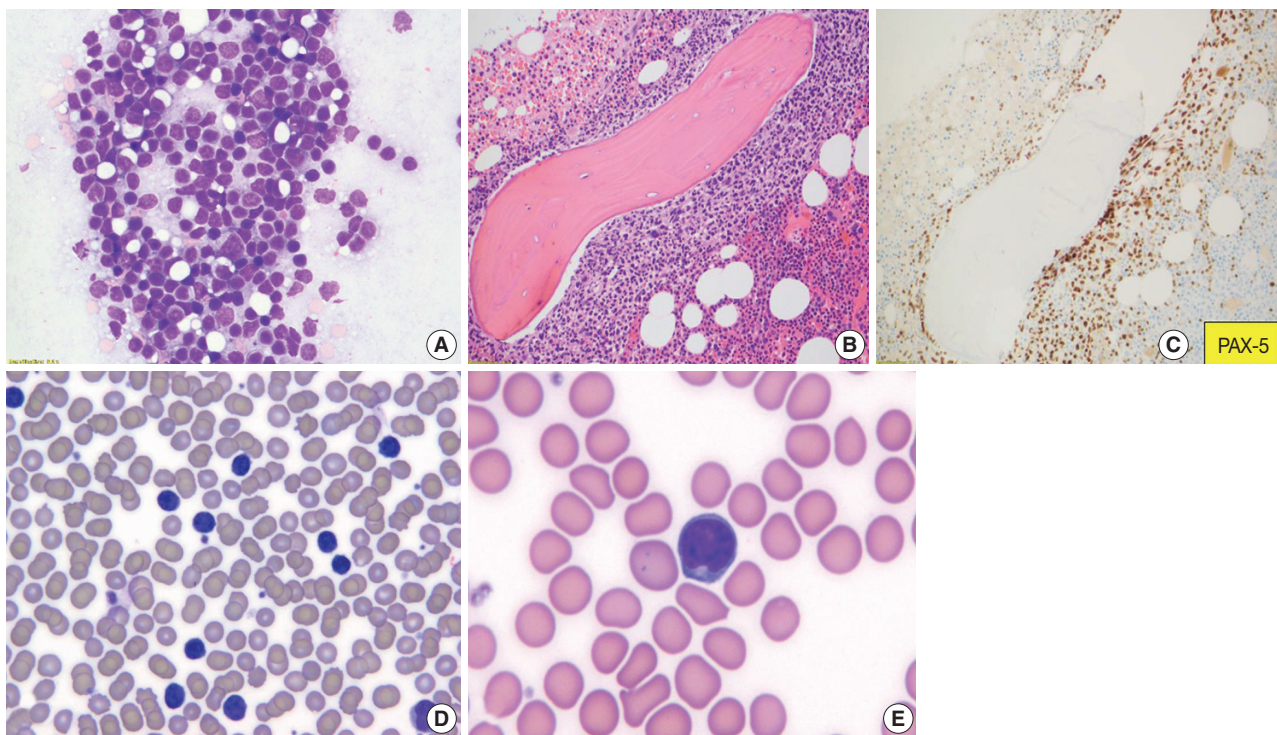


Fig. 4. Follicular lymphoma, fine-needle aspirate smear. Paratrabeular pattern of involvement in the bone marrow and peripheral blood smear involvement. Wright-Giemsa-stained smears (A, D, E), H&E-stained slide (B), and immunohistochemical stain (C). Fine-needle aspiration of a lymph node from a patient with FL, grade 1–2, demonstrates a mixture of centrocytes and centroblasts (A). Bone marrow core biopsy specimen involved by follicular lymphoma is shown. The neoplasm has a paratrabeular pattern of distribution (B). PAX-5 highlights neoplastic B-cells (C). Peripheral blood smear from a patient with follicular lymphoma demonstrates leukemic involvement by centrocytes (D) with deeply cleaved nuclei (E).

FL cases are negative for T cell markers CD2, CD3, CD4, CD5, CD7, CD8, and are usually negative for CD43 and cyclin D1 [1,51]. A small subset of cases is positive for CD5, including a subset of instances of the floral variant of FL [52].

The morphologic appreciation of follicular patterns in FL is usually adequate. Still, it can be supported by identifying FDC networks underlying the follicular aggregates, which are generally positive for CD21, CD23, and/or CD35 [22]. Another clue for a nodular pattern in FL is the accumulation of reactive T-cells at the periphery of the nodules. CXCL13 is another FDC-associated IHC marker that tends to be positive in most FL cases with

FDCs when negative for other FDC-associated IHC markers [53].

Ki-67 assesses the proliferation rate of follicular lymphomas, and the Ki-67 proliferation index correlates with FL grade. Most low-grade FL has proliferative rates <20%. However, about 20% of low-grade FL have a high proliferation rate (>30%). These follicular lymphomas appear to behave more aggressively, similar to grade 3A or grade 3B FL. We report these cases as FL grade 1 to 2 with a high proliferation fraction. We include diagnostic comments indicating that these cases may be more clinically aggressive than typical low-grade FL [54]. It is recommended

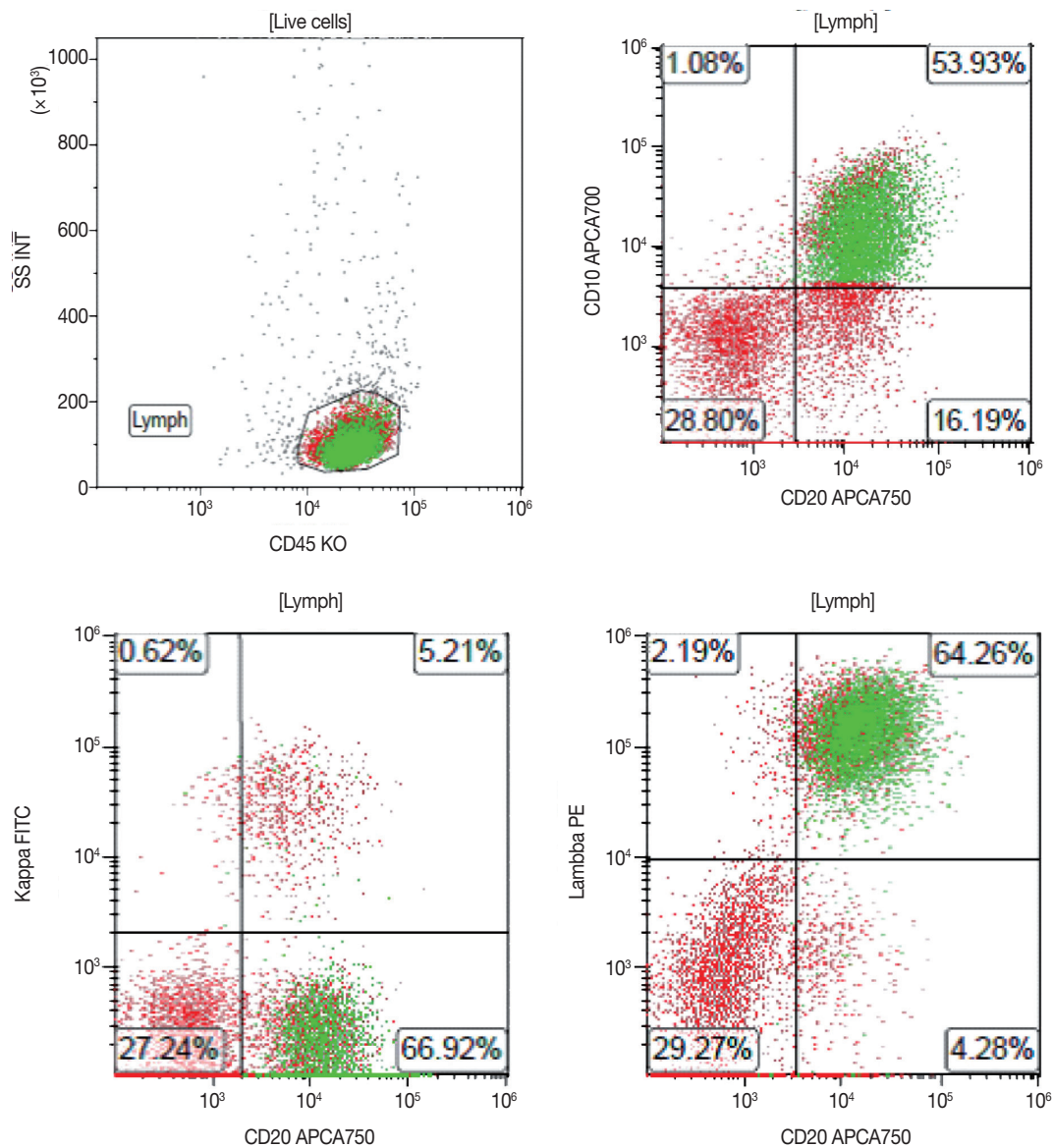


Fig. 5. A representative case of the flow cytometric immunophenotype of follicular lymphoma. Flow cytometry immunophenotyping of a lymph node fine-needle aspirate specimen from a patient with follicular lymphoma confirms that the lymphoma cells, gated by expression of CD45, co-express CD20 and CD10, with surface light chain restriction for lambda.

to assess Ki-67 in follicles. However, if interfollicular areas are more extensive than follicular ones, we estimate the Ki-67 proliferation based on an average of the entire neoplasm [22]. FLs with polarized follicles may have higher Ki-67 proliferative rates present in the dark zone of the follicle, and this should not be interpreted as a high proliferation index in FL [22].

Peripheral blood is commonly involved (at a low level) in ~90% of FL cases. This feature can be detected by flow cytometry or molecular methods if not observed easily in peripheral blood smear. Absolute lymphocytosis with a high count is present in 5%–10% of cases [19]. Neoplastic cells are typically small to intermediate in size with highly indented nuclei, known as buttock cells.

The typical immunophenotype of FL as identified by flow cytometry is CD19⁺ (dim), CD20⁺ (bright), CD10⁺ (uniform), CD5⁻, CD23⁻, CD200⁻, CD11c⁻, with surface expression of restricted immunoglobulin κ-chain or immunoglobulin λ-chain (Fig. 5).

Conventional cytogenetic analysis can detect t(14;18)(q32;q21) *IGH-BCL2* in up to 90% of FL cases (Fig. 6) [55].

Fluorescent in-situ hybridization (FISH) is more sensitive than PCR-based approaches in detecting *IGH-BCL2* due to variation in breakpoint regions [56]. Rare cases of FL have the juxtaposition of the Ig light chain promoters to *BCL2*: t(2;18)(p11;q21) and t(18;22)(q21;q11) [57].

The absence of a *BCL2* rearrangement in a suspected low-grade FL is unusual. In contrast, the absence of such a rearrangement in grade 3 cases should not be interpreted as evidence against a diagnosis of follicular lymphoma, particularly in grade 3B FL.

Loss of 1p36, which contains *TNFRSF14*, is common in FL [11,13]. 3q27 *BCL6* rearrangement or amplification is present mainly in FL 3B. In the absence of *BCL2* rearrangement in grade 3 cases, FISH studies for *BCL6* rearrangements can be performed.

MYC rearrangement/activation of *MYC* is rare in FL (<5%). In the absence of histologic transformation, these cases are still called FL and are not classified as high-grade B-cell lymphoma. More extensive studies are needed to evaluate if *MYC*-rearrangement in FL has prognostic significance [58,59]. However, some of the FL with *MYC*-rearrangement are associated with transformation to DLBCL. These cases are categorized as double-hit

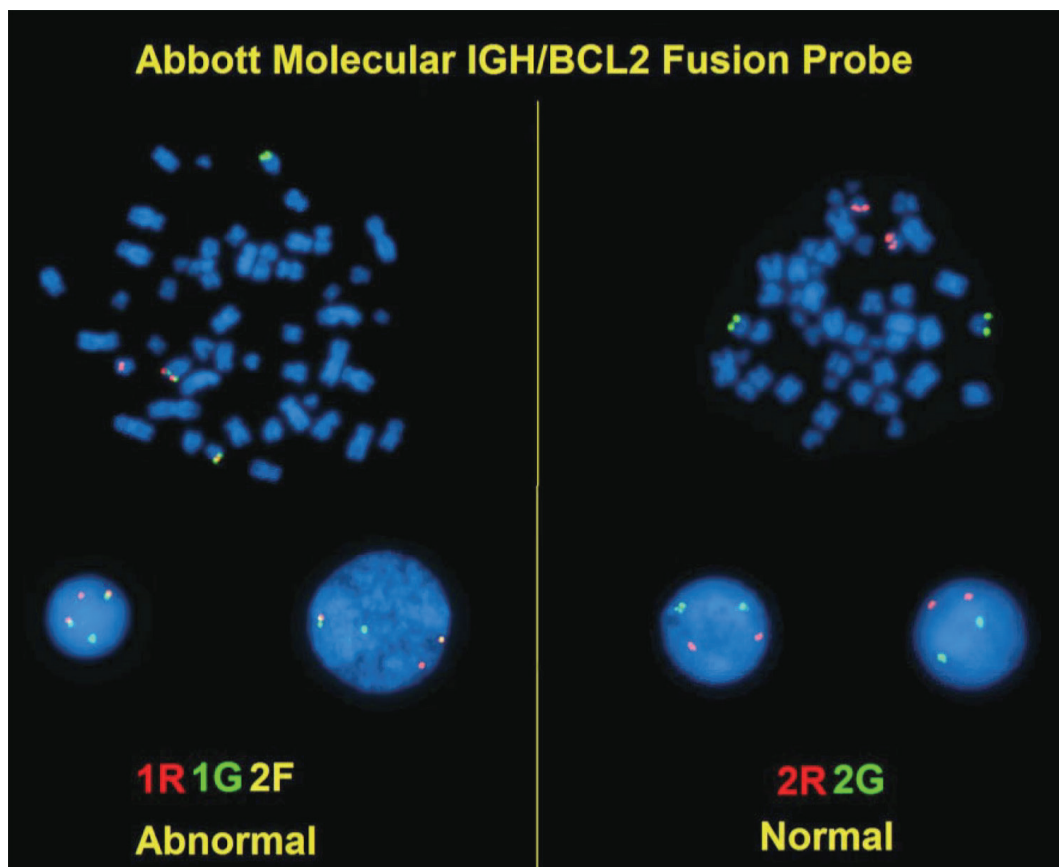


Fig. 6. *IGH/BCL2* dual-color fluorescent in-situ hybridization (FISH). FISH on a fixed, paraffin-embedded tissue section of follicular lymphoma using dual-fusion probes for *BCL2* (red) and *IGH* (green). The t(14;18)(q32;q21) *IGH/BCL2* fusion gene is a yellow signal.

lymphoma, in the category of high-grade B-cell lymphoma, if transformed and have *BCL2* or *BCL6* translocation in addition to *MYC*-rearrangement [60]. Other genetic alterations associated with transformation to DLBCL include the inactivation of *TP53* and *CDKN2A* [61,62].

Frequent genetic alterations in FL include: *BCL2*, *KMT2D/MLL2*, *EPHA7*, *EZH2*, *BCL6*, *CREBBP*, and *TNFRSF14* mutations. Less common genetic alterations are *ARID1A*, *CARD11*, *TNFAIP3*, *MYC*, *FOXO1*, and *TP53* mutation/alteration. Comparative genomic hybridization has detected gains in 1, 2p15, 6p, 7p, 7q, 8q, 12q, 18p, 18q, X chromosomes and losses in 1p36, 3q, 6q, 9p, 10q, 11q, 13q, 17p chromosomes [1,10,63].

Finally, monoclonal B-cell populations in FL can be detected by monoclonal Ig heavy and light chain gene rearrangements detected by BIOMED-2 primer sets in multiplex polymerase chain reaction [64,65].

DIFFERENTIAL DIAGNOSIS

Reactive follicular hyperplasia

In reactive follicular hyperplasia, follicles are primarily located in the cortex, are more widely separated, show variation in size and shape, the polarization of germinal centers into light and dark zones (higher proliferation), frequent mitoses, tingible body macrophages in germinal centers, and sharply demarcated mantle zones. There is usually no evidence of monoclonality by Ig rearrangement studies, and $t(14;18)(q32;q21)$ is not identified [66]. Flow cytometry evidence of monotypic light chain expression, uniform expression of CD10, decreased intensity of CD19, CD20, and CD38, are also features that would support the diagnosis of FL over reactive follicular hyperplasia. However, rare cases of re-

active lymph nodes can show monotypic light chain expression among B-cells, especially in children [67-69].

Progressive transformation of germinal centers

Nodules are 3–5 times larger than background reactive follicles in the progressive transformation of germinal centers. It may be hard to separate this entity from the floral variant of FL on morphology (Fig. 7). By IHC, germinal center B-cells are negative for *BCL2* in the progressive transformation of germinal centers, and there is no evidence of monoclonality or $t(14;18)(q32;q21)$ [25].

Castleman disease, hyaline vascular variant

Follicles are more widely spaced and have concentric mantle zones. Follicles are depleted of germinal center B-cells, and there are prominent FDCs. Lymphoid cells of the atretic follicles are negative for *BCL6* by IHC, and residual germinal center B-cells do not express *BCL2* [23].

Nodular lymphocyte-predominant Hodgkin lymphoma

NLPHL has larger nodules than FL, and the nodules are more vaguely circumscribed. Most cells in nodules are small round lymphocytes. Centrocytes and centroblasts are absent. The presence of lymphocyte predominant (LP) cells which are negative for CD10 and *BCL2*, is the clue to the diagnosis of NLPHL. Interestingly, LP cells might express some germinal-center-associated markers, including *BCL6*, *HGAL*, *LMO2*, which may add to the difficulty of differentiating NLPHL B-cell rich nodular areas from FL [70]. In NLPHL, $t(14;18)(q32;q21)$ is not identified [22].

Lymphocyte-rich classic Hodgkin lymphoma

There are commonly large nodules with eccentrically located

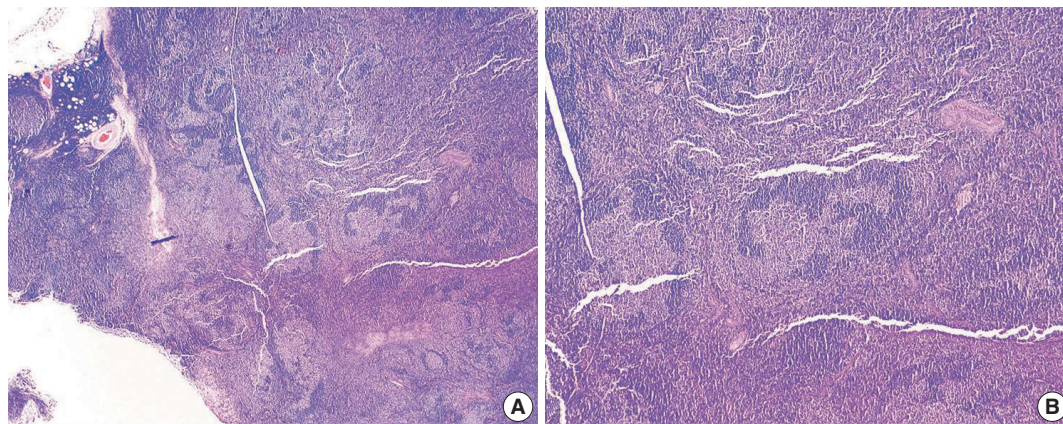


Fig. 7. Floral variant of follicular lymphoma. H&E-stained excisional biopsy (A, B) shows the morphology of follicular lymphoma with large and lobulated follicles, in some areas resembling flower petals (A). The darker mantle zone lymphocytes are infiltrating the pale follicular lymphoma cells (B).

germinal centers and expanded mantle zones in this neoplasm. There are Reed-Sternberg and Hodgkin cells, usually present within the expanded mantle zones. Reed-Sternberg and Hodgkin cells are positive for CD15, CD30, and PAX5 (dim) and negative for CD45, OCT2, BOB1, and CD79a. BCL6 positive germinal center B-cells do not co-express BCL2.

Mantle cell lymphoma

Mantle cell lymphoma (MCL) can resemble low-grade FL if it has in nodular or mantle zone pattern. Lymphoma cells of MCL are usually positive for CD5, CD43, cyclin D1, and negative for CD10. *t(11;14)(q13;q32)/IGH-CCND1* is the hallmark of MCL.

Nodal marginal zone lymphoma

In nodal marginal zone lymphoma (MZL) lymphocytes with monocytoid features, frequent plasmacytic differentiation, and colonization of germinal centers by a monotypic and monoclonal B-cell population is identified. The neoplastic cells express pan-B-cell markers and are BCL2 positive by IHC. However, they are negative for CD5, CD10, cyclin D1, BCL6, LMO2, and other germinal center-associated markers. Expression of germinal center cell markers, including dual expression of BCL2 and BCL6 in rare cases of MZL, especially extranodal MZL, is an essential diagnostic pitfall to be aware of [71]. Positive IHC stain for IRTA1 and MNDA favor the diagnosis of MZL [72].

PROGNOSTIC FACTORS AND THERAPEUTIC MODALITIES

FL patients have a median overall survival of > 15 years with different 5-year progression-free survival based on disease characteristics, comorbidities, therapies used, and therapeutic response [73]. Short remission after treatment has a poor prognosis [74].

FL may transform into an aggressive lymphoma. In ~25% to 35% of cases, FL progress to DLBCL, usually with the DLBCL showing biologic similarity to germinal center derived DLBCL [75-77]. As mentioned previously, a small subset of FL may progress to high-grade B-cell lymphomas with *MYC*, *BCL2*, and/or *BCL6* translocations, and rare cases may progress to lymphoblastic lymphoma or relapse as classic Hodgkin lymphoma.

Other clinical prognostic factors in FL include:

Follicular Lymphoma International Prognostic Index (FLIPI), based on the following criteria, was published before the era of rituximab therapy [78]:

- Age (≥ 60 vs. < 60 years)

- Ann Arbor stage (III-IV vs. I-II)

- Hemoglobin level (< 120 vs. ≥ 120 g/L)

- Number of nodal areas involved (> 4 vs. ≤ 4)

- Serum LDH level (above normal versus normal or below)

Three risk groups based on FLIPI are: low risk (score 0-1), intermediate-risk (score 2), and high risk (score 3-5), predicting 10-year overall survival of 70%, 50%, and 35%, respectively.

FLIPI2 system (in patients treated with rituximab) [79]:

- High serum $\beta 2$ microglobulin

- Largest involved lymph node > 6 cm

- BM involvement

- Hemoglobin < 12 g/dL

- Age > 60 years

M7 FLIPI better characterizes prognostic risk by incorporating the mutational status of seven genes included in this model: *EZH2*, *ARID1A*, *MEF2B*, *EP300*, *FOXO1*, *CREBBP*, and *CARD11* [80].

Other histopathologic adverse prognostic factors include:

- High histologic grade (especially grade 3B) and presence of DLBCL [81]

- Low-grade FL or grade 3A FL with a high proliferation index ($> 30\%$) behaves similar to high-grade FL [54]

Cytogenetic adverse prognostic factors:

- Complex karyotype

- Both *BCL2* and *MYC* rearrangement

- *Del6q25-27*; *del17p* and/ or mutations of *TP53* [82,83]

TREATMENT

Standardized first-line therapy for FL [10]:

(1) Stage I or contiguous stage II (non-bulky): localized radiotherapy +/- systemic chemotherapy

(2) Stage I or stage II (bulky), or non-contiguous stage II: Anti-CD20 monoclonal antibody ± chemotherapy; anti-CD20 monoclonal antibody ± chemotherapy and/or radiotherapy

(3) Stage III or stage IV: anti-CD20 monoclonal antibody (in those with low tumor burden or elderly); anti-CD20 monoclonal antibody + chemotherapy (+/- maintenance anti-CD20)

Patients with advanced-stage disease and a low tumor burden also can undergo watchful waiting.

FL is generally very responsive to radiation and chemotherapy. Radiation alone can provide a long-lasting remission in some patients with limited disease. In more advanced stages, physicians may use one or more chemotherapy drugs or the monoclonal antibody rituximab (Rituxan) alone or with other agents.

Standard combination regimens include:

- R-Bendamustine (rituximab and bendamustine)
- R-CHOP (rituximab, cyclophosphamide, doxorubicin, vincristine, and prednisone)
- R-CVP (rituximab, cyclophosphamide, vincristine, and prednisone)
- Chemotherapy, radiation, monoclonal antibodies, and chimeric antigen receptor T cell therapy, like axicabtagene ciloleucel, may be used to treat relapsed/refractory FL [84].

The bispecific antibody, mosunetuzumab, which targets CD20 and CD3, redirects and recruits endogenous T-cells to the proximity of CD20-expressing B-cells; it has promising clinical activity in patients with relapsed or refractory FL [85].

Standard second-line regimens include:

- Bendamustine (Treanda) with or without rituximab (Rituxan) or obinutuzumab (Gazyva) [86]
- Copanlisib (Aliqopa): phosphoinositide 3-kinase (PI3K) inhibitor [87]
- Duvelisib (Copiktra): PI3K inhibitor [88]
- Idelalisib (Zydelig): PI3K inhibitor [88]
- Umbralisib (UKONIQ): PI3K inhibitor [89]
- Tazemetostat (TAZVERIK): inhibitor of EZH2 [90]
- Abexinostat, vorinostat, and mocetinostat: Histone deacetylase inhibitors [91,92]
- Polatuzumab vedotin, an antibody–drug conjugate targeting the CD79b component of the BCR [93]
- Hu5F9-G4, an antibody targeting CD47 (which is overexpressed on cancer cells): enables the killing of tumor cells by macrophages by disrupting the inhibitory effect of CD47 on macrophage phagocytosis [94].

CONCLUSION

FL is the most common indolent B-cell lymphoma and originates from the lymphoid follicle's germinal center B-cells (centrocytes and centroblasts).

In summary, we discussed the importance of morphologic classification and interpretation of ancillary studies in the accurate diagnosis of FL. Although many cases of FLs are typical and histopathologic features are straightforward, differentiating FL from mimickers, either from other lymphomas or reactive conditions, requires awareness of different morphologic patterns in FL and pitfalls in the interpretation of ancillary tests.

The overall survival for most patients is prolonged, but relapses are frequent. Understanding mutational abnormalities and signaling pathways, in addition to the t(14;18) (q32;q21) translocation and *BCL2* mutation, will further help to identify innovative

treatment approaches and application of immunotherapy and targeted therapy in patients with FL.

Ethics Statement

Not applicable.

Availability of Data and Material

The datasets generated or analyzed during the study are available from the corresponding author on reasonable request.

Code Availability

Not applicable.

ORCID

Mahsa Khanlari <https://orcid.org/0000-0002-6412-6943>
Jennifer R. Chapman <https://orcid.org/0000-0002-6214-4152>

Author Contributions

Writing—review & editing: MK, JRC. Approval of final manuscript: all authors.

Conflicts of Interest

The authors declare that they have no potential conflicts of interest to disclose.

Funding Statement

No funding to declare.

References

1. Jaffe ES, Harris NL, Swerdlow SH, et al. Follicular lymphoma. In: Swerdlow SH, Campo E, Harris NL, et al., eds. WHO classification of tumours of haematopoietic and lymphoid tissues. 4th ed. Lyon: IARC Press, 2017; 266-77.
2. Brill NE, Baehr G, Rosenthal N. Generalized giant lymph follicle hyperplasia of lymph nodes and spleen; a hitherto undescribed type. *Am J Med* 1952; 13: 570-4.
3. Lukes RJ, Butler JJ. The pathology and nomenclature of Hodgkin's disease. *Cancer Res* 1966; 26: 1063-83.
4. Lennert K. History of the European Association for Haematopathology. New York: Springer, 2006.
5. Harris NL, Jaffe ES, Stein H, et al. A revised European-American classification of lymphoid neoplasms: a proposal from the International Lymphoma Study Group. *Blood* 1994; 84: 1361-92.
6. Anderson JR, Armitage JO, Weisenburger DD. Epidemiology of the non-Hodgkin's lymphomas: distributions of the major subtypes differ by geographic locations. Non-Hodgkin's Lymphoma Classification Project. *Ann Oncol* 1998; 9: 717-20.
7. A clinical evaluation of the International Lymphoma Study Group classification of non-Hodgkin's lymphoma. The Non-Hodgkin's Lymphoma Classification Project. *Blood* 1997; 89: 3909-18.
8. Roulland S, Faroudi M, Mamessier E, Sungalee S, Salles G, Nadel B. Early steps of follicular lymphoma pathogenesis. *Adv Immunol* 2011; 111: 1-46.
9. Sungalee S, Mamessier E, Morgado E, et al. Germinal center reentries of BCL2-overexpressing B cells drive follicular lymphoma progression. *J Clin Invest* 2014; 124: 5337-51.
10. Carbone A, Roulland S, Ghoghini A, et al. Follicular lymphoma. *Nat*

- Rev Dis Primers 2019; 5: 83.
11. Green MR. Chromatin modifying gene mutations in follicular lymphoma. *Blood* 2018; 131: 595-604.
 12. Green MR, Kihira S, Liu CL, et al. Mutations in early follicular lymphoma progenitors are associated with suppressed antigen presentation. *Proc Natl Acad Sci U S A* 2015; 112: E1116-25.
 13. Green MR, Gentles AJ, Nair RV, et al. Hierarchy in somatic mutations arising during genomic evolution and progression of follicular lymphoma. *Blood* 2013; 121: 1604-11.
 14. Mamessier E, Broussais-Guillaumot F, Chetaille B, et al. Nature and importance of follicular lymphoma precursors. *Haematologica* 2014; 99: 802-10.
 15. Goldin LR, Bjorkholm M, Kristinsson SY, Turesson I, Landgren O. Highly increased familial risks for specific lymphoma subtypes. *Br J Haematol* 2009; 146: 91-4.
 16. Skibola CF, Bracci PM, Halperin E, et al. Genetic variants at 6p21.33 are associated with susceptibility to follicular lymphoma. *Nat Genet* 2009; 41: 873-5.
 17. Smith S. Transformed lymphoma: what should I do now? *Hematology Am Soc Hematol Educ Program* 2020; 2020: 306-11.
 18. Trecourt A, Mauduit C, Szablewski V, et al. Plasticity of mature B cells between follicular and classic Hodgkin lymphomas: a series of 22 cases expanding the spectrum of transdifferentiation. *Am J Surg Pathol* 2022;46:58-70.
 19. Sarkozy C, Baseggio L, Feugier P, et al. Peripheral blood involvement in patients with follicular lymphoma: a rare disease manifestation associated with poor prognosis. *Br J Haematol* 2014; 164: 659-67.
 20. Yoo C, Yoon DH, Suh C. Serum beta-2 microglobulin in malignant lymphomas: an old but powerful prognostic factor. *Blood Res* 2014; 49: 148-53.
 21. Bain BJ. Diagnosis of follicular lymphoma from the peripheral blood. *Am J Hematol* 2018;93:1111-2.
 22. Medeiros LJ, O'Malley DP, Caraway NP, Vega F, Elenitoba-Johnson KS, Lim MS. AFIP atlas of tumor pathology, series 4. Tumors of the lymph nodes and spleen. Follicular lymphoma. 4th ed. Washington, DC: American Registry of Pathology, 2017; 205-38.
 23. Pina-Oviedo S, Miranda RN, Lin P, Manning JT, Medeiros LJ. Follicular lymphoma with hyaline-vascular Castleman-like features: analysis of 6 cases and review of the literature. *Hum Pathol* 2017; 68: 136-46.
 24. Kojima M, Yamanaka S, Yoshida T, et al. Histological variety of floral variant of follicular lymphoma. *APMIS* 2006; 114: 626-32.
 25. Osborne BM, Butler JJ. Follicular lymphoma mimicking progressive transformation of germinal centers. *Am J Clin Pathol* 1987; 88: 264-9.
 26. Coffing BN, Lim MS. Signet ring cell lymphoma in a patient with elevated CA-125. *J Clin Oncol* 2011; 29: e416-8.
 27. Cong P, Raffeld M, Teruya-Feldstein J, Sorbara L, Pittaluga S, Jaffe ES. In situ localization of follicular lymphoma: description and analysis by laser capture microdissection. *Blood* 2002; 99: 3376-82.
 28. Jegalian AG, Eberle FC, Pack SD, et al. Follicular lymphoma in situ: clinical implications and comparisons with partial involvement by follicular lymphoma. *Blood* 2011; 118: 2976-84.
 29. Vogelsberg A, Steinhilber J, Mankel B, et al. Genetic evolution of in situ follicular neoplasia to aggressive B-cell lymphoma of germinal center subtype. *Haematologica* 2021; 106: 2673-81.
 30. Schmidt J, Salaverria I, Haake A, et al. Increasing genomic and epigenomic complexity in the clonal evolution from in situ to manifest t(14;18)-positive follicular lymphoma. *Leukemia* 2014; 28: 1103-12.
 31. Kosmidis P, Bonzheim I, Dufke C, et al. Next generation sequencing of the clonal IGH rearrangement detects ongoing mutations and interfollicular trafficking in in situ follicular neoplasia. *PLoS One* 2017; 12: e0178503.
 32. Adam P, Katzenberger T, Eifert M, et al. Presence of preserved reactive germinal centers in follicular lymphoma is a strong histopathologic indicator of limited disease stage. *Am J Surg Pathol* 2005; 29: 1661-4.
 33. Marks E, Shi Y. Duodenal-type follicular lymphoma: a clinicopathologic review. *Arch Pathol Lab Med* 2018; 142: 542-7.
 34. Hellmuth JC, Louissaint A Jr, Szczepanowski M, et al. Duodenal-type and nodal follicular lymphomas differ by their immune micro-environment rather than their mutation profiles. *Blood* 2018; 132: 1695-702.
 35. Sato Y, Ichimura K, Tanaka T, et al. Duodenal follicular lymphomas share common characteristics with mucosa-associated lymphoid tissue lymphomas. *J Clin Pathol* 2008; 61: 377-81.
 36. Katzenberger T, Kalla J, Leich E, et al. A distinctive subtype of t(14;18)-negative nodal follicular non-Hodgkin lymphoma characterized by a predominantly diffuse growth pattern and deletions in the chromosomal region 1p36. *Blood* 2009; 113: 1053-61.
 37. Siddiqi IN, Friedman J, Barry-Holson KQ, et al. Characterization of a variant of t(14;18) negative nodal diffuse follicular lymphoma with CD23 expression, 1p36/TNFRSF14 abnormalities, and STAT6 mutations. *Mod Pathol* 2016; 29: 570-81.
 38. Finn LS, Viswanatha DS, Belasco JB, et al. Primary follicular lymphoma of the testis in childhood. *Cancer* 1999; 85: 1626-35.
 39. Sovani V, Harvey C, Haynes AP, McMillan AK, Clark DM, O'Connor SR. Bone marrow trephine biopsy involvement by lymphoma: review of histopathological features in 511 specimens and correlation with diagnostic biopsy, aspirate and peripheral blood findings. *J Clin Pathol* 2014; 67: 389-95.
 40. Torlakovic E, Torlakovic G, Brunning RD. Follicular pattern of bone marrow involvement by follicular lymphoma. *Am J Clin Pathol* 2002; 118: 780-6.
 41. Mollejo M, Rodriguez-Pinilla MS, Montes-Moreno S, et al. Splenic follicular lymphoma: clinicopathologic characteristics of a series of 32 cases. *Am J Surg Pathol* 2009; 33: 730-8.
 42. Howard MT, Dufresne S, Swerdlow SH, Cook JR. Follicular lymphoma of the spleen: multiparameter analysis of 16 cases. *Am J Clin Pathol* 2009; 131: 656-62.
 43. Ferry JA, Leval L, Louissaint A, Harris NL. Follicular lymphoma. In: Jaffe ES, Arber DA, Campo E, Harris NL, Quintanilla-Martinez L, eds. *Hematopathology*. 2nd ed. Philadelphia: Elsevier, 2017; 321-52.
 44. Menter T, Gasser A, Juskevicius D, Dirnhofer S, Tzankov A. Diagnostic utility of the germinal center-associated markers GCET1, HGAL, and LMO2 in hematolymphoid neoplasms. *Appl Immunohistochem Mol Morphol* 2015; 23: 491-8.
 45. Pittaluga S, Ayoubi TA, Wlodarska I, et al. BCL-6 expression in reactive lymphoid tissue and in B-cell non-Hodgkin's lymphomas. *J Pathol* 1996; 179: 145-50.
 46. Marafioti T, Copie-Bergman C, Calaminici M, et al. Another look at follicular lymphoma: immunophenotypic and molecular analyses identify distinct follicular lymphoma subgroups. *Histopathology* 2013; 62: 860-75.
 47. Bosga-Bouwer AG, van Imhoff GW, Boonstra R, et al. Follicular lymphoma grade 3B includes 3 cytogenetically defined subgroups

- with primary t(14;18), 3q27, or other translocations: t(14;18) and 3q27 are mutually exclusive. *Blood* 2003; 101: 1149-54.
48. Guo Y, Karube K, Kawano R, et al. Low-grade follicular lymphoma with t(14;18) presents a homogeneous disease entity otherwise the rest comprises minor groups of heterogeneous disease entities with Bcl2 amplification, Bcl6 translocation or other gene aberrances. *Leukemia* 2005; 19: 1058-63.
 49. Nann D, Ramis-Zaldivar JE, Muller I, et al. Follicular lymphoma t(14;18)-negative is genetically a heterogeneous disease. *Blood Adv* 2020; 4: 5652-65.
 50. Kendrick SL, Redd L, Muranyi A, et al. BCL2 antibodies targeted at different epitopes detect varying levels of protein expression and correlate with frequent gene amplification in diffuse large B-cell lymphoma. *Hum Pathol* 2014; 45: 2144-53.
 51. Lai R, Weiss LM, Chang KL, Arber DA. Frequency of CD43 expression in non-Hodgkin lymphoma: a survey of 742 cases and further characterization of rare CD43+ follicular lymphomas. *Am J Clin Pathol* 1999; 111: 488-94.
 52. Tiesinga JJ, Wu CD, Inghirami G. CD5+ follicle center lymphoma. Immunophenotyping detects a unique subset of "floral" follicular lymphoma. *Am J Clin Pathol* 2000; 114: 912-21.
 53. Chang KC, Huang X, Medeiros LJ, Jones D. Germinal centre-like versus undifferentiated stromal immunophenotypes in follicular lymphoma. *J Pathol* 2003; 201: 404-12.
 54. Wang SA, Wang L, Hochberg ER, Muzikansky A, Harris NL, Hasserjian RP. Low histologic grade follicular lymphoma with high proliferation index: morphologic and clinical features. *Am J Surg Pathol* 2005; 29: 1490-6.
 55. Hoglund M, Sehn L, Connors JM, et al. Identification of cytogenetic subgroups and karyotypic pathways of clonal evolution in follicular lymphomas. *Genes Chromosomes Cancer* 2004; 39: 195-204.
 56. Espinet B, Bellosillo B, Melero C, et al. FISH is better than BIOMED-2 PCR to detect IgH/BCL2 translocation in follicular lymphoma at diagnosis using paraffin-embedded tissue sections. *Leuk Res* 2008; 32: 737-42.
 57. Leich E, Hoster E, Wartenberg M, et al. Similar clinical features in follicular lymphomas with and without breaks in the BCL2 locus. *Leukemia* 2016; 30: 854-60.
 58. Chaudhary S, Brown N, Song JY, et al. Relative frequency and clinicopathologic characteristics of MYC-rearranged follicular lymphoma. *Hum Pathol* 2021; 114: 19-27.
 59. Bisso A, Sabo A, Amati B. MYC in germinal center-derived lymphomas: mechanisms and therapeutic opportunities. *Immunol Rev* 2019; 288: 178-97.
 60. Pasqualucci L, Khiabani H, Fangazio M, et al. Genetics of follicular lymphoma transformation. *Cell Rep* 2014; 6: 130-40.
 61. Huet S, Tesson B, Jais JP, et al. A gene-expression profiling score for prediction of outcome in patients with follicular lymphoma: a retrospective training and validation analysis in three international cohorts. *Lancet Oncol* 2018; 19: 549-61.
 62. Elenitoba-Johnson KS, Gascoyne RD, Lim MS, Chhanabai M, Jaffe ES, Raffeld M. Homozygous deletions at chromosome 9p21 involving p16 and p15 are associated with histologic progression in follicle center lymphoma. *Blood* 1998; 91: 4677-85.
 63. Bouska A, McKeithan TW, Deffenbacher KE, et al. Genome-wide copy-number analyses reveal genomic abnormalities involved in transformation of follicular lymphoma. *Blood* 2014; 123: 1681-90.
 64. Evans PA, Pott C, Groenen PJ, et al. Significantly improved PCR-based clonality testing in B-cell malignancies by use of multiple immunoglobulin gene targets. Report of the BIOMED-2 Concerted Action BHM4-CT98-3936. *Leukemia* 2007; 21: 207-14.
 65. Bagg A, Brazier RM, Arber DA, Bijwaard KE, Chu AY. Immunoglobulin heavy chain gene analysis in lymphomas: a multi-center study demonstrating the heterogeneity of performance of polymerase chain reaction assays. *J Mol Diagn* 2002; 4: 81-9.
 66. Weiss LM, O'Malley D. Benign lymphadenopathies. *Mod Pathol* 2013; 26 Suppl 1: S88-96.
 67. Mantei K, Wood BL. Flow cytometric evaluation of CD38 expression assists in distinguishing follicular hyperplasia from follicular lymphoma. *Cytometry B Clin Cytom* 2009; 76: 315-20.
 68. Seegmiller AC, Hsi ED, Craig FE. The current role of clinical flow cytometry in the evaluation of mature B-cell neoplasms. *Cytometry B Clin Cytom* 2019; 96: 20-9.
 69. Khanlari M, Wang SA, Tang G, Saluja K, Medeiros LJ, Thakral B. CD45-negative follicular lymphoma: a rare diagnostic pitfall of a common entity. *Cytometry B Clin Cytom* 2021; 100: 406-8.
 70. Younes S, Rojansky RB, Menke JR, Gratzinger D, Natkunam Y. Pitfalls in the diagnosis of nodular lymphocyte predominant Hodgkin lymphoma: variant patterns, borderlines and mimics. *Cancers (Basel)* 2021; 13: 3021.
 71. Poveda J, Cassidy DP, Zhou Y, et al. Expression of germinal center cell markers by extranodal marginal zone lymphomas of MALT type within colonized follicles, a diagnostic pitfall with follicular lymphoma. *Leuk Lymphoma* 2021; 62: 1116-22.
 72. Wang Z, Cook JR. IRTA1 and MNDA expression in marginal zone lymphoma: utility in differential diagnosis and implications for classification. *Am J Clin Pathol* 2019; 151: 337-43.
 73. Link BK, Day BM, Zhou X, et al. Second-line and subsequent therapy and outcomes for follicular lymphoma in the United States: data from the observational National LymphoCare Study. *Br J Haematol* 2019; 184: 660-3.
 74. Casulo C, Byrtek M, Dawson KL, et al. Early relapse of follicular lymphoma after rituximab plus cyclophosphamide, doxorubicin, vincristine, and prednisone defines patients at high risk for death: an analysis from the National LymphoCare Study. *J Clin Oncol* 2015; 33: 2516-22.
 75. Sarkozy C, Maurer MJ, Link BK, et al. Cause of death in follicular lymphoma in the first decade of the rituximab era: a pooled analysis of French and US cohorts. *J Clin Oncol* 2019; 37: 144-52.
 76. Kridel R, Chan FC, Mottok A, et al. Histological transformation and progression in follicular lymphoma: a clonal evolution study. *PLoS Med* 2016; 13: e1002197.
 77. Lee AY, Connors JM, Klimo P, O'Reilly SE, Gascoyne RD. Late relapse in patients with diffuse large-cell lymphoma treated with MA-COP-B. *J Clin Oncol* 1997; 15: 1745-53.
 78. Solal-Celigny P, Roy P, Colombat P, et al. Follicular lymphoma international prognostic index. *Blood* 2004; 104: 1258-65.
 79. Federico M, Bellei M, Marcheselli L, et al. Follicular lymphoma international prognostic index 2: a new prognostic index for follicular lymphoma developed by the international follicular lymphoma prognostic factor project. *J Clin Oncol* 2009; 27: 4555-62.
 80. Pastore A, Jurinovic V, Kridel R, et al. Integration of gene mutations in risk prognostication for patients receiving first-line immunotherapy for follicular lymphoma: a retrospective analysis of a prospective clinical trial and validation in a population-based registry. *Lancet Oncol* 2015; 16: 1111-22.

81. Wahlin BE, Yri OE, Kimby E, et al. Clinical significance of the WHO grades of follicular lymphoma in a population-based cohort of 505 patients with long follow-up times. *Br J Haematol* 2012; 156: 225-33.
82. Ross CW, Ouillette PD, Saddler CM, Shedden KA, Malek SN. Comprehensive analysis of copy number and allele status identifies multiple chromosome defects underlying follicular lymphoma pathogenesis. *Clin Cancer Res* 2007; 13: 4777-85.
83. Khanlari M, Wang SA, Fowler NH, et al. Concurrent TP53 mutation and deletion in refractory low-grade follicular lymphoma. *Clin Lymphoma Myeloma Leuk* 2021; 21: e626-9.
84. Ollila TA, Olszewski AJ. Chemotherapy-free management of follicular and marginal zone lymphoma. *Cancer Manag Res* 2021; 13: 3935-52.
85. Schuster SJ. Bispecific antibodies for the treatment of lymphomas: promises and challenges. *Hematol Oncol* 2021; 39 Suppl 1: 113-6.
86. Mondello P, Steiner N, Willenbacher W, et al. Bendamustine plus rituximab versus R-CHOP as first-line treatment for patients with follicular lymphoma grade 3A: evidence from a multicenter, retrospective study. *Oncologist* 2018; 23: 454-60.
87. Dreyling M, Morschhauser F, Bouabdallah K, et al. Phase II study of copanlisib, a PI3K inhibitor, in relapsed or refractory, indolent or aggressive lymphoma. *Ann Oncol* 2017; 28: 2169-78.
88. Pagel JM, Burke JM, Leslie LA. Refining the management of relapsed or refractory follicular lymphoma: case scenarios. *Clin Adv Hematol Oncol* 2020; 18 Suppl 20: 20-1.
89. Pongas G, Cheson B. Recent advances in the management of patients with relapsed/refractory follicular lymphoma. *Blood Lymphat Cancer* 2021; 11: 55-66.
90. Italiano A, Soria JC, Toulmonde M, et al. Tazemetostat, an EZH2 inhibitor, in relapsed or refractory B-cell non-Hodgkin lymphoma and advanced solid tumours: a first-in-human, open-label, phase 1 study. *Lancet Oncol* 2018; 19: 649-59.
91. Evens AM, Balasubramanian S, Vose JM, et al. A phase I/II multicenter, open-label study of the oral histone deacetylase inhibitor abexinostat in relapsed/refractory lymphoma. *Clin Cancer Res* 2016; 22: 1059-66.
92. Ribrag V, Kim WS, Bouabdallah R, et al. Safety and efficacy of abexinostat, a pan-histone deacetylase inhibitor, in non-Hodgkin lymphoma and chronic lymphocytic leukemia: results of a phase II study. *Haematologica* 2017; 102: 903-9.
93. Sawalha Y, Maddocks K. Profile of polatuzumab vedotin in the treatment of patients with relapsed/refractory non-Hodgkin Lymphoma: a brief report on the emerging clinical data. *Onco Targets Ther* 2020; 13: 5123-33.
94. Advani R, Flinn I, Popplewell L, et al. CD47 blockade by Hu5F9-G4 and rituximab in non-Hodgkin's lymphoma. *N Engl J Med* 2018; 379: 1711-21.

Clinicopathological differences in radiation-induced organizing hematomas of the brain based on type of radiation treatment and primary lesions

Myung Sun Kim¹, Se Hoon Kim¹, Jong-Hee Chang², Mina Park³, Yoon Jin Cha¹

Departments of ¹Pathology and ²Neurosurgery, Yonsei University College of Medicine, Seoul;
³Department of Radiology, Gangnam Severance Hospital, Yonsei University College of Medicine, Seoul, Korea

Background: Radiation-induced organizing hematoma (RIOH) is a sporadic form of cavernous hemangioma (CH) that occurs after cerebral radiation. RIOH lesions are distinct histologically from de novo CH; however, detailed research on this subject is lacking. In the present study, the clinical and histological features of RIOHs were evaluated based on causative lesions. **Methods:** The present study included 37 RIOHs confirmed by surgical excision from January 2009, to May 2020, in Yonsei Severance Hospital. All cases were divided into subgroups based on type of radiation treatment (gamma knife surgery [GKS], n=24 vs. conventional radiation therapy [RT], n=13) and pathology of the original lesion (arteriovenous malformation, n=14; glioma, n=12; metastasis, n=4; other tumors, n=7). The clinicopathological results were compared between the groups. **Results:** Clinical data of multiplicity, latency, and size and wall thickness of the original tumors and RIOHs were analyzed. The GKS group showed shorter latency (5.85±4.06 years vs. 11.15±8.27 years, p=.046) and thicker tumor wall (693.7±565.7 μm vs. 406.9±519.7 μm, p=.049) than the conventional RT group. Significant difference was not found based on original pathology. **Conclusions:** RIOH is more likely to occur earlier with thick tumor wall in subjects who underwent GKS than in patients who underwent conventional RT. These results indicate the clinical course of RIOH differs based on type of treatment and might help determine the duration of follow-up.

Key Words: Radiation-induced organizing hematoma; Cavernous hemangioma; Gamma knife surgery; Radiation therapy; Latency

Received: June 28, 2021 Revised: August 24, 2021 Accepted: August 30, 2021

Corresponding Author: Yoon Jin Cha, MD, PhD, Department of Pathology, Gangnam Severance Hospital, Yonsei University College of Medicine, 211 Eonju-ro, Gangnam-gu, Seoul 06273, Korea
 Tel: +82-2-2019-3540, Fax: +82-2-3463-2103, E-mail: yooncha@yuhs.ac

Radiation-induced cavernous hemangioma (RICH) refers to a localized vascular, tumor-like lesion that develops after cerebral radiation [1-3]. The lesion occurs mainly in children and young people, with variable latency periods after radiation treatment and diverse original lesions, including arteriovenous malformation (AVM), glioma, and metastatic tumor [4,5]. Similar to de novo cavernous hemangioma (CH), RICH appears as an enhancing lesion with popcorn-like appearance and partial hemosiderin rim on magnetic resonance imaging (MRI) and is observed histologically as a vascular-rich hemorrhagic lesion [6-8]. Thus, RICH has been regarded as a sporadic form of de novo CH that appears as a late complication of cerebral radiation [9,10].

Recently, in several studies in which RICH was compared with de novo CH, RICH was shown a potentially distinct group

of diseases with different pathogenesis compared with previously known CHs [6,11-13]. Previous research has reported that RICH following stereotactic radiosurgery shows some distinguishing features on MRI such as an unilocular cystic area with some solid component and prominent perilesional edema, and de novo CH appears to have a complete hemosiderin rim and less prominent perilesional edema [6]. Furthermore, RICH is more likely to be an inactive organizing hematoma rather than a vascular malformation. Therefore, the term “radiation-induced organizing hematoma (RIOH)” was proposed to describe the lesions more appropriately and replace the term RICH, which might be a misnomer for these lesions [6]. All the authors of the current study agreed to this concept, and the term RIOH, instead of RICH, was used throughout the manuscript.

Detailed studies on RIOH are limited. In particular, RIOH lesions have been reported irrespective of radiation dose, type of malignancy, or radiation type, such as gamma knife surgery (GKS) or conventional radiation therapy (RT) [11]. However, studies to improve the understanding of RIOH lesions have not been conducted. In the present study, RIOH lesions were better defined, and their clinicopathological characteristics, including original pathology and type of radiation treatment, were compared.

MATERIALS AND METHODS

Patient selection and clinicopathological examination

Between January 2009 and May 2020, a total of 37 cases of pathologically confirmed RIOH was selected from Severance Hospital. For each case, the size of both the original tumor and RIOH was obtained. The size of original tumor was measured from preoperative imaging, and the size of RIOH were obtained through microscopic examination. The difference between the maximal diameter of primary tumor and RIOH was measured. All the pathologic slides were reviewed, and the tumor wall thickness of RIOH was measured at the thickest point of the submitted tissue under light microscope.

All medical records were reviewed, and clinical data including age at the time of RIOH detection, sex, radiologic findings, locations of the original tumor and RIOH, multiplicity, and latency period were compared between the original tumor and RIOH. A radiologist (M.P.) reviewed all MRI scans of patients, focusing on differences in radiologic findings including perilesional edema and hemosiderin rim depending on type of RT. Furthermore, information on previous treatments was collected. Cases were classified into two groups based on previous type of radiation (GKS, $n = 24$ vs. conventional RT, $n = 13$) and into four groups based on preceding pathology of the original tumor (AVM, $n = 14$; glioma, $n = 12$; metastasis, $n = 4$; other tumors, $n = 7$). The clinicopathological parameters were analyzed. For patients who had been treated multiple times or who underwent both GKS and RT, the groups and latency were divided and calculated based on timing and method of the last treatment.

Statistical analysis

Statistical analyses were performed using SPSS ver. 21.0 (IBM Corp., Armonk, NY, USA). Continuous and categorical variables were analyzed using the non-parametric Mann-Whitney U test and the chi-square test, respectively, and $p < .05$ was considered statistically significant.

RESULTS

Patient characteristics

A total of 37 samples was included in the study. Baseline patient characteristics are summarized in Table 1. RIOH samples were from 14 males (37.8%) and 23 females (62.2%). Twenty-four patients (64.9%) underwent GKS, and 13 (35.1%) were treated with conventional RT. Original tumor pathologies were as follows: AVM ($n = 14$, 37.8%), brain tumors (11 gliomas and 1 ependymoma; $n = 12$, 32.4%), metastasis ($n = 4$, 10.8%), and other tumors (3 schwannomas, two nasopharyngeal cancers, one pituitary tumor, and one craniopharyngioma; $n = 7$, 18.9%). The cases of nasopharyngeal cancer were subcategorized into 'other tumors' in this study because postoperative RT often is used for nasopharyngeal cancer, and the central nervous system area usually is included in the radiation field.

Clinicopathological differences between RIOH lesions

The overall results of the clinical and pathological comparisons are summarized in Tables 2 and 3. RIOH cases were divided into two groups based on previous type of radiation (GKS or conventional RT). Histologically, RIOH shows a hematoma-like area with a reduced number of hyalinized thin-walled vessels with fibrin and infiltrating foamy macrophages in the vessel walls. Conversely, de novo CH shows a thick, hyalinized wall without prominent macrophage infiltration (Fig. 1). The results

Table 1. Baseline characteristics of the patients ($n = 37$)

Characteristic	No. (%)
Age at the time of RIOH detection (yr), mean \pm SD	46.57 \pm 13.79
Sex	
Male	14 (37.8)
Female	23 (62.2)
Original pathology	
AVM	14 (37.8)
Brain tumor	12 (32.4)
Metastasis	4 (10.8)
Other tumors	7 (19.0)
Type of treatment	
GKS	24 (64.9)
RTx	13 (35.1)
Tumor location	
Frontal lobe	10 (27.0)
Parietal lobe	5 (13.5)
Temporal lobe	6 (16.2)
Occipital lobe	4 (10.8)
Other (including sellar lesion)	12 (32.5)

RIOH, radiation-induced organizing hematoma; SD, standard deviation; AVM, arteriovenous malformation; GKS, gamma knife surgery; RTx, radiation therapy.

Table 2. Clinicopathological differences between 37 radiation-induced organizing hematomas

Variable	Radiation treatment		p-value	Original pathology				p-value
	GKS (n=24)	RTx (n=13)		AVM (n=14)	Brain tumor (n=12)	Metastasis (n=4)	Others (n=7)	
Tumor size (cm)								
Primary tumor	3.35±1.22	3.04±1.08	.387	3.87±1.26	2.85±1.04	2.92±0.60	2.85±1.05	.081
RIOH	2.01±0.80	1.51±0.55	.055	2.06±0.82	1.50±0.68	2.20±0.41	1.75±0.75	.459
(Size differences)	1.34±1.33	1.53±1.28	.695	1.81±1.49	1.35±1.25	0.72±0.45	1.10±1.23	.425
Tumor wall thickness (µm)	693.7±565.7	406.9±519.7	.049	714.2±610.9	560.0±630.6	362.5±47.8	538.5±518.0	.752
Latency (yr)	5.85±4.06	11.15±8.27	.046	8.92±7.01	7.55±5.06	2.28±3.45	8.68±7.28	.161

Values are presented as mean±SD.

GKS, gamma knife surgery; RTx, radiation therapy; AVM, arteriovenous malformation; RIOH, radiation-induced organizing hematoma; SD, standard deviation.

Table 3. Correlation between multiplicity and treatment/original pathology

	Total	Multiplicity		p-value
		No	Yes	
GKS	24	21 (87.5)	3 (12.5)	.586
RTx	13	11 (84.6)	2 (15.4)	
AVM	14	13 (92.8)	1 (7.2)	.155
Brain tumor	12	10 (83.3)	2 (16.7)	
Metastasis	4	2 (50.0)	2 (50.0)	
Others	7	7 (100)	0	

GKS, gamma knife surgery; RTx, radiation therapy; AVM, arteriovenous malformation.

showed significantly shorter latency in the GKS group than in the conventional RT group (5.85 ± 4.06 years vs. 11.15 ± 8.27 years, $p = .046$). In addition, the RIOH in the GKS group had significantly thicker tumor wall than that in the conventional RT group (693.7 ± 565.7 µm vs. 406.9 ± 519.7 µm, $p = .049$) (Fig. 2). Significant differences were not observed in age, tumor size of primary tumor, or RIOH. The primary tumor size did not differ between groups. However, the size of RIOH lesions tended to be larger in the GKS group than in the conventional RT group ($p = .055$). The multiplicity of RIOH was not significantly different between the groups. In terms of original pathology, the four groups based on preceding pathology were compared, and no significant differences were found in any of the clinicopathological parameters.

The results of the radiologic findings are summarized in Table 4. All patients with GKS-induced RIOH and 11 patients with RT-induced RIOH showed perilesional edema on T2-weighted images. Seven patients in the GKS-induced RIOH group showed subacute stage hemorrhage on T1-weighted images, and 21 showed hemosiderin rim deposit on T2-weighted images. Similarly, nine patients in the RT-induced RIOH group showed subacute stage hemorrhage, and 11 cases showed hemosiderin rim. Significant difference in radiologic image findings including perilesional edema ($p = .223$), subacute stage hemor-

rhage ($p = .059$) and hemosiderin deposit in MR image ($p = .679$), was not observed between the GKS and RTx groups.

No significant differences were found in other parameters. In the GKS group, the mean age at the time of RIOH diagnosis was 46.9 years; the mean sizes of primary tumor and RIOH were 3.35 cm and 2.01 cm, respectively; and size difference between primary tumor and RIOH was 1.34 cm. In the conventional RT group, the mean age was 45.8 years; the sizes of primary tumor and RIOH measured 3.04 cm and 1.51 cm on average, respectively; and the size difference between primary tumor and RIOH was 1.53 cm. However, the size of RIOH lesions tended to be larger in the GKS group than in the conventional RT group ($p = .055$).

In terms of original pathology, the four groups based on preceding pathology were compared. The mean age in the AVM, brain tumor, metastasis, and other tumors groups was 43.1 years, 43.5 years, 57.2 years, and 52.7 years, respectively. The mean sizes of the primary tumor and RIOH were 3.87 cm and 2.06 cm in the AVM group, 2.85 cm and 1.50 cm in the brain tumor group, 2.92 cm and 2.20 cm in the metastasis group, and 2.85 cm and 1.75 cm in the other tumors group, respectively. The size difference was 1.81 cm, 1.35 cm, 0.72 cm, and 1.10 cm in the AVM, brain tumor, metastasis, and other tumors groups, respectively. The mean tumor wall thickness was 714.2 µm in the AVM group, 560.0 µm in the brain tumor group, 362.5 µm in the metastasis group, and 538.5 µm in the other tumors group. The average latency in the AVM, brain tumor, metastasis, and other tumors groups was 8.92 years, 7.55 years, 2.28 years, and 8.68 years, respectively. No significant difference was found in any of the clinicopathological parameters.

Three patients in the GKS group showed multiplicity, two in the conventional RT group, 1 in the AVM group, 2 in the brain tumor group, and two in the metastasis group; however, statistical difference was not found between the groups.

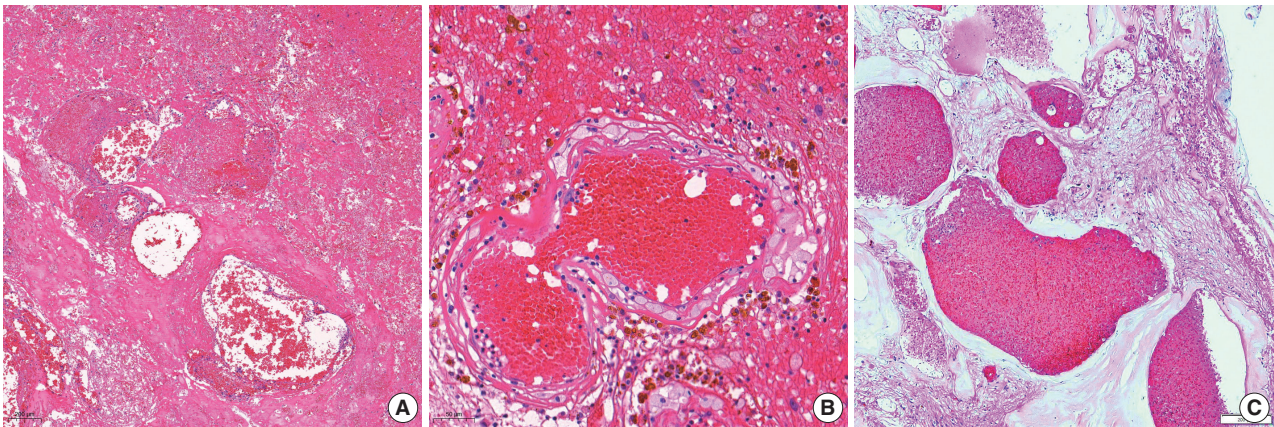


Fig. 1. The histology of radiation-induced organizing hematoma (RIOH) and de novo cavernous hemangioma (CH); Microscopically, RIOH shows a hematoma-like area composed of hyalinized vessels with fibrin and infiltrating foamy macrophages (A, B), and de novo CH consists of clusters of well-formed vascular lumens (C).

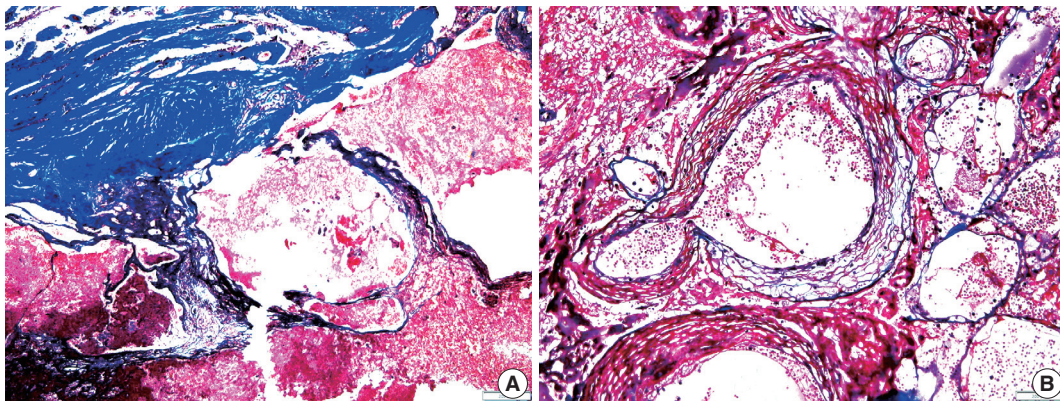


Fig. 2. Gamma knife surgery-induced radiation-induced cavernous hemangioma (RIOH) shows relatively thicker tumor walls (A) compared with conventional radiation therapy-induced RIOH (B) (Masson's trichrome).

Table 4. Radiological differences between GKS-induced and conventional RTx-induced RIOH

	Perilesional edema			p-value	Subacute stage hemorrhage (T1 high)			p-value	Hemosiderin deposit (T2 dark rim)		p-value
	Total	Absent	Present		Absent	Present	Absent		Present		
GKS	24	0	23 (95.8) ^a	.223	9 (37.5)	7 (29.1) ^b	.059	2 (8.3)	21 (87.5) ^a	.679	
RTx	13	2 (15.3)	11 (84.6)		4 (30.7)	9 (69.2)		2 (15.3)	11 (84.6)		

GKS, gamma knife surgery; RTx, radiation therapy; RIOH, radiation-induced organizing hematoma; MRI, magnetic resonance imaging.

^aOne case was undetectable on MRI; ^bEight cases were excluded that did not include the T1 series in preoperative MRI.

DISCUSSION

RIOH has been considered a sporadic form of de novo CH occurring as a late complication of cerebral radiation. RIOH occurs in children mainly after the use of cerebral radiation to treat medulloblastoma, glioma, or AVM or for prophylactic treatment of hematological malignancies such as acute lymphoblastic leukemia [4,5,14,15]. However, RIOH is rare in adults

[14,16]. In a previous study with 84 cases of RIOH, the average age at diagnosis was 20.6 years, the median was 17 years, and the average latency to development of RIOH was 10.3 years, with a median of 8 years [11]. One rare case of RIOH has been diagnosed at 52 years after RT [17].

The pathophysiology of RIOH is not well-known; however, two hypotheses have been suggested: occult CHs that were previously present respond to radiation and become apparent; de

novo formation of the lesion in response to radiation [10]. The de novo mechanisms might include a series of processes, such as vascular injury, proliferation of the vascular wall, necrosis, and ischemia due to narrowing of the lumen. Previous studies showed increased vascular endothelial growth factor after exposure to radiation in rats, supporting this hypothesis [18].

Patients with de novo CH can be treated with antiepileptic drugs and regular follow-up but are usually recommended to undergo surgery if possible in case the symptoms worsen or the size changes due to the risk of bleeding. In RIOH, which is regarded a sporadic form of de novo CM, surgical treatment is considered the standard treatment option following the treatment algorithm for de novo CM. However, if RIOH is considered a separate disease entity with different pathogenesis and clinical course than de novo CM, conservative treatment modalities could be considered in addition to invasive surgical treatments, which could cause neurological side effects. Therefore, several studies have been conducted to compare the pathogenesis of RIOH and de novo CH, and several notable results were reported. Compared with de novo CH, RIOH was found to develop at younger age, symptoms at the time of diagnosis were milder, and tended to be more multifocal. However, the prevalence of a hemorrhagic event, the most fatal complication, was not significantly different [11-13].

Considering the hematoma-like area and infiltration of foamy macrophage, RIOH appears more likely to be an inactive hemangioma-like lesion, which might be closer to a recanalized cavity hematoma induced by high-dose radiation than to vascular malformation [6]. Therefore, we suggest the use of the term RIOH rather than RICH.

In the present study, we hypothesized that RIOH would show clinical and histological differences depending on treatment type or primary pathology. Based on the treatment type, the GKS group showed shorter latency. In previous studies, several factors affecting the duration of the latency period have been reported, including radiation dose > 30 Gy and RT before 10 years of age [11,14,15,19], with increased risk of hemorrhagic event [9]. Hypothetically, the shorter latency observed in the GKS group might be due to its requirement of a higher dose in a smaller target area compared with conventional RT or focused damage that could accelerate tissue necrosis and tumorigenesis.

The present study had several limitations. First, the small sample size might have led to skewed statistical results. Second, although all available clinical, radiologic, and pathologic data were collected, some parameters might be inconsistent in retrospec-

tive analysis. Third, the subjects were older in the present study. As previously stated, RIOH occurs primarily in younger patients, however, in the present study, the mean age of the subjects was 46.6 years, which is an older age group compared with other reports (median 31.1 years [12]; mean age at the time of radiation 10.4 years with mean latency of 10.3 years [11]). Histopathological differences can exist in the RIOH of older subjects compared with younger subjects and could affect the results. However, only 37 patients were included in this study, most of whom were in their 30s or older, explaining why the results differ from those of previous studies. Further research with a larger cohort is needed to verify the results.

We hypothesized that the size of RIOH after conventional RT would be larger than after GKS because conventional RT is applied for larger lesions. However, the average size of the lesion tended to be larger in the GKS group, although the difference was not statistically significant. Furthermore, we hypothesized that the size difference between primary tumor and RIOH would be greater in the GKS group than in the RT group; however, significant difference was not observed. The repeated treatment applied in the same lesion, the error in the measurement of the radiological/pathological size, and the limitations of the present study described above might have affected these results.

In summary, RIOH after GKS tended to occur earlier and had thinner tumor wall than RIOH after conventional RT. The original pathology of RIOH had no effect on the histologic and clinical features of RIOH. These results suggest that the clinical course of RIOH differs based on type of treatment. Understanding the unique pathophysiology of RIOH, one of the most well-known complications of cerebral radiation, has become more important as the survival rate of brain tumor patients increases. Therefore, further investigation in the form of prospective studies with larger cohorts is required to elucidate more detailed clinical and histologic features of patients to provide appropriate medical management and predict the clinical course more accurately.

Ethics Statement

This retrospective study was approved by the Institutional Review Board of Severance Hospital (4-2020-0186), and patient informed consent was waived. All procedures were performed in accordance with the 1964 Declaration of Helsinki and its later amendments or comparable ethical standards.

Availability of Data and Material

All data generated or analyzed during the study are included in this published article (and its supplementary information files).

Code Availability

Not applicable.

ORCID

Myung Sun Kim <https://orcid.org/0000-0003-1521-2586>
 Se Hoon Kim <https://orcid.org/0000-0001-7516-7372>
 Jong-Hee Chang <https://orcid.org/0000-0003-1509-9800>
 Mina Park <https://orcid.org/0000-0002-2005-7560>
 Yoon Jin Cha <https://orcid.org/0000-0002-5967-4064>

Author Contributions

Conceptualization: YJC, SHK. Data curation and interpretation: MSK, YJC, MP, SHK. Supervision: SHK, JHC, YJC. Writing—original draft: MSK, YJC. Writing—review & editing: YJC, JHC, SHK. Approval of final manuscript: all authors.

Conflicts of Interest

S.H.K., a contributing editor of the *Journal of Pathology and Translational Medicine*, was not involved in the editorial evaluation or decision to publish this article. All remaining authors have declared no conflicts of interest.

Funding Statement

No funding to declare.

References

1. Heckl S, Aschoff A, Kunze S. Radiation-induced cavernous hemangiomas of the brain: a late effect predominantly in children. *Cancer* 2002; 94: 3285-91.
2. Park YS, Kim SH, Chang JH, Chang JW, Park YG. Radiosurgery for radiosurgery-induced cavernous malformation. *World Neurosurg* 2011; 75: 94-8.
3. Vinchon M, Leblond P, Caron S, Delestret I, Baroncini M, Coche B. Radiation-induced tumors in children irradiated for brain tumor: a longitudinal study. *Childs Nerv Syst* 2011; 27: 445-53.
4. Humpal T, Bruhl K, Bohl J, Schwarz M, Stoeter P, Gutjahr P. Cerebral haemorrhage in long-term survivors of childhood acute lymphoblastic leukaemia. *Eur J Pediatr* 1997; 156: 367-70.
5. Larson JJ, Ball WS, Bove KE, Crone KR, Tew JM, Jr. Formation of intracerebral cavernous malformations after radiation treatment for central nervous system neoplasia in children. *J Neurosurg* 1998; 88: 51-6.
6. Cha YJ, Nahm JH, Ko JE, et al. Pathological Evaluation of Radiation-Induced Vascular Lesions of the Brain: Distinct from De Novo Cavernous Hemangioma. *Yonsei Med J* 2015; 56: 1714-20.
7. Hegde AN, Mohan S, Lim CC. CNS cavernous haemangioma: “popcorn” in the brain and spinal cord. *Clin Radiol* 2012; 67: 380-8.
8. Mann P, Kleinschmidt-DeMasters BK. CNS Masson Tumors: Frequent Association With Therapeutic Radiation. *Am J Surg Pathol* 2016; 40: 81-93.
9. Koike T, Yanagimachi N, Ishiguro H, et al. High incidence of radiation-induced cavernous hemangioma in long-term survivors who underwent hematopoietic stem cell transplantation with radiation therapy during childhood or adolescence. *Biol Blood Marrow Transplant* 2012; 18: 1090-8.
10. Nimjee SM, Powers CJ, Bulsara KR. Review of the literature on de novo formation of cavernous malformations of the central nervous system after radiation therapy. *Neurosurg Focus* 2006; 21: e4.
11. Keezer MR, Del Maestro R. Radiation-induced cavernous hemangiomas: case report and literature review. *Can J Neurol Sci* 2009; 36: 303-10.
12. Cutsforth-Gregory JK, Lanzino G, Link MJ, Brown RD, Jr, Flemming KD. Characterization of radiation-induced cavernous malformations and comparison with a nonradiation cavernous malformation cohort. *J Neurosurg* 2015; 122: 1214-22.
13. Duhem R, Vinchon M, Leblond P, Soto-Ares G, Dhellemmes P. Cavernous malformations after cerebral irradiation during childhood: report of nine cases. *Childs Nerv Syst* 2005; 21: 922-5.
14. Furuse M, Miyatake SI, Kuroiwa T. Cavernous malformation after radiation therapy for astrocytoma in adult patients: report of 2 cases. *Acta Neurochir (Wien)* 2005; 147: 1097-101.
15. Mariniello G, De Liso M, Russo C, et al. Radiation-induced brain cavernomas in elderly: review of the literature and a rare case report. *Acta Biomed* 2019; 90: 77-83.
16. Sasagawa Y, Akai T, Itou S, Iizuka H. Gamma knife radiosurgery-induced cavernous hemangioma: case report. *Neurosurgery* 2009; 64: E1006-7.
17. Bejjani GK, Caputy AJ, Kurtzke RN, Duong DH, Sekhar LN. Remote hemorrhage of a pontine cavernous angioma fifty-two years after cerebral irradiation. *Acta Neurochir (Wien)* 1997; 139: 583-4.
18. Tsao MN, Li YQ, Lu G, Xu Y, Wong CS. Upregulation of vascular endothelial growth factor is associated with radiation-induced blood-spinal cord barrier breakdown. *J Neuropathol Exp Neurol* 1999; 58: 1051-60.
19. Strenger V, Sovinz P, Lackner H, et al. Intracerebral cavernous hemangioma after cranial irradiation in childhood. Incidence and risk factors. *Strahlenther Onkol* 2008; 184: 276-80.

Association of PTTG1 expression with invasiveness of non-functioning pituitary adenomas

Su Jung Kum, Hye Won Lee, Soon Gu Kim, Hyungsik Park, Ilseon Hwang, Sang Pyo Kim

Department of Pathology, Keimyung University Dongsan Medical Center, Daegu, Korea

Background: Pituitary tumor transforming gene 1 (PTTG1), paired-like homeodomain 2 (PITX2), and galectin-3 have been widely studied as predictive biomarkers for various tumors and are involved in tumorigenesis and tumor progression. We evaluated the usefulness of PTTG1, PITX2, and galectin-3 as predictive biomarkers for invasive non-functioning pituitary adenomas (NFPAs) by determining the relationship between the expressions of these three proteins and the invasiveness of the NFPAs. We also investigated whether PTTG1, E-cadherin, and Ki-67, which are known to be related to each other, show a correlation with NFPA features. **Methods:** A retrospective study was conducted on 87 patients with NFPAs who underwent surgical removal. The NFPAs were classified into three groups based on magnetic resonance imaging findings of suprasellar extension and cavernous sinus invasion. Immunohistochemical staining for PTTG1, PITX2, galectin-3, E-cadherin, and Ki-67 was performed on tissue microarrays. **Results:** PTTG1 expression showed a statistically significant correlation with the invasiveness of NFPAs, whereas PITX2 and galectin-3 did not have a relationship with the invasiveness of NFPAs. Moreover, there was no association among PTTG1, E-cadherin, and Ki-67 expression. **Conclusions:** PTTG1 has the potential to serve as a predictive biomarker for invasive NFPA. Furthermore, this study may serve as a reference for the development of PTTG1-targeted therapeutic agents.

Key Words: Non-functioning pituitary adenomas; Pituitary tumor transforming gene expression; Invasiveness

Received: July 30, 2021 **Revised:** August 25, 2021 **Accepted:** August 31, 2021

Corresponding Author: Sang Pyo Kim, MD, PhD, Department of Pathology, Keimyung University Dongsan Hospital, Keimyung University School of Medicine, 1095 Dalgubeol-daero, Dalseo-gu, Daegu 42601, Korea

Tel: +82-53-258-7398, Fax: +82-53-258-7382, E-mail: smkim5@kmu.ac.kr

Corresponding Author: Ilseon Hwang, MD, PhD, Department of Pathology, Keimyung University Dongsan Hospital, Keimyung University School of Medicine, 1095 Dalgubeol-daero, Dalseo-gu, Daegu 42601, Korea

Tel: +82-53-258-7396, Fax: +82-53-258-7382, E-mail: ilseon@dsmc.or.kr

Pituitary adenoma is a common neuroendocrine tumor that accounts for approximately 17% of all primary intracranial neoplasms [1]. While most of these tumors are benign, some show aggressive patterns such as invasion into surrounding structures. In contrast to the functioning pituitary adenomas, which are usually quickly detected due to symptoms of excess hormone secretion, the detection of a non-functioning pituitary adenoma (NFPA) is relatively delayed. As a result, NFPAs are usually found as macroadenomas (1–4 cm) or giant adenomas (> 4 cm) with suprasellar extension (SSE), which tend to invade into the cavernous sinus. The effectiveness of hormone control therapy for NFPA is limited, and surgical removal is the only effective treatment [2,3]. Based on these aspects, it is clinically important to identify prognostic markers of NFPAs.

In the 2004 World Health Organization (WHO) classification,

three subcategories were proposed for the classification of primary pituitary tumors: typical, atypical, and carcinoma [4]. Atypical pituitary adenoma was diagnosed based on histopathological features, including a high Ki-67 proliferation index (> 3%), p53 expression, and a high mitotic count. However, as the WHO classification was revised in 2017, the term “atypical pituitary adenoma” is no longer recommended based on studies reporting that this subtype does not reflect prognosis [5-7]. Instead, histological or radiological invasiveness status has emerged as an important factor for predicting prognosis, which was also introduced in the 2017 WHO classification [5,8]. In general, two factors are predominantly used to evaluate the invasiveness status of pituitary adenoma: SSE and cavernous sinus invasion (CSI). CSI is directly associated with prognosis [9]. On the other hand, there are many studies indicating that SSE alone lacks prognostic

value [10-12]. However, several grading systems combining SSE and CSI have shown significant prognostic value and are currently widely used [13].

Until the term “atypical pituitary adenoma” was accepted, p53 was generally used as a biomarker for aggressive pituitary adenoma [14]. However, as various studies asserting that p53 is not suitable as a prognostic marker have been published, there is now no biomarker of aggressive pituitary adenomas with proven validity [9,15,16]. Currently, only a few candidate proteins are being studied [17].

This study focused on the pituitary tumor transforming gene 1 (PTTG1), paired-like homeodomain 2 (PITX2), and galectin-3 proteins as predictive biological markers for invasive NFPAs. PTTG1 and PITX2 are not widely used markers, but it has been continually reported that these proteins are related to tumors and their aggressiveness in various organs. PTTG1 is an oncogene that participates in mitosis, DNA repair, angiogenesis, and cell proliferation [18-21]. PTTG1 is also known to induce tumor aggressiveness by being involved in epithelial-to-mesenchymal transition (EMT) and down-regulating E-cadherin expression [19,22,23]. PITX2, a member of the paired-like homeobox transcription factor family, regulates cell cycle regulators such as cyclin D1, cyclin D2, and c-Myc. Galectin-3 is a well-known prognostic and diagnostic marker in various organs that is involved in various biological processes, including cell growth, angiogenesis, cell adhesion, and tumor progression [24,25].

In this study, we aimed to determine the correlation between PTTG1, PITX2, and galectin-3 expression levels and to evaluate the various clinicopathologic characteristics of the NFPAs, including invasiveness status. Moreover, we evaluated the relationships among PTTG1, E-cadherin, and Ki-67 in NFPAs. This is the first study to investigate the biological significance of PTTG1, PITX2, and galectin-3 in Korean patients with NFPAs.

MATERIALS AND METHODS

Patients and tissue specimens

The archived specimens of 124 patients with NFPAs, obtained from 2000 to 2019 by surgical resection, including the transphenoidal approach, at Keimyung University Dongsan Hospital (Daegu, Korea), were analyzed in this study. A pathological diagnosis of the surgical specimens was made based on hematoxylin and eosin staining and immunohistochemical staining for six pituitary hormones (growth hormone, thyroid-stimulating hormone, prolactin, follicle-stimulating hormone, luteinizing hormone, and adrenocorticotrophic hormone). Clinical confirmation

that these adenomas did not exhibit excess hormone secretion was based on checking the patients' serum hormone levels and the absence of hormone-related symptoms. Cases showing positive immunohistochemical staining but not associated with clinical evidence of excess hormone secretion were diagnosed as NFPAs. Sufficient tissue for the construction of microarrays was available from 87 of the 124 cases. Clinical data, including age, sex, symptoms, recurrence, and survival status, were obtained via retrospective chart review.

Radiographic analysis

Tumor size and invasion status were evaluated using magnetic resonance imaging (MRI). Tumor size was recorded as the longest diameter. CSI was evaluated based on the criteria presented by Cottier et al. [26]. The samples were then classified into three groups: group I, neither SSE nor CSI; group II, only one of SSE or CSI; and group III, both SSE and CSI. We considered that a higher group level indicated a more aggressive tumor.

Construction of tissue microarrays

Four tissue microarray (TMA) blocks were constructed from archived, formalin-fixed paraffin blocks of the 87 samples with sufficient tumor cells. After checking the tumor cell-rich areas on the hematoxylin and eosin slides, a 3-mm-diameter core was collected from each sample and then arranged on premade recipient paraffin blocks (UB06-3, UNITMA, Seoul, Korea).

Immunohistochemistry

Sections (5 µm in thickness) were obtained from the four TMA blocks described above. Immunohistochemical staining for PTTG1, E-cadherin, Ki-67, PITX2, and galectin-3 was performed using an automated slide-processing system (Benchmark XT, Ventana Medical Systems, Tucson, AZ, USA). The cut sections were pretreated with Cell Conditioner 1 (CC1, #950-124, Ventana Medical Systems) for 40 minutes. The sections were then incubated with PTTG1 antibody (1:200, #34-1500, Thermo Fisher Scientific, Waltham, MA, USA), PITX2 antibody (1:50, #ab32832, Abcam, Cambridge, UK), galectin-3 antibody (1:200, #18-0393, Thermo Fisher Scientific), E-cadherin antibody (1:400, #M3612, Dako, Glostrup, Denmark), and Ki-67 antibody (1:200, #ab16667, Abcam) for 32 minutes each. The OptiView DAB Detection Kit (#760-700, Ventana Medical Systems) was used for chromogenic detection.

Protein expression was evaluated by scoring the intensity of each stain on a scale of 0 (negative), 1 (weak), 2 (moderate), and 3 (strong). Since the proportion of each stain was uniform in most

of the tumors, the expression level was determined only by the intensity of the stain. For Ki-67 staining, the stained cells were counted using a computer-assisted image analyzer (GenASIS HiPath, Applied Spectral Imaging Inc., Carlsbad, CA, USA).

Statistical analysis

The chi-squared test was used to determine the differences among expression groups of PTTG1, PITX2, galectin-3, and E-cadherin associated with clinical characteristics (e.g., SSE, CSI, sex, and recurrence). Linear-by-linear association was used to evaluate the correlation of the three invasiveness groups with PTTG1, PITX2, and galectin-3 expression levels. The independent t-test was used to analyze the relationships among the three candidate biomarkers and clinical factors including age, tumor size, and Ki-67 index. Analysis of variance was used to determine the differences between the three invasiveness groups associated with age and tumor size. An ordinal logistic regression model was used to compare the influences of individual factors, including PTTG1, PITX2, galectin-3, E-cadherin, Ki-67, age, sex, and tumor size, on NFPA invasiveness. All analyses were performed using IBM SPSS Statistics for Windows, ver. 25 (IBM Corp., Armonk, NY, USA). Statistical significance was set at $p < 0.05$.

RESULTS

Patient characteristics

The characteristics of the 87 patients with NFPA are shown in Table 1. The median age at diagnosis was 54 years (range, 16 to 83 years). Among these 87 patients, 48 (55.2%) were men and 39 (45.8%) were women. The mean tumor size (\pm standard

deviation [SD]) was 28.3 ± 12.5 mm, and there were two cases with missing tumor size data.

Overall, 77 patients (88.5%) showed SSE and 33 cases (37.9%) showed CSI on MRI (Table 1). Among the 87 patients, seven (8.0%) were in group I, 50 (57.5%) were in group II (SSE only, 47; CSI only, 3), and 30 (34.5%) were in group III (Fig. 1).

Thirty-five patients (40.2%) underwent post-operative radiotherapy. During each follow-up period (mean, 66 months; range, 0.5 to 209 months), tumor recurrences were observed in

Table 1. Clinical characteristics of patients with non-functioning pituitary adenomas

Clinical characteristic	No. (%)
Age (yr)	
Median (range)	54 (16–83)
Sex	
Male	48 (55.2)
Female	39 (44.8)
Tumor size (mm) ^a	
Mean \pm SD	28.3 \pm 12.5
Postoperative radiotherapy	
Yes	35 (40.2)
No	52 (59.8)
Recurrence	
Present	16 (18.4)
Absent	71 (81.6)
Suprasellar extension	
Present	77 (88.5)
Absent	10 (11.5)
Cavernous sinus invasion	
Present	33 (37.9)
Absent	54 (62.1)

SD, standard deviation.

^aUnknown tumor size in two cases.

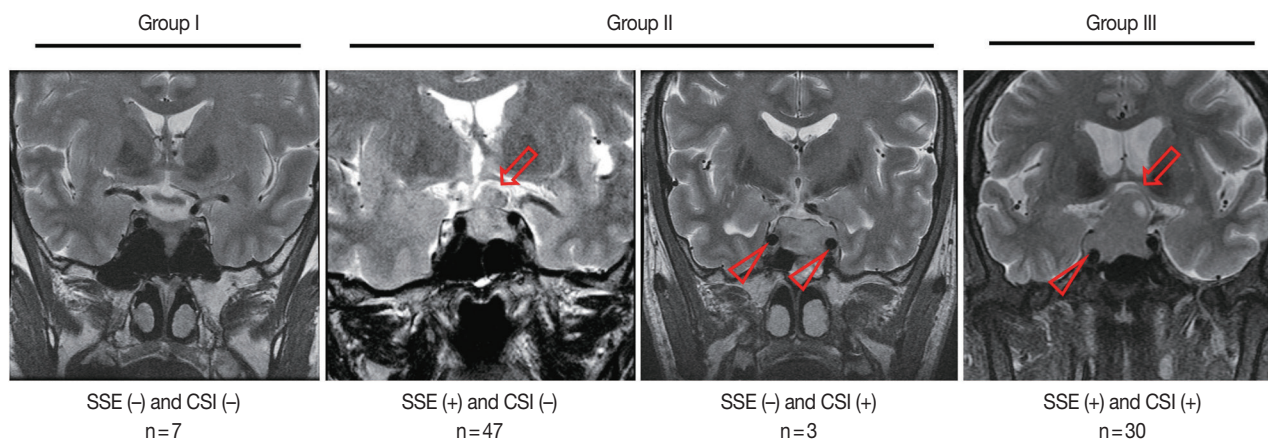


Fig. 1. Invasiveness groups of non-functioning pituitary adenoma (NFPA) based on suprasellar extension (SSE) and cavernous sinus invasion (CSI) on magnetic resonance imaging (MRI). The representative MRI images of SSE (arrows) and CSI (arrowheads) are shown. NFPAs were classified into three groups based on the MRI findings: group I, neither SSE nor CSI; group II, only one of SSE or CSI; group III, both SSE and CSI.

16 patients (18.4%), and non-disease-related death was observed in one patient. Disease-related death was not observed.

Expression levels of PTTG1, PITX2, and galectin-3 and their relationship with invasiveness of NFPA

The individual staining patterns and scores of PTTG1, PITX2, and galectin-3 are shown in Fig. 2. Staining of PTTG1 was observed in a cytoplasmic and paranuclear pattern. In PTTG1 staining, a score of 0 was considered no expression, scores of 1 and 2 were considered low expression, and a score of 3 was considered high expression. Staining of PITX2 and galectin-3

showed both nuclear and cytoplasmic patterns. In PITX2 and galectin-3 staining, a score of 0 was considered no expression, a score of 1 was considered low expression, and scores of 2 and 3 were considered high expression. Expression levels of PITX2 and galectin-3 were applied differently from PTTG1 because there were too few cases with scores of 3 in PITX2 and galectin-3 staining, making it difficult to calculate the appropriate statistics. Ten (11.5%) specimens were negative for PTTG1, and 52 (59.8%) and 25 (28.7%) specimens showed low and high PTTG1 expression, respectively. In PITX2 staining, 21 (24.1%) of the specimens showed no expression, 30 (34.5%) showed low

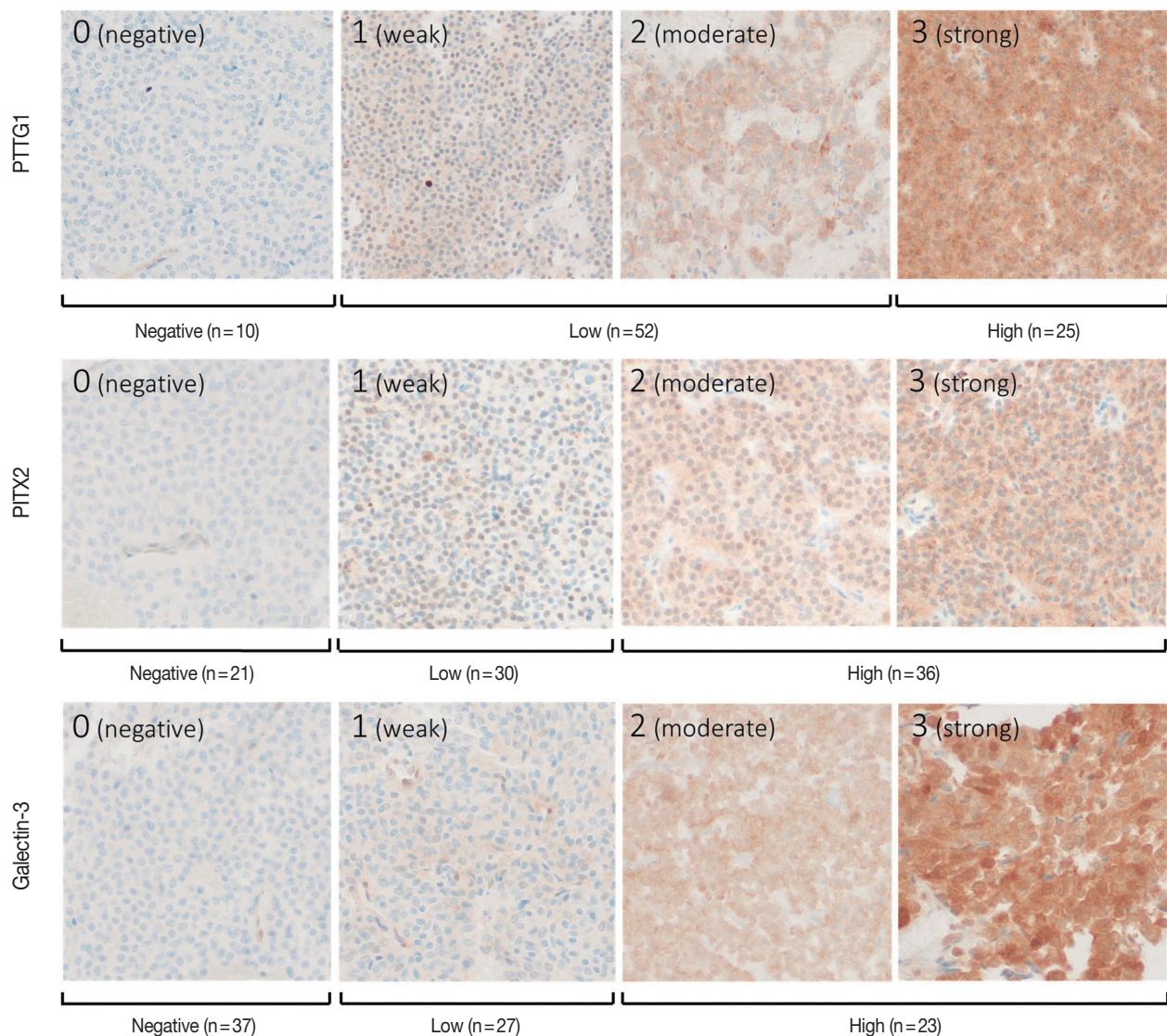


Fig. 2. Scoring of immunohistochemical staining for pituitary tumor transforming gene (PTTG1), paired-like homeodomain 2 (PITX2), and galectin-3. The intensity of immunohistochemical stains was scored from 0 (negative) to 3 (strong). PTTG1: a score of 0 was regarded as negative, scores of 1 and 2 were regarded as low, and a score of 3 was regarded as high expression. PITX2 and galectin-3: a score of 0 was regarded as negative, a score of 1 was regarded as low, and scores of 2 and 3 were regarded as high expression.

expression, and 36 (41.4%) showed high expression. In galectin-3 staining, 37 (42.5%) specimens showed no expression, 27 (31.0%) showed low expression, and 23 (26.4%) showed high expression.

PTTG1 expression was significantly correlated with NFPA invasiveness. In the high PTTG1 expression group, SSE or CSI was observed more frequently than in the negative or low PTTG1 expression group ($p = .033$) (Table 2). Similarly, the higher invasiveness group showed higher PTTG1 expression, and the lower invasiveness group showed lower PTTG1 expression ($p = .003$) (Table 3, Fig. 3). There was no association between PITX2 or galectin-3 expression and invasiveness (Table 3). As described above, expression levels of PITX2 and galectin-3 were applied differently from PTTG1 because the number of cases with scores of 3 in PITX2 and galectin-3 was too few (score 1, low expression; scores 2 and 3, high expression). Nevertheless, even when the expression levels of PITX2 and galectin-3 were classified in the same way as PTTG1 expression (scores 1 and 2, low expression; score 3, high expression), there was no statistically signifi-

cant correlation between PITX2 and galectin-3 expression and NFPA invasiveness ($p = .271$ for PITX2, $p = .997$ for galectin-3).

PTTG1, PITX2, and galectin-3 did not show any relationship with other clinical characteristics, such as age, sex, tumor size, and recurrence. Even in the group without post-operative radiotherapy, there was no correlation between PTTG1 expression and recurrence (Table 2).

Relationships of E-cadherin loss and Ki-67 index with PTTG1 expression

The individual staining patterns of E-cadherin and Ki-67 are shown in Fig. 4. The E-cadherin stained in a membranous pattern. A score of 0 was considered negative, and scores of 1 to 3 were considered positive for E-cadherin staining. Forty-eight (55.2%) of the specimens were negative, and 39 (44.8%) showed positive E-cadherin expression. In the high PTTG1 expression group, 11 (44.0%) showed negative E-cadherin expression. In the negative or low PTTG1 expression group, 37 (59.7%) showed negative E-cadherin expression (Table 2). There was no significant correlation between the expression of E-cadherin and PTTG1.

Table 2. Clinicopathologic characteristics according to PTTG1 expression

Variable	Negative or low PTTG1 (n=62)	High PTTG1 (n=25)	p-value
Age (yr)			.656
Median (range)	53 (31–83)	55 (16–83)	
Sex			.183
Male	37 (59.7)	11 (44.0)	
Female	25 (40.3)	14 (56.0)	
Invasiveness status			.033 ^a
Suprasellar extension			
Present	52 (83.9)	25 (100)	
Absent	10 (16.1)	0	
Cavernous sinus invasion			.027 ^a
Present	19 (30.6)	14 (56.0)	
Absent	43 (69.4)	11 (44.0)	
Tumor size (mm) ^b			.612
Mean ± SD	29.0 ± 13.5	26.5 ± 9.2	
Recurrence			.329
Present	13 (21.0)	3 (12.0)	
Absent	49 (79.0)	22 (88.0)	
Present (N-PRT)	11 (28.9)	0 (0.0)	.103
Absent (N-PRT)	27 (71.1)	14 (100.0)	
E-cadherin			.183
Positive (score 1–3)	25 (40.3)	14 (56.0)	
Negative (score 0)	37 (59.7)	11 (44.0)	
Ki-67 index (%)			.389
Mean ± SD	1.3 ± 1.1	1.8 ± 2.5	

Values are presented as number (%) unless otherwise indicated. PTTG1, pituitary tumor transforming gene 1; SD, standard deviation; N-PRT, no post-operative radiotherapy. ^aStatistically significant ($p < .05$); ^bUnknown tumor size in two cases with low PTTG1 expression.

Table 3. Clinicopathologic characteristics according to tumor invasiveness group

Variable	Tumor invasion group			p-value
	I (n=7)	II (n=50)	III (n=30)	
Age (yr)				.605
Median (range)	50 (42–71)	55 (16–83)	54.5 (31–83)	
Sex (%)				.790
Male	3 (42.9)	28 (56.0)	17 (56.7)	
Female	4 (57.1)	22 (44.0)	13 (43.3)	
Tumor size (mm) ^a				< .001 ^b
Mean ± SD	17.2 ± 5.1	25.9 ± 9.2	35.3 ± 15.0	
PTTG1 (%)				.013 ^b
High	0	11 (22.0)	14 (46.7)	
Negative or low	7 (100)	39 (78.0)	16 (53.3)	
PITX2 (%)				.745
High	3 (42.9)	19 (38.0)	14 (46.7)	
Low or negative	4 (57.1)	31 (62.0)	16 (53.3)	
Galectin-3 (%)				.605
High	1 (14.3)	15 (30.0)	7 (23.3)	
Low or negative	6 (85.7)	35 (70.0)	23 (76.7)	
E-cadherin (%)				.989
Positive	3 (42.9)	23 (46.0)	13 (43.3)	
Negative	4 (57.1)	27 (54.0)	17 (56.7)	
Ki-67 index (%)				.681
Mean ± SD	1.5 ± 0.8	1.6 ± 2.0	1.2 ± 1.1	

Values are presented as number (%) unless otherwise indicated. SD, standard deviation; PTTG1, pituitary tumor transforming gene 1; PITX2, paired-like homeodomain 2. ^aUnknown tumor size in two cases in group III; ^bStatistically significant ($p < .05$).

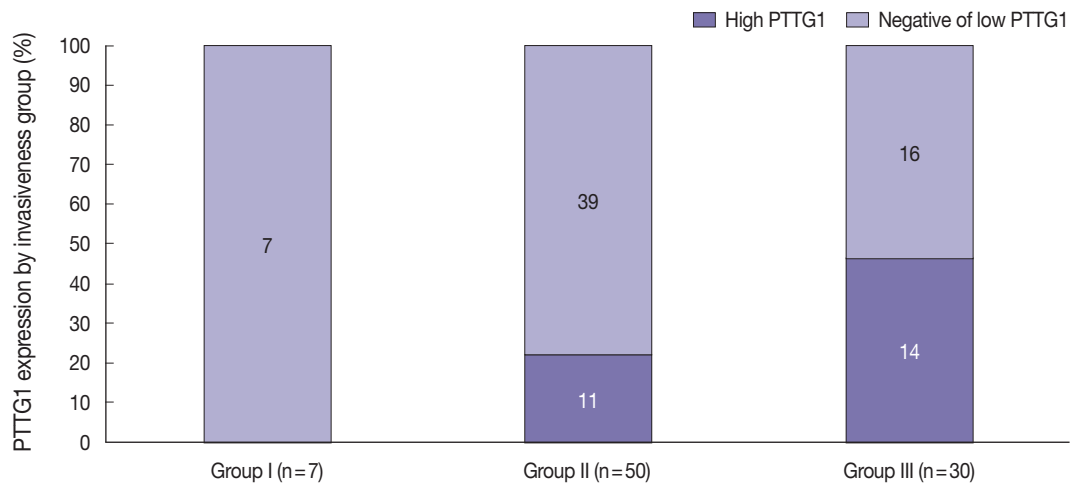


Fig. 3. Stacked column chart showing the ratio of pituitary tumor transforming gene (PTTG1) expression in each invasiveness group. As the level of invasiveness increased, the proportion of high PTTG1 expression tended to increase.

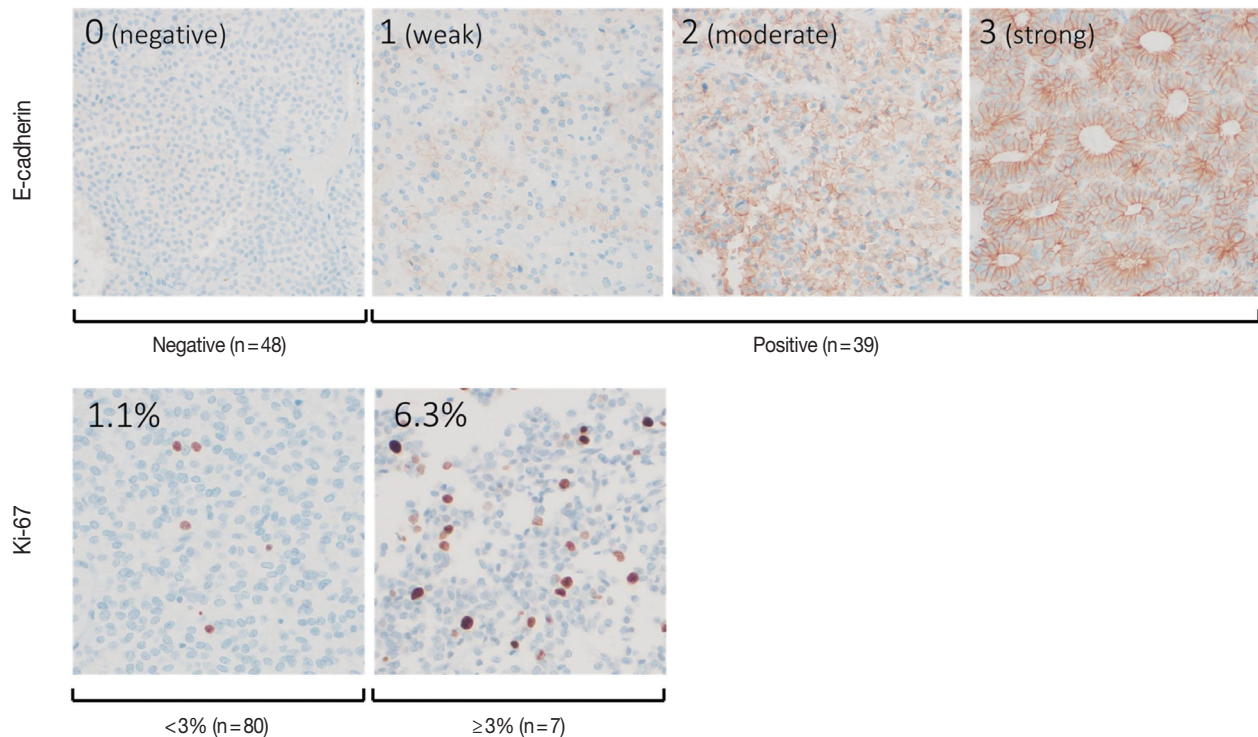


Fig. 4. Scoring of immunohistochemical staining for E-cadherin and Ki-67. E-cadherin: a score of 0 was regarded as negative, and scores of 1 to 3 were regarded as positive expression. Ki-67 index was measured by image analyzer, and two samples of the stain are shown.

The Ki-67 staining showed nuclear staining, and the overall average index (\pm SD) was $1.4\% \pm 1.4\%$. The average Ki-67 index in the high PTTG1 expression group was $1.8\% \pm 2.5\%$, which was higher than that observed in the negative or low PTTG1 expression group ($1.3\% \pm 1.1\%$) (Table 2). Ki-67 expression tended to be associated with PTTG1 expression; however, this result was not statistically significant ($p = .389$).

Other clinical factors associated with aggressive features of NFPA

The tumor invasiveness was significantly correlated with the tumor size: the higher the level of the invasion group, the larger the tumor size ($p < .001$) (Table 3, Fig. 5A). In addition, tumor size was associated with the recurrence of NFPA (Fig. 5B). As the size of the tumor increased, the NFPA tended to recur. How-

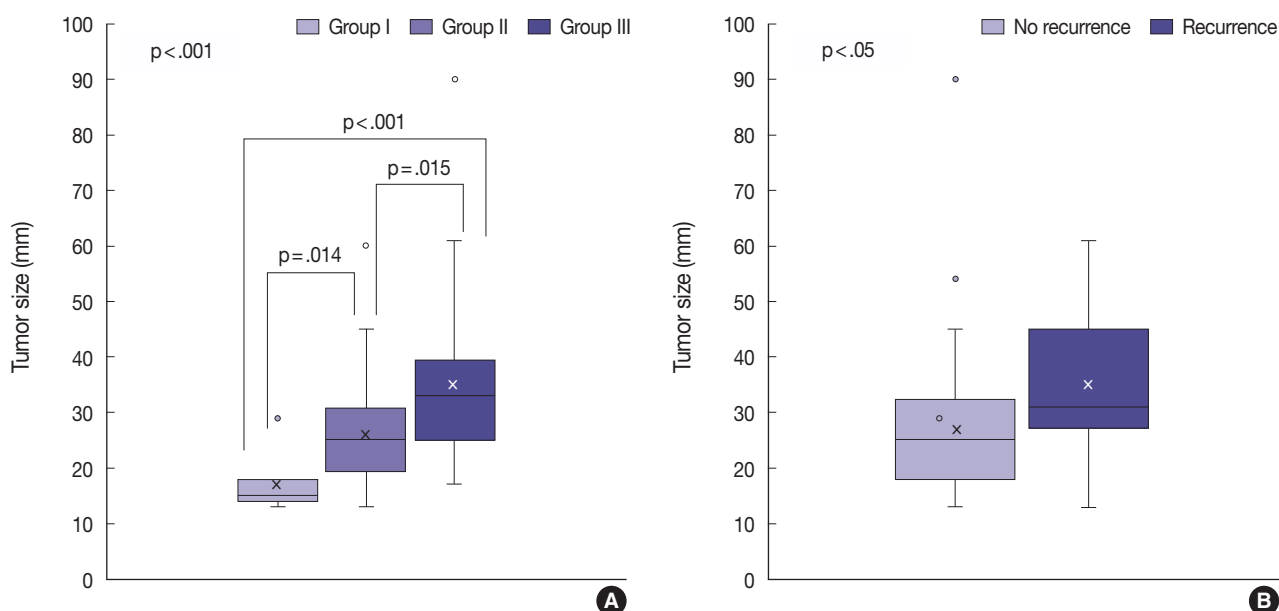


Fig. 5. Box plots of the distribution of the tumor size by invasion group and recurrence. A larger tumor size was associated with higher invasiveness (A) and a higher recurrence rate (B).

Table 4. Multivariate analysis (ordinal logistic regression test) of invasiveness groups associated with clinicopathologic variables

Variable	Estimate	p-value	95% Confidence interval
Age	0.030	.180	-0.014 to 0.074
Sex	-0.085	.876	-1.152 to 0.983
Tumor size	0.13	< .001 ^a	0.069 to 0.191
PTTG1	2.518	.001 ^a	1.086 to 3.950
PITX2	-0.320	.391	-1.052 to 0.411
Galectin-3	0.195	.575	-0.485 to 0.875
E-cadherin	0.482	.498	-0.914 to 1.879
Ki-67 index	0.347	.696	-1.398 to 2.093

PTTG1, pituitary tumor transforming gene 1; PITX2, paired-like homeodomain 2.

^aStatistically significant ($p < .05$).

ever, post-operative radiotherapy was not considered in this study.

Multivariate analysis of NFPA invasiveness

Multivariate analysis using ordinal logistic regression showed that PTTG1 expression and tumor size were statistically associated with tumor invasiveness levels ($p = .001$ for PTTG1, $p < .001$ for tumor size) (Table 4). The other variables including PITX2, galectin-3, E-cadherin, Ki-67, age, and sex did not show any relationships with the tumor invasiveness groups. In addition, the PTTG1 expression and the tumor size were statistically independent of each other and of other variables including PITX2, galectin-3, E-cadherin, Ki-67, age, and sex (Table 4).

DISCUSSION

Although several studies have shown PTTG1 overexpression in pituitary adenomas and in tumors of other organs, a limited number of studies have investigated the relationship between PTTG1 expression and tumor invasiveness [18,27,28]. A meta-analysis of these studies concluded that there was a significant relationship between PTTG1 expression and the invasiveness of pituitary adenomas [29]. However, most of these studies were limited to a specific subtype of functioning pituitary adenomas or did not distinguish functioning adenomas from non-functioning adenomas.

In this study, we performed an analysis limited to NFPA, and demonstrated that PTTG1 expression was significantly correlated with the invasiveness of NFPA. Only a few previous studies have explored PTTG1 expression and invasiveness status limited to NFPA [18,27,30]. A study by Trott et al. [30] revealed that PTTG1 expression and the invasiveness status of NFPA had an important correlation. Additionally, research by McCabe et al. [18] revealed PTTG1 overexpression in both invasive NFPA and invasive functioning pituitary adenomas. The results of the present study support these two previous studies. In contrast, a previous study conducted by Zhang et al. [27] did not identify a correlation between PTTG1 expression and invasiveness in NFPA but did reveal the correlation in functioning pituitary adenomas. However, the number of the NFPA samples in the study by Zhang et al. [27] was 30, which was smaller than those

included in the studies that confirmed the significant correlation between PTTG1 and NFPA invasiveness, including our study; the numbers of NFPA samples were 56 for the study by Trott et al. [30], 92 for the study by McCabe et al. [18], and 87 for the present study. It is therefore reasonable to assume that PTTG1 expression is correlated with NFPA invasiveness, as it is in other organ tumors.

Several studies revealed a correlation between PTTG1 expression and the recurrence of pituitary adenomas [30-32]. One of these studies by Fillippella et al. [31] did not report the factor of postoperative radiotherapy. Additionally, other studies by Trott et al. [30] and Noh et al. [32] excluded the patients who underwent postoperative radiotherapy. The present study did not reveal a correlation between PTTG1 expression and recurrence of the tumor. We also analyzed PTTG1 expression and recurrence in a group of patients who did not undergo post-operative radiotherapy, but no meaningful results were obtained, contrary to the results of previous studies.

A few studies have demonstrated that PITX2 expression is increased in pituitary adenomas, highlighting a correlation between PITX2 overexpression and the aggressiveness of NFPA [33,34]. In comparison, however, the results of the present study did not show a relationship between PITX2 expression and NFPA invasiveness. These contradictory results are probably due to the small number of cases in our study. However, since few studies have been conducted on this subject to date, more data should be acquired to establish the relationship between PITX2 expression and NFPA invasiveness.

In pituitary adenoma, galectin-3 expression is increased in functioning pituitary adenomas, especially in functioning corticotroph adenomas, but not in NFPA [35,36]. In addition, there have been several studies on galectin-3 and the aggressive behavior of pituitary adenoma, which demonstrated that galectin-3 expression is positively correlated with the aggressiveness of pituitary adenomas, but not in NFPA [36,37]. In the present study with only NFPA, the intensity of galectin-3 staining was varied, and there was no correlation with the invasiveness of NFPA. Although we noted a high intensity of galectin-3 staining in our study, the validity of this result should be reassessed because we did not compare the intensity in NFPA with that in functioning adenomas.

As PTTG1 was the only protein that showed an association with the invasiveness of NFPA in this study, further investigation was performed on the relationship among PTTG1, E-cadherin, and Ki-67. Based on the previous studies, which showed an association between PTTG1 and E-cadherin loss in the process

of EMT in other organs (e.g., head and neck, esophagus, ovary, and breast), we hypothesized that E-cadherin is correlated with PTTG1 expression in NFPA; this is the first study on PTTG1 and E-cadherin in pituitary adenoma [19,22,23]. However, we could not identify the relationship between PTTG1 expression and E-cadherin loss in NFPA. This may be due to the small number of cases, but it may also be the result of PTTG1 not being the main causative factor for E-cadherin loss. There are several epigenetic mechanisms that induce E-cadherin loss other than PTTG1, including some microRNAs (e.g., miR-192, miR-200, and miR-205) and the hypermethylation of *CDH1* promoter, a gene encoding E-cadherin [38,39]. The results of our study suggest that the factors such as the microRNAs and the hypermethylation of *CDH1* promoter may play a greater role than PTTG1 in inducing E-cadherin loss in pituitary adenomas.

There have been previous studies on PTTG1 expression and cell proliferation, but the results are conflicting [40-43]. Studies by Heaney et al. [40] and Wang et al. [41] revealed that PTTG1 promoted cell proliferation. However, studies by Mu et al. [42] and Yu et al. [43] revealed that there was no correlation between PTTG1 and cell proliferation, which is consistent with the results of the present study. In terms of its ability to inhibit chromatid separation during mitosis, PTTG1 is expected to inhibit cell proliferation, but its ability to induce angiogenesis or disrupt the DNA repair system may promote cell proliferation. As there are contradictory views in many studies, the relationship between PTTG1 expression and cell proliferation needs to be further studied.

Additionally, we determined that the invasiveness status and recurrence of NFPA were significantly correlated with tumor size. According to many studies, pituitary adenomas show aggressive behavior as the size of the tumor increases, which is consistent with the results of our study [44]. However, with respect to tumor recurrence, previous studies have shown that tumor recurrence is not influenced by tumor size, which contradicts the results of the present study [45]. Although the results of our study revealed a correlation between tumor size and recurrence, it should be noted that the factor of post-operative radiotherapy was not considered.

In conclusion, we demonstrated here that PTTG1 has the potential to be a predictive marker for the invasiveness of NFPA. Although there are many previous studies that have explored the relationship between PTTG1 expression and tumors including pituitary adenoma, in the present study, we elucidated the role of PTTG1, particularly in NFPA, for the first time. Furthermore, we provide evidence for the development of PTTG1-tar-

geted agents and references for studies on the correlation between PTTG1 and various tumors, which have been continually reported.

Ethics Statement

This study was approved by the Institutional Review Board of the Keimyung University Dongsan Medical Center, with waiver of informed consent (DSMC 2021-02-036).

Availability of Data and Material

The datasets generated or analyzed during the study are available from the corresponding author on reasonable request.

Code Availability

Not applicable.

ORCID

Su Jung Kum <https://orcid.org/0000-0003-4871-3707>
 Hye Won Lee <https://orcid.org/0000-0001-8540-524X>
 Soon Gu Kim <https://orcid.org/0000-0002-1436-8442>
 Hyungsik Park <https://orcid.org/0000-0001-5476-3853>
 Ilseon Hwang <https://orcid.org/0000-0002-6122-4417>
 Sang Pyo Kim <https://orcid.org/0000-0003-0948-2408>

Author Contributions

Conceptualization: SPK. Data curation: SJK, IH. Formal analysis: IH, SGK, SJK. Investigation: SJK, HP. Methodology: SPK, SJK. Resources: HWL. Supervision: SPK, IH. Visualization: SJK, IH. Writing—original draft: SJK, IH. Writing—review & editing: SJK, SPK, IH, HWL. Approval of final manuscript: all authors.

Conflicts of Interest

The authors declare that they have no potential conflicts of interest.

Funding Statement

This work was supported by the research promoting grant from the Institute for Cancer Research Keimyung University Dongsan Medical Center in 2018.

References

- Gadella MR, Trivellini G, Hernandez Ramirez LC, Korbonits M. Genetics of pituitary adenomas. *Front Horm Res* 2013; 41: 111-40.
- Greenman Y, Cooper O, Yaish I, et al. Treatment of clinically non-functioning pituitary adenomas with dopamine agonists. *Eur J Endocrinol* 2016; 175: 63-72.
- Greenman Y, Tordjman K, Osher E, et al. Postoperative treatment of clinically nonfunctioning pituitary adenomas with dopamine agonists decreases tumour remnant growth. *Clin Endocrinol (Oxf)* 2005; 63: 39-44.
- DeLellis RA, Lloyd RV, Heitz PU, Eng C. World Health Organization classification of tumours: pathology and genetics of tumours of endocrine organs. Lyons: IARC Press, 2004.
- Lloyd RV, Osamura RY, Kloppel G, Rosai J. WHO classification of tumours of endocrine organs. Lyons: IARC Press, 2012; 11-3.
- Saeger W, Ludecke DK, Buchfelder M, Fahlbusch R, Quabbe HJ, Petersenn S. Pathohistological classification of pituitary tumors: 10 years of experience with the German Pituitary Tumor Registry. *Eur J Endocrinol* 2007; 156: 203-16.
- Zada G, Woodmansee WW, Ramkissoon S, Amadio J, Nose V, Laws ER Jr. Atypical pituitary adenomas: incidence, clinical characteristics, and implications. *J Neurosurg* 2011; 114: 336-44.
- Scoazec JY, Couvelard A, Reseau T. Classification of pancreatic neuroendocrine tumours: changes made in the 2017 WHO classification of tumours of endocrine organs and perspectives for the future. *Ann Pathol* 2017; 37: 444-56.
- Trouillas J, Roy P, Sturm N, et al. A new prognostic clinicopathological classification of pituitary adenomas: a multicentric case-control study of 410 patients with 8 years post-operative follow-up. *Acta Neuropathol* 2013; 126: 123-35.
- Matsuyama J. Ki-67 expression for predicting progression of postoperative residual pituitary adenomas: correlations with clinical variables. *Neurol Med Chir (Tokyo)* 2012; 52: 563-9.
- Chiloiro S, Doglietto F, Trapasso B, et al. Typical and atypical pituitary adenomas: a single-center analysis of outcome and prognosis. *Neuroendocrinology* 2015; 101: 143-50.
- Kim JS, Lee YS, Jung MJ, Hong YK. The predictive value of pathologic features in pituitary adenoma and correlation with pituitary adenoma recurrence. *J Pathol Transl Med* 2016; 50: 419-25.
- Mooney MA, Hardesty DA, Sheehy JP, et al. Rater reliability of the hardy classification for pituitary adenomas in the magnetic resonance imaging era. *J Neurol Surg B Skull Base* 2017; 78: 413-8.
- Thapar K, Scheithauer BW, Kovacs K, Pernicone PJ, Laws ER Jr. p53 expression in pituitary adenomas and carcinomas: correlation with invasiveness and tumor growth fractions. *Neurosurgery* 1996; 38: 765-70.
- Oliveira MC, Marroni CP, Pizarro CB, Pereira-Lima JF, Barbosa-Coutinho LM, Ferreira NP. Expression of p53 protein in pituitary adenomas. *Braz J Med Biol Res* 2002; 35: 561-5.
- Salehi F, Agur A, Scheithauer BW, Kovacs K, Lloyd RV, Cusimano M. Biomarkers of pituitary neoplasms: a review (Part II). *Neurosurgery* 2010; 67: 1790-8.
- Sav A, Rotondo F, Syro LV, Scheithauer BW, Kovacs K. Biomarkers of pituitary neoplasms. *Anticancer Res* 2012; 32: 4639-54.
- McCabe CJ, Khaira JS, Boelaert K, et al. Expression of pituitary tumour transforming gene (PTTG) and fibroblast growth factor-2 (FGF-2) in human pituitary adenomas: relationships to clinical tumour behaviour. *Clin Endocrinol (Oxf)* 2003; 58: 141-50.
- Shah PP, Kakar SS. Pituitary tumor transforming gene induces epithelial to mesenchymal transition by regulation of Twist, Snail, Slug, and E-cadherin. *Cancer Lett* 2011; 311: 66-76.
- Zou H, McGarry TJ, Bernal T, Kirschner MW. Identification of a vertebrate sister-chromatid separation inhibitor involved in transformation and tumorigenesis. *Science* 1999; 285: 418-22.
- Salehi F, Kovacs K, Scheithauer BW, Lloyd RV, Cusimano M. Pituitary tumor-transforming gene in endocrine and other neoplasms: a review and update. *Endocr Relat Cancer* 2008; 15: 721-43.
- Feng W, Xiaoyan X, Shenglei L, Hongtao L, Guozhong J. PTTG1 cooperated with GLI1 leads to epithelial-mesenchymal transition in esophageal squamous cell cancer. *Oncotarget* 2017; 8: 92388-400.
- Yoon CH, Kim MJ, Lee H, et al. PTTG1 oncogene promotes tumor malignancy via epithelial to mesenchymal transition and expansion of cancer stem cell population. *J Biol Chem* 2012; 287: 19516-27.
- Nangia-Makker P, Honjo Y, Sarvis R, et al. Galectin-3 induces endothelial cell morphogenesis and angiogenesis. *Am J Pathol* 2000; 156: 899-909.

25. Yoshii T, Fukumori T, Honjo Y, Inohara H, Kim HR, Raz A. Galectin-3 phosphorylation is required for its anti-apoptotic function and cell cycle arrest. *J Biol Chem* 2002; 277: 6852-7.
26. Cottier JP, Destrieux C, Brunereau L, et al. Cavernous sinus invasion by pituitary adenoma: MR imaging. *Radiology* 2000; 215: 463-9.
27. Zhang X, Horwitz GA, Heaney AP, et al. Pituitary tumor transforming gene (PTTG) expression in pituitary adenomas. *J Clin Endocrinol Metab* 1999; 84: 761-7.
28. Raverot G, Wierinckx A, Dantony E, et al. Prognostic factors in prolactin pituitary tumors: clinical, histological, and molecular data from a series of 94 patients with a long postoperative follow-up. *J Clin Endocrinol Metab* 2010; 95: 1708-16.
29. Li Y, Zhou LP, Ma P, et al. Relationship of PTTG expression with tumor invasiveness and microvessel density of pituitary adenomas: a meta-analysis. *Genet Test Mol Biomarkers* 2014; 18: 279-85.
30. Trott G, Ongaratti BR, de Oliveira Silva CB, et al. PTTG overexpression in non-functioning pituitary adenomas: Correlation with invasiveness, female gender and younger age. *Ann Diagn Pathol* 2019; 41: 83-9.
31. Filippella M, Galland F, Kujas M, et al. Pituitary tumour transforming gene (PTTG) expression correlates with the proliferative activity and recurrence status of pituitary adenomas: a clinical and immunohistochemical study. *Clin Endocrinol (Oxf)* 2006; 65: 536-43.
32. Noh TW, Jeong HJ, Lee MK, Kim TS, Kim SH, Lee EJ. Predicting recurrence of nonfunctioning pituitary adenomas. *J Clin Endocrinol Metab* 2009; 94: 4406-13.
33. Tamura R, Ohara K, Morimoto Y, et al. PITX2 expression in non-functional pituitary neuroendocrine tumor with cavernous sinus invasion. *Endocr Pathol* 2019; 30: 81-9.
34. Acunzo J, Roche C, Defilles C, et al. Inactivation of PITX2 transcription factor induced apoptosis of gonadotroph tumoral cells. *Endocrinology* 2011; 152: 3884-92.
35. Jin L, Riss D, Ruebel K, et al. Galectin-3 expression in functioning and silent ACTH-producing adenomas. *Endocr Pathol* 2005; 16: 107-14.
36. Zhang Y, He N, Zhou J, Chen Y. The relationship between MRI invasive features and expression of EMMPRIN, galectin-3, and microvessel density in pituitary adenoma. *Clin Imaging* 2011; 35: 165-73.
37. Righi A, Morandi L, Leonardi E, et al. Galectin-3 expression in pituitary adenomas as a marker of aggressive behavior. *Hum Pathol* 2013; 44: 2400-9.
38. Qian ZR, Sano T, Yoshimoto K, et al. Tumor-specific downregulation and methylation of the CDH13 (H-cadherin) and CDH1 (E-cadherin) genes correlate with aggressiveness of human pituitary adenomas. *Mod Pathol* 2007; 20: 1269-77.
39. Wong TS, Gao W, Chan JY. Interactions between E-cadherin and microRNA deregulation in head and neck cancers: the potential interplay. *Biomed Res Int* 2014; 2014: 126038.
40. Heaney AP, Horwitz GA, Wang Z, Singson R, Melmed S. Early involvement of estrogen-induced pituitary tumor transforming gene and fibroblast growth factor expression in prolactinoma pathogenesis. *Nat Med* 1999; 5: 1317-21.
41. Wang Z, Moro E, Kovacs K, Yu R, Melmed S. Pituitary tumor transforming gene-null male mice exhibit impaired pancreatic beta cell proliferation and diabetes. *Proc Natl Acad Sci U S A* 2003; 100: 3428-32.
42. Mu YM, Oba K, Yanase T, et al. Human pituitary tumor transforming gene (hPTTG) inhibits human lung cancer A549 cell growth through activation of p21(WAF1/CIP1). *Endocr J* 2003; 50: 771-81.
43. Yu R, Cruz-Soto M, Li Calzi S, Hui H, Melmed S. Murine pituitary tumor-transforming gene functions as a securin protein in insulin-secreting cells. *J Endocrinol* 2006; 191: 45-53.
44. Dekkers OM, Karavitaki N, Pereira AM. The epidemiology of aggressive pituitary tumors (and its challenges). *Rev Endocr Metab Disord* 2020; 21: 209-12.
45. Roelfsema F, Biermasz NR, Pereira AM. Clinical factors involved in the recurrence of pituitary adenomas after surgical remission: a structured review and meta-analysis. *Pituitary* 2012; 15: 71-83.

Clinicopathologic implication of PD-L1 gene alteration in primary adrenal diffuse large B cell lymphoma

Ki Rim Lee^{1,2}, Jiwon Koh^{2,3}, Yoon Kyung Jeon^{2,3}, Hyun Jung Kwon^{1,2}, Jeong-Ok Lee^{4,5}, Jin Ho Paik^{1,2}

¹Department of Pathology, Seoul National University Bundang Hospital, Seongnam;

²Department of Pathology, Seoul National University College of Medicine, Seoul;

³Department of Pathology, Seoul National University Hospital, Seoul;

⁴Department of Internal Medicine, Seoul National University Bundang Hospital, Seongnam;

⁵Department of Internal Medicine, Seoul National University College of Medicine, Seoul, Korea

Background: Primary adrenal (PA) diffuse large B cell lymphoma (DLBCL) was previously reported as an aggressive subset of DLBCL, but its genetic features were not sufficiently characterized. From our previous study of DLBCL with programmed death-ligand 1 (PD-L1) gene alterations, we focused on PD-L1 gene alterations in PA-DLBCL with clinicopathologic implications. **Methods:** We performed fluorescence in situ hybridization for PD-L1 gene translocation and amplification in PA-DLBCL (n=18) and comparatively analyzed clinicopathologic characteristics with systemic non-adrenal (NA)-DLBCL (n=90). **Results:** PA-DLBCL harbored distinctive features (vs. NA-DLBCL), including high international prognostic index score (3–5) (72% [13/18] vs. 38% [34/90], p=.007), poor Eastern Cooperative Oncology Group performance score (≥2) (47% [7/15] vs. 11% [10/90], p=.003), elevated serum lactate dehydrogenase (LDH) (78% [14/18] vs. 51% [44/87], p=.035) and MUM1 expression (87% [13/15] vs. 60% [54/90], p=.047). Moreover, PA-DLBCL showed frequent PD-L1 gene alterations (vs. NA-DLBCL) (39% [7/18] vs. 6% [5/86], p=.001), including translocation (22% [4/18] vs. 3% [3/87], p=.016) and amplification (17% [3/18] vs. 2% [2/87], p=.034). Within the PA-DLBCL group, PD-L1 gene-altered cases (vs. non-altered cases) tended to have B symptoms (p=.145) and elevated LDH (p=.119) but less frequent bulky disease (≥10 cm) (p=.119). In the survival analysis, PA-DLBCL had a poor prognosis for overall survival (OS) and progression-free survival (PFS) (vs. NA-DLBCL; p=.014 and p=.004). Within the PA-DLBCL group, PD-L1 translocation was associated with shorter OS and PFS (p<.001 and p=.012). **Conclusions:** PA-DLBCL is a clinically aggressive and distinct subset of DLBCL with frequent PD-L1 gene alterations. PD-L1 gene translocation was associated with poor prognosis in PA-DLBCL.

Key Words: Malignant lymphoma; Diffuse large B cell lymphoma; Adrenal gland; PD-L1

Received: September 6, 2021 **Revised:** September 26, 2021 **Accepted:** October 5, 2021

Corresponding Author: Jin Ho Paik, MD, PhD, Department of Pathology, Seoul National University Bundang Hospital, 82, Gumi-ro 173beon-gil, Bundang-gu, Seongnam 13620, Korea

Tel: +82-31-787-7717, Fax: +82-31-787-4012, E-mail: paikjh@snu.ac.kr

Malignant lymphomas have been classified and updated by distinctive morphologic, clinical, and genetic features [1]. Classical Hodgkin lymphoma (cHL) has activated programmed death-ligand 1 (PD-L1) signaling, while it is derived from B cells [2-5]. For B cell-derived neoplasms with intact B cell antigen expression, including diffuse large B cell lymphoma (DLBCL), the clinicopathologic significance of PD-L1 gene alteration has not been well characterized. In our previous retrospective study of DLBCL, PD-L1 gene alterations, including translocation and amplification, were observed in 14% of non-germinal center B cell-like (non-GCB) subtype [6]. Interestingly, frequent alteration of the

PD-L1 gene was observed in several anatomic site-specific subtypes of DLBCL, including primary mediastinal large B cell lymphoma, primary DLBCL of the central nervous system (CNS) and primary testicular DLBCL [7,8]. These phenomena suggest that PD-L1 gene alteration may also play an important pathogenic role in a delicately defined subset of DLBCL.

Adrenal gland has a unique microenvironment with potential features of immune sanctuary sites and locally increased immunosuppressive hormones [9,10]. It is rarely involved by malignant lymphomas usually with secondary spread from systemic extra-adrenal lymphomas [11]. Primary adrenal lymphoma accounts

for only < 1% of non-Hodgkin lymphomas and 3% of extranodal lymphomas, and DLBCL is the most common histologic type [11,12]. Primary adrenal DLBCL (PA-DLBCL) was reported to frequently have clinicopathologic features such as elevated lactate dehydrogenase (LDH), presence of B symptoms, non-GCB subtype, Bcl-6 gene rearrangement and worse prognosis [11,13,14].

In our previous study of DLBCL, PD-L1 gene alteration was observed in one out of three cases of the PA-DLBCL subset, providing a clue for further investigation of PD-L1 gene alteration in PA-DLBCL [6]. Furthermore, we also focused on several studies relating PD-L1 upregulation with clinical aggressiveness [15,16]. These findings raised questions about the prevalence of PD-L1 gene alterations in PA-DLBCL as well as its role in presumed clinical aggressiveness [14]. Herein, we hypothesized that the clinicopathologic features of PA-DLBCL may be associated with PD-L1 gene alterations. We investigated (1) the clinicopathologic characteristics of PA-DLBCL, including the frequency of PD-L1 gene alterations, and (2) the associations between PD-L1 gene alterations and clinicopathologic variables, including prognosis.

MATERIALS AND METHODS

Patients and samples

From 20 cases of DLBCL, not otherwise specified (NOS) that occurred primarily in the adrenal gland, i.e., “primary adrenal DLBCL (PA-DLBCL)” retrospectively retrieved from the archives of pathology records between May 2003 and January 2013 at Seoul National University Bundang Hospital (SNUBH) and Seoul National University Hospital, two cases were excluded due to inappropriate tissue conditions and failure to meet the clinical criteria. Therefore, a total of 18 cases of PA-DLBCL were finally enrolled. To elucidate the unique clinicopathologic features of PA-DLBCL, systemic cases of DLBCL, NOS diagnosed at SNUBH during the same period was used as a reference group of “non-adrenal (NA)-DLBCL” group containing 90 cases [6]. Considering the characteristics of the previously described PA-DLBCL [11,13], we defined PA-DLBCL as “de novo DLBCL with one or more adrenal gland mass-forming and/or hypermetabolic lesion(s) as the most dominant lesion” for the purpose of the present study. Specifically, the “PA-DLBCL” group included the following cases: (1) cases of DLBCL, NOS according to the World Health Organization (WHO) 2016 criteria with no prior history of lymphoma, (2) cases with unequivocal adrenal-dominant mass lesions (maximal diameter: adrenal mass > 2 of NA mass) measured by computed tomography (CT) and/or ¹⁸F-positron emission tomography (PET)-CT, and (3) cases proven by

appropriate pathologic studies. The following cases were excluded from the “PA-DLBCL” group for the purpose of clarity of this study: (1) widely disseminated DLBCL cases, (2) cases with widespread node-based disease, and (3) any distinct entities including ‘DLBCL of the CNS’, ‘primary mediastinal large B cell lymphoma’, ‘primary testicular DLBCL’, so-called ‘gray-zone lymphomas’ and lymphomas associated with Epstein-Barr virus or human immunodeficiency virus. All samples in this study were archived materials of formalin-fixed paraffin-embedded tissues obtained from biopsy or surgical specimens.

The pathologic diagnosis was reviewed by two pathologists (KRL and JHP) by WHO 2016 criteria, and the ‘cell of origin’ subtype was determined by Han’s algorithm [1,17]. Clinical findings were retrieved from medical records.

Fluorescence in situ hybridization for PD-L1 gene

We investigated the genetic alterations of the PD-L1 (CD274) gene (translocation, copy number gain, and amplification) by using fluorescence in situ hybridization (FISH) staining, as previously described [6]. A PD-L1 break-apart probe (9p24.1) (catalog No. PDL1BA-20-ORGR) from Empire Genomics (Buffalo, NY) was used to detect the translocation, and a PD-L1 (orange)/chromosome 9 (green) probe set (9p24.1/9p21.33) (catalog No. PDL1-CHR09-20-ORGR) from the same company was used to detect the copy number gain and amplification. To determine translocation, copy number gain and amplification, more than 200 cells with non-overlapping nuclei were counted. Separation of orange and green signals in more than 15% of cells was interpreted as the presence of translocation. Copy number gain and amplification were defined as orange/green signal (PD-L1 gene/chromosome 9) ratios > 2 and > 4, respectively. In the case of clustered signals, we counted them as 12 copies. In our series of PA-DLBCL, there were no cases with copy number gain or cases with concurrent translocation and copy number gain/amplification.

Statistical analysis

SPSS Statistics ver. 19 (IBM Corp., Armonk, NY, USA) was used for statistical analysis. Chi-square and Fisher exact tests were used to compare clinicopathologic features. Kaplan-Meier analysis was used to draw survival curves using the log-rank test. A Cox proportional hazard model was used for multivariate survival analysis. Overall survival (OS) was defined as the time interval from the date of diagnosis to the date of last follow-up or death. Progression-free survival (PFS) was defined as the time interval from the date of treatment to the date of progression with radiologic confirmation using CT and/or PET-CT after treatment or

Table 1. Clinicopathologic features of PA-DLBCL and NA-DLBCL patients

Clinicopathologic characteristic	PA-DLBCL	NA-DLBCL	p-value
Age (yr)			.796
≤60	9 (50.0)	42 (46.7)	
>60	9 (50.0)	48 (53.3)	
Sex			.667
Men	10 (55.6)	45 (50.0)	
Women	8 (44.4)	45 (50.0)	
B symptoms			.082 ^a
Absent	10 (55.6)	69 (76.7)	
Present	8 (44.4)	21 (23.0)	
ECOG PS			.003 ^a
<2	8 (53.3)	80 (88.9)	
≥2	7 (46.7)	10 (11.1)	
Serum LDH			.035
Normal	4 (22.2)	43 (49.4)	
Elevated	14 (77.8)	44 (50.6)	
Ann Arbor stage			.796
I-II	9 (50.0)	42 (46.7)	
III-IV	9 (50.0)	48 (53.3)	
International prognostic index			.007
0-2	5 (27.8)	56 (62.2)	
3-5	13 (72.0)	34 (37.8)	
Bone marrow involvement			>.99 ^a
Absent	13 (86.7)	70 (84.3)	
Present	2 (13.3)	13 (15.7)	
Bulky mass (> 10 cm)			.084 ^a
<10	14 (77.8)	83 (92.2)	
≥10	4 (22.0)	7 (7.8)	
Hans classification			.224 ^a
GCB	2 (13.3)	25 (30.1)	
Non-GCB	13 (86.7)	58 (69.9)	
BCL2 expression			.349
Negative	4 (26.7)	35 (39.3)	
Positive	11 (73.3)	54 (60.7)	
BCL6 expression			.079
Negative	4 (26.7)	46 (51.1)	
Positive	11 (73.3)	44 (48.9)	
CD10 expression			.459 ^a
Negative	15 (93.8)	76 (84.4)	
Positive	1 (6.2)	14 (15.6)	
MUM1 expression			.047
Negative	2 (13.3)	36 (40.0)	
Positive	13 (86.7)	54 (60.0)	
Treatment			.585
R-CHOP	17 (94.4)	81 (90.0)	
R-others	1 (5.6)	4 (4.4)	
Others	0 (0.0)	5 (5.6)	
Total	18 (100.0)	90 (100.0)	

Values are presented as number (%).

PA, primary adrenal; DLBCL, diffuse large B cell lymphoma; NA, non-adrenal; ECOG PS, Eastern Cooperative Oncology Group performance status; LDH, lactate dehydrogenase; GCB, germinal center B cell.

^ap-values were calculated by Pearson's chi-square test (2-sided) or Fisher's exact test (2-sided).

the date of death. All p-values reported were two-sided, and statistical significance was accepted when they were less than .05.

RESULTS

Clinicopathologic characteristics of PA-DLBCL

To characterize the clinicopathologic features of PA-DLBCL, we analyzed the clinicopathologic parameters of the PA-DLBCL group with a reference group of NA-DLBCL (Table 1). As for clinical variables, compared to NA-DLBCL, PA-DLBCL patients showed high international prognostic index (IPI) score (3–5) (72% [13/18] in PA-DLBCL vs. 38% [34/90] in NA-DLBCL, $p = .007$), poor Eastern Cooperative Oncology Group performance score (ECOG PS) (≥ 2) (47% [7/15] in PA-DLBCL vs. 11% [10/90] in NA-DLBCL, $p = .003$), elevated LDH (78% [14/18] in PA-DLBCL vs. 51% [44/87] in NA-DLBCL, $p = .035$) with trends for high frequency of B symptoms (44% [8/18] in PA-DLBCL vs. 23% [21/90] in NA-adrenal DLBCL, $p = .082$) and bulky disease (≥ 10 cm) (22% [4/18] in PA-DLBCL vs. 8% [7/90] in NA-adrenal DLBCL, $p = .084$). However, the two groups showed a similar distribution of high-stage disease (50% [9/18] in PA-DLBCL vs. 53% [48/90] in NA-DLBCL).

Pathologically, the PA-DLBCL group showed frequent MUM1 expression (87% [13/15] in PA-DLBCL vs. 60% [54/90] in NA-adrenal DLBCL, $p = .047$) with trends for Bcl-6 expression (73% [11/15] in PA-DLBCL vs. 49% [44/90] in NA-adrenal DLBCL, $p = .079$).

Taken together, PA-DLBCL group harbored aggressive clinicopathologic features even with similar stage, compared to NA-DLBCL.

Table 2. PD-L1 genetic alteration in PA-DLBCL and NA-DLBCL

PD-L1 genetic status	PA-DLBCL	NA-DLBCL	p-value
PD-L1 translocation			.016
Absent	14 (77.8)	84 (96.6)	
Present	4 (22.2)	3 (3.4)	
PD-L1 amplification			.034
Absent	15 (83.3)	85 (97.7)	
Present	3 (16.7)	2 (2.3)	
PD-L1 genetic alteration			.001
Absent	11 (61.1)	81 (94.2)	
Present	7 (38.9)	5 (5.8)	
Total	18 (100.0)	87 (100.0)	

Values are presented as number (%).

p-values were calculated by Fisher's exact test (2-sided).

PD-L1, programmed death-ligand 1; PA, primary adrenal; DLBCL, diffuse large B cell lymphoma; NA, non-adrenal.

PD-L1 gene alteration by using fluorescence in situ hybridization

We next analyzed the frequency of PD-L1 gene alterations, including translocation and amplification, by using the FISH method. As shown in Table 2 and Fig. 1, PD-L1 gene alteration in PA-DLBCL accounted for 39% (7/18), including translocation in 22% (4/18) and amplifications in 17% (3/18), which were much higher frequencies than NA-DLBCL with PD-L1 gene alteration in 6% [5/86], including translocation in 3% (3/87) and amplification in 2% (2/87) ($p = .001$, $p = .016$, and $p = .034$, respectively). Therefore, the PA-DLBCL group had a significantly higher frequency of PD-L1 gene alterations than the NA-DLBCL group.

Associations between clinicopathologic variables and PD-L1 gene alterations in PA-DLBCL

We next investigated associations between PD-L1 gene alter-

ations and clinicopathologic parameters within the PA-DLBCL group. As shown in Table 3, PA-DLBCL with PD-L1 gene alteration tended to have elevated serum LDH (100% [7/7] in the PD-L1–altered group vs. 64% [7/11] in non-altered group) and B symptoms (71% [5/7] in the PD-L1–altered group vs. 27% [3/11] in non-altered group). In contrast, there was a tendency for less frequent bulky disease (≥ 10 cm) in the PD-L1–altered group (0% [0/7] in the PD-L1–altered group vs. 36% [4/11] in non-altered group).

Survival analysis

As shown in Fig. 2, the PA-DLBCL group showed inferior OS and PFS compared to the NA-DLBCL group ($p = .014$ and $p = .004$) (Fig. 2A, B). When survival was analyzed within the PA-DLBCL group (Table 4), PD-L1 gene alteration did not significantly affect OS or PFS ($p > .05$) (Fig. 2C, D). When the survival effect of PD-L1 translocation was analyzed, the PD-L1 translo-

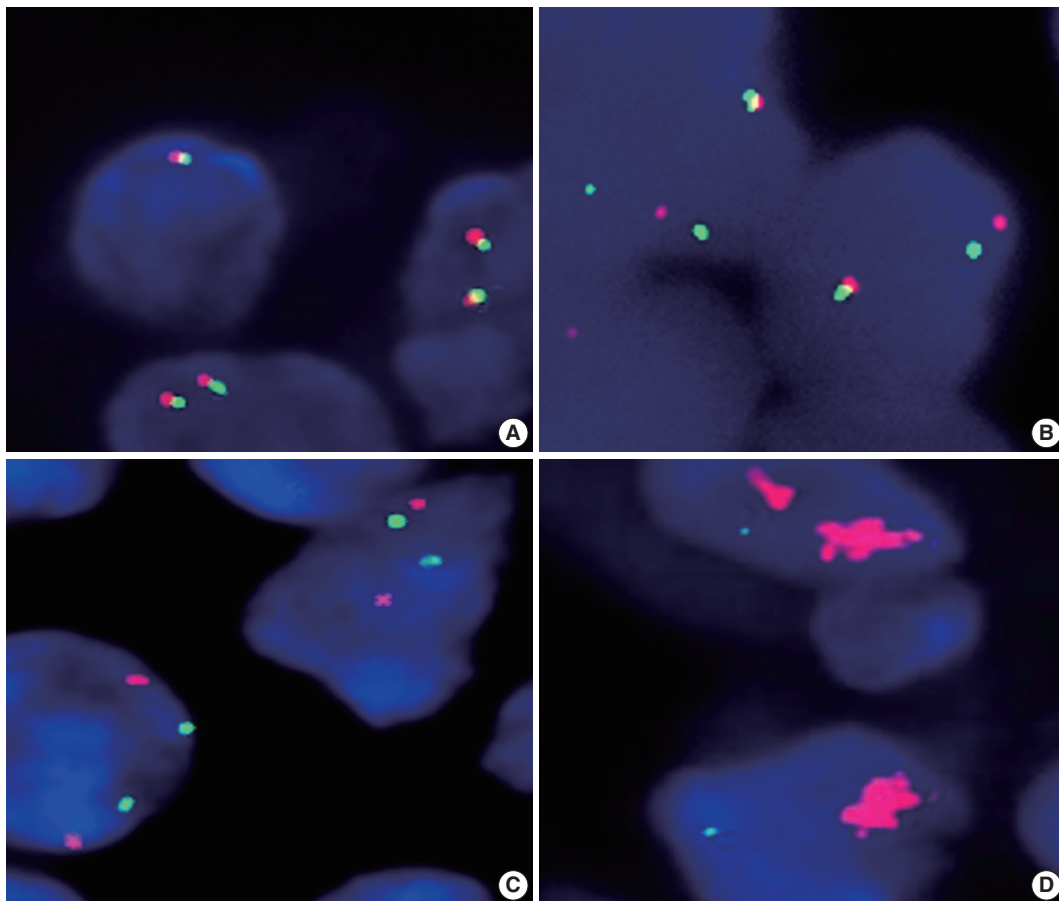


Fig. 1. Fluorescence in situ hybridization analysis of the programmed death-ligand 1 (PD-L1) gene in diffuse large B cell lymphoma. By using a dual-color orange/green break-apart probe, non-split fused signal indicates the absence of translocation (A), while separate orange and green signals indicate the presence of translocation (B). By using a copy number analysis probe, orange (PD-L1 gene) and green (chromosome 9) signals showed a nearly 1:1 ratio in cases with no gain or amplification of the PD-L1 gene (C), in contrast to amplified orange signals indicating PD-L1 gene amplification (D).

Table 3. Clinicopathologic features of primary adrenal diffuse large B cell lymphoma according to PD-L1 gene alteration

Clinicopathologic characteristic	Absence of PD-L1 genetic alteration	Presence of PD-L1 genetic alteration	p-value
Age (yr)			> .99
≤60	6 (54.5)	4 (57.1)	
>60	5 (45.5)	3 (42.9)	
Sex			> .99
Male	6 (54.5)	4 (57.1)	
Female	5 (45.5)	3 (42.9)	
B symptoms			.145
Absent	8 (72.7)	2 (28.6)	
Present	3 (27.3)	5 (71.4)	
ECOG PS			.619
<2	5 (62.5)	3 (42.9)	
≥2	3 (37.5)	4 (57.1)	
Serum LDH			.119
Normal	4 (36.4)	0	
Elevated	7 (63.6)	7 (100.0)	
Ann Arbor stage			.335
I-II	4 (36.4)	5 (71.4)	
III-IV	7 (63.6)	2 (28.6)	
International prognostic index			.596
0-2	4 (36.4)	1 (14.3)	
3-5	7 (63.6)	6 (85.7)	
Bone marrow involvement			.486
Absent	7 (77.8)	6 (100.0)	
Present	2 (22.2)	0	
Bulky disease (cm)			.119
<10	7 (63.6)	7 (100.0)	
≥10	4 (36.4)	0	
Mass size (cm)	7.4±3.2	5.5±1.6	.157 ^a
Hans classification			> .99
GCB	1 (10.0)	1 (20.0)	
Non-GCB	9 (90.0)	4 (80.0)	
BCL2 expression			.560
Negative	2 (20.0)	2 (40.0)	
Positive	8 (80.0)	3 (60.0)	
BCL6 expression			> .99
Negative	3 (30.0)	1 (20.0)	
Positive	7 (70.0)	4 (80.0)	
CD10 expression			> .99
Negative	9 (90.0)	6 (100.0)	
Positive	1 (10.0)	0	
MUM1 expression			> .99
Negative	1 (10.0)	1 (20.0)	
Positive	9 (90.0)	4 (80.0)	
Total	11 (100.0)	7 (100.0)	

Values are presented as number (%) or mean ± SD.

PDL1, programmed death-ligand 1; ECOG PS, Eastern Cooperative Oncology Group performance status; LDH, lactate dehydrogenase; GCB, germinal center B cell.

^ap-values were calculated by Fisher's exact test (2-sided) or Spearman's correlation (2-sided; rho = -0.456).

cation group showed inferior OS and PFS ($p < .001$ and $p = .012$) (Fig. 2E, F). However, PD-L1 gene amplification was not associated with prognosis. Among the conventional prognostic markers, ECOG PS was a significant predictor for PFS ($p = .039$). In multivariate analysis, all variables were not significant due to the limited number of cases.

DISCUSSION

In our study, we demonstrated that PD-L1 gene alterations were more frequent in PA-DLBCL than in NA-DLBCL and tended to be associated with aggressive clinical parameters such as the presence of B symptoms or high LDH. Patients with PD-L1 translocation but not amplification revealed inferior survival in PA-DLBCL.

DLBCLs in certain primary anatomic sites, such as the mediastinum, CNS or testis, are classified as specific types because of their distinct molecular pathogenesis. PD-L1/PD-L2 signaling has been reported to be activated in these lymphomas [7,8]. Although PA-DLBCL is not defined as a special type based on anatomic sites, it is usually associated with aggressive features and distinct pathologic characteristics [12,14]. Our study also supported that PA-DLBCL had aggressive features with a high rate of PD-L1 gene alteration, suggesting unique clinicopathologic characteristics.

Because of the rarity of PA-DLBCL, its clinicopathologic features, including pathogenic mechanism and clinical behavior, have not been well characterized. Several previous reports revealed aggressive features of PA-DLBCL, such as frequent B symptoms, elevated serum LDH, bulky mass formation and predominance of the non-GCB subtype, which are in concordance with our results [11-14]. In the present study, compared to the NA-DLBCL group, the PA-DLBCL group showed frequent poor ECOG PS (≥ 2), high IPI (3-5) and poor prognosis, suggesting the intrinsic aggressive features of PA-DLBCL [11,12], even with a nearly equal proportion of high-stage (III-IV) disease in both groups (50% vs. 53%).

The biological role of the programmed death-1/PD-L1 axis was revealed as the induction and maintenance of peripheral tolerance in T cells to prevent autoimmune reactions. However, inhibitory signals via this pathway hamper the proliferation and function of effector T cells, resulting in immune evasion in antitumor immunity [18]. Recently, several studies have suggested that cancer cell-intrinsic PD-L1 signaling contributes to the proliferation, migration and invasion of various types of cancer cells, including lymphoma cells [19]. In this context, these extrinsic

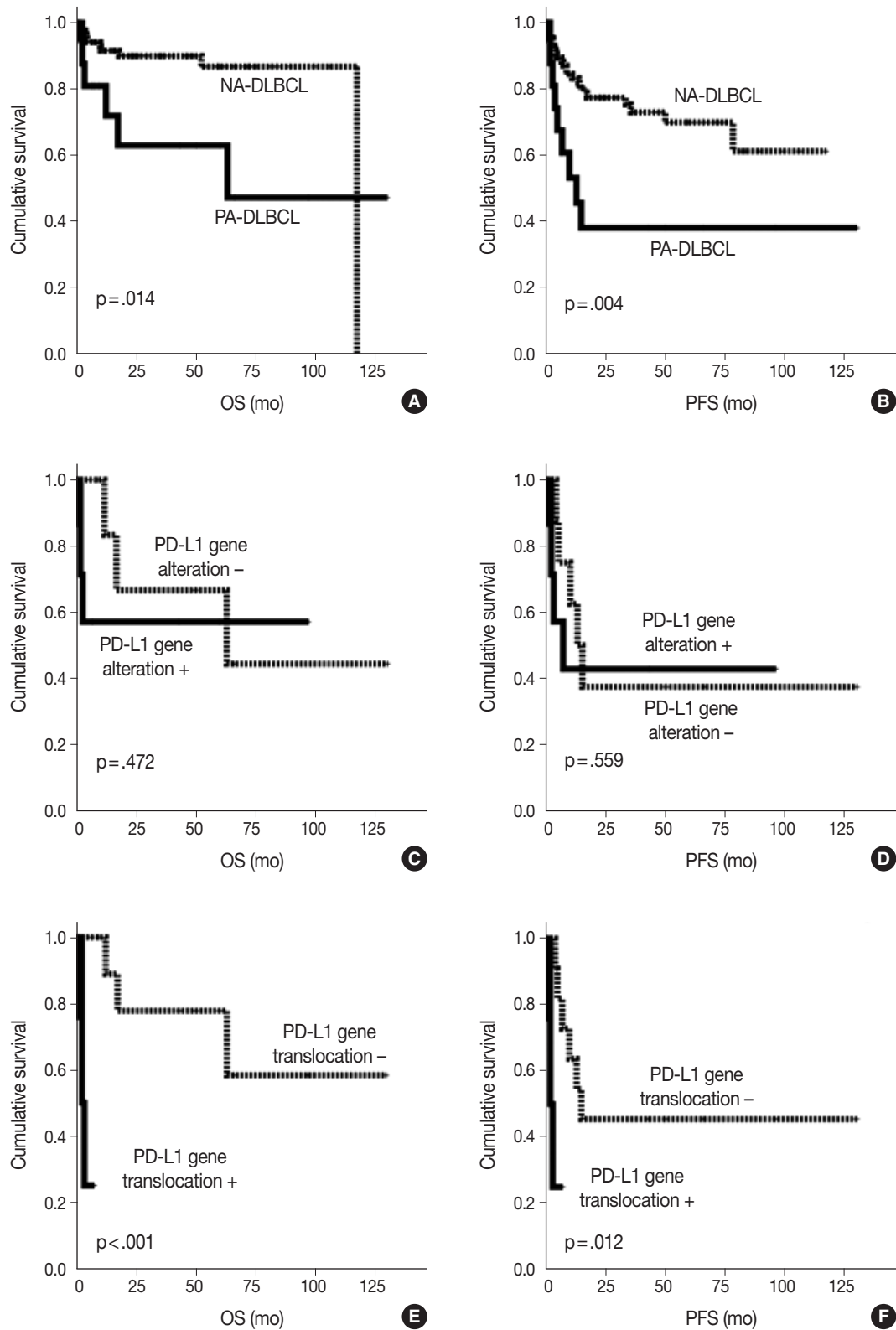


Fig. 2. Kaplan-Meier curves of overall survival (OS) and progression-free survival (PFS) in diffuse large B cell lymphoma (DLBCL) patients. OS (A) and PFS (B) of primary adrenal (PA)- and non-adrenal (NA)-DLBCL patients. OS (C) and PFS (D) of PA-DLBCL patients by the presence of programmed death-ligand 1 (PD-L1) gene alterations. OS (E) and PFS (F) of PA-DLBCL patients by the presence of PD-L1 gene translocation.

Table 4. Univariate survival analysis according to clinicopathologic variables and PD-L1 gene alteration in primary adrenal diffuse large B cell lymphoma

Clinicopathologic variable	p-value	
	Progression-free survival	Overall survival
Age (≤ 60 vs. > 60)	.139	.192
Sex (male vs. female)	.910	.656
ECOG PS (< 2 vs. ≥ 2)	.039	.661
B symptoms (absent vs. present)	.206	.704
Serum LDH (normal vs. elevated)	.768	.267
International prognostic index (0–2 vs. 3–5)	.057	.260
Bone marrow involvement (absent vs. present)	.986	.431
Bulky disease (< 10 cm vs. ≥ 10 cm)	.158	.873
Ann Arbor stage (I–II vs. III–IV)	.535	.857
Hans classification (GCB vs. non-GCB)	.942	.992
PD-L1 gene alteration (– vs. +)	.559	.472
PD-L1 gene amplification (– vs. +)	.317	.139
PD-L1 gene translocation (– vs. +)	.012	$< .001$

PD-L1, programmed death-ligand 1; ECOG PS, Eastern Cooperative Group performance status; LDH, lactate dehydrogenase; GCB, germinal center B cell.

and intrinsic effects of PD-L1 signaling may help to constitute the features of PD-L1–altered cancers. In our PA-DLBCL group, we observed that PD-L1 gene alteration had trends for frequent B symptoms, elevated serum LDH and relatively less bulky mass lesions, suggesting that PD-L1–altered tumor cells may tend to secrete mediators producing systemic reactions at a relatively early phase of mass formation.

The aggressive clinicopathologic nature of PA-DLBCL could not be fully explained by PD-L1 gene alteration due to its limited prevalence (39%). Another genetic feature of PA-DLBCL includes Bcl-6 gene rearrangement [14], which is common in both GCB and non-GCB DLBCLs [1,20,21]. A recent functional study in a mouse model revealed that Bcl-6 suppressed PD-L1/PD-L2 expression in germinal center (GC) B cells [22]. However, the functional role of Bcl-6 on PD-L1 in the post-GC B cell context is not definite and remains to be investigated further.

In summary, we observed that PA-DLBCL had characteristic clinicopathologic features, including high IPI, inferior outcome, and frequent PD-L1 gene alteration. Within this PA-DLBCL group, PD-L1 gene translocation was a significant poor prognostic marker predicting OS and PFS. Our results suggest that PA-DLBCL can be a distinct entity with frequent PD-L1 genetic alterations and may provide insight into the potentially shared pathogenesis of DLBCL of the mediastinum, CNS, testis, and adrenal gland.

Ethics Statement

This study was approved by the Institutional Review Board of Seoul National University Bundang Hospital (B-1306-208-301) and Seoul National University (No. 1506-080-681), and informed consent was waived due to the retrospective design using archived material in this study.

Availability of Data and Material

The datasets generated or analyzed during the study are available from the corresponding author on reasonable request.

Code Availability

Not applicable.

ORCID

Ki Rim Lee <https://orcid.org/0000-0001-8774-1204>
 Jiwon Koh <https://orcid.org/0000-0002-7687-6477>
 Yoon Kyung Jeon <https://orcid.org/0000-0001-8466-9681>
 Hyun Jung Kwon <https://orcid.org/0000-0001-8822-7899>
 Jeong-Ok Lee <https://orcid.org/0000-0001-9402-6372>
 Jin Ho Paik <https://orcid.org/0000-0002-2792-0419>

Author Contributions

Conceptualization: KRL, JHP. Data curation: KRL, JK, YKJ, HJK, JOL, JHP. Formal analysis: KRL, JHP. Funding acquisition: JHP. Investigation: KRL, JK, YKJ, JOL, HJK, JHP. Methodology: KRL, JHP. Writing—original draft: KRL, JHP. Writing—review & editing: KRL, JK, YKJ, JOL, JHP. Approval of final manuscript: all authors.

Conflicts of Interest

J.H.P., a contributing editor of the *Journal of Pathology and Translational Medicine*, was not involved in the editorial evaluation or decision to publish this article. All remaining authors have declared no conflicts of interest.

Funding Statement

This study was supported by the Basic Science Research Program through the National Research Foundation (NRF) of Korea funded by the Ministry of Science and ICT (NRF-2019R1F1A1061920) and the Development Fund from Seoul National University (grant No.: 800-20190386) funded by the HUNKIM Family Charitable Foundation.

References

1. Swerdlow SH, Campo E, Pileri SA, et al. The 2016 revision of the World Health Organization classification of lymphoid neoplasms. *Blood* 2016; 127: 2375-90.
2. Nagasaki J, Togashi Y, Sugawara T, et al. The critical role of CD4+ T cells in PD-1 blockade against MHC-II-expressing tumors such as classic Hodgkin lymphoma. *Blood Adv* 2020; 4: 4069-82.
3. Xu-Monette ZY, Zhou J, Young KH. PD-1 expression and clinical PD-1 blockade in B-cell lymphomas. *Blood* 2018; 131: 68-83.
4. Roemer MG, Advani RH, Ligon AH, et al. PD-L1 and PD-L2 genetic alterations define classical Hodgkin lymphoma and predict outcome. *J Clin Oncol* 2016; 34: 2690-7.
5. Ansell SM, Lesokhin AM, Borrello I, et al. PD-1 blockade with nivolumab in relapsed or refractory Hodgkin's lymphoma. *N Engl J Med* 2015; 372: 311-9.
6. Kwon HJ, Yang JM, Lee JO, Lee JS, Paik JH. Clinicopathologic implication of PD-L1 and phosphorylated STAT3 expression in diffuse large B cell lymphoma. *J Transl Med* 2018; 16: 320.

7. Twa DD, Chan FC, Ben-Neriah S, et al. Genomic rearrangements involving programmed death ligands are recurrent in primary mediastinal large B-cell lymphoma. *Blood* 2014; 123: 2062-5.
8. Chapuy B, Roemer MG, Stewart C, et al. Targetable genetic features of primary testicular and primary central nervous system lymphomas. *Blood* 2016; 127: 869-81.
9. Cohen R, Jonchere V, De La Fouchardiere C, et al. Adrenal gland as a sanctuary site for immunotherapy in patients with microsatellite instability-high metastatic colorectal cancer. *J Immunother Cancer* 2021; 9: e001903.
10. Mushtaq RR, Gao D, Raeburn C, Tobin RP, Robinson W. Adrenal metastases in malignant melanoma, is it a privileged site? *J Clin Oncol* 2019; 37(15 Suppl): e21016.
11. Rashidi A, Fisher SI. Primary adrenal lymphoma: a systematic review. *Ann Hematol* 2013; 92: 1583-93.
12. Kim YR, Kim JS, Min YH, et al. Prognostic factors in primary diffuse large B-cell lymphoma of adrenal gland treated with rituximab-CHOP chemotherapy from the Consortium for Improving Survival of Lymphoma (CISL). *J Hematol Oncol* 2012; 5: 49.
13. Laurent C, Casasnovas O, Martin L, et al. Adrenal lymphoma: presentation, management and prognosis. *QJM* 2017; 110: 103-9.
14. Mozos A, Ye H, Chuang WY, et al. Most primary adrenal lymphomas are diffuse large B-cell lymphomas with non-germinal center B-cell phenotype, BCL6 gene rearrangement and poor prognosis. *Mod Pathol* 2009; 22: 1210-7.
15. Audrito V, Serra S, Stingi A, et al. PD-L1 up-regulation in melanoma increases disease aggressiveness and is mediated through miR-17-5p. *Oncotarget* 2017; 8: 15894-911.
16. Gao Q, Wang XY, Qiu SJ, et al. Overexpression of PD-L1 significantly associates with tumor aggressiveness and postoperative recurrence in human hepatocellular carcinoma. *Clin Cancer Res* 2009; 15: 971-9.
17. Hans CP, Weisenburger DD, Greiner TC, et al. Confirmation of the molecular classification of diffuse large B-cell lymphoma by immunohistochemistry using a tissue microarray. *Blood* 2004; 103: 275-82.
18. Bardhan K, Anagnostou T, Boussiotis VA. The PD1:PD-L1/2 pathway from discovery to clinical implementation. *Front Immunol* 2016; 7: 550.
19. Hudson K, Cross N, Jordan-Mahy N, Leyland R. The extrinsic and intrinsic roles of PD-L1 and its receptor PD-1: implications for immunotherapy treatment. *Front Immunol* 2020; 11: 568931.
20. Pasqualucci L, Dalla-Favera R. The genetic landscape of diffuse large B-cell lymphoma. *Semin Hematol* 2015; 52: 67-76.
21. Iqbal J, Greiner TC, Patel K, et al. Distinctive patterns of BCL6 molecular alterations and their functional consequences in different subgroups of diffuse large B-cell lymphoma. *Leukemia* 2007; 21: 2332-43.
22. Peng C, Hu Q, Yang F, Zhang H, Li F, Huang C. BCL6-mediated silencing of PD-1 ligands in germinal center B cells maintains follicular T cell population. *J Immunol* 2019; 202: 704-13.

Polo-like kinase 4 as a potential predictive biomarker of chemoradioresistance in locally advanced rectal cancer

Hyunseung Oh¹, Soon Gu Kim², Sung Uk Bae³, Sang Jun Byun⁴, Shin Kim⁵,
 Jae-Ho Lee⁶, Ilseon Hwang¹, Sun Young Kwon¹, Hye Won Lee¹

Departments of ¹Pathology and ²Education Support Center, ³Division of Colorectal Surgery, Department of Surgery, Departments of ⁴Radiation Oncology, ⁵Immunology, and ⁶Anatomy, Keimyung University School of Medicine, Daegu, Korea

Background: Polo-like kinase 4 (PLK4) is a serine/threonine protein kinase located in the centriole of the chromosome during the cell cycle. PLK4 overexpression has been described in a variety of many common human epithelial tumors. Conversely, PLK4 acts as a haploinsufficient tumor suppressor in some situations, highlighting the importance of strict regulation of PLK4 expression, activity, and function. Meanwhile, the importance of chemoradiation resistance in rectal cancer is being emphasized more than ever. We aimed to analyze PLK4 expression and the tumor regression grade (TRG) in patients with rectal cancer, treated with chemoradiotherapy (CRT).

Methods: A retrospective study was conducted on 102 patients with rectal cancer who received preoperative CRT. Immunohistochemistry for PLK4 in paraffin-embedded tissue was performed from the biopsy and surgical specimens. **Results:** We found significant association between high expression of PLK4 and poor response to neoadjuvant CRT (according to both Mandard and The Korean Society of Pathologists TRG systems) in the pre-CRT specimens. Other clinicopathologic parameters did not reveal any correlation with PLK4 expression. **Conclusions:** This study revealed an association between high expression of PLK4 in the pre-CRT specimens and TRG. Our results indicated that PLK4 could potentially be a new predictor for CRT effect in patients with rectal cancer.

Key Words: Polo-like kinase 4; Rectal neoplasms; Chemoradiotherapy; Biomarker

Received: August 5, 2021 **Revised:** September 29, 2021 **Accepted:** October 7, 2021

Corresponding Author: Hye Won Lee, MD, PhD, Department of Pathology, Keimyung University School of Medicine, 1095 Dalgubeol-daero, Dalseo-gu, Daegu 42601, Korea
 Tel: +82-53-258-4260, Fax: +82-53-258-7382, E-mail: hwlee@dsmc.or.kr

The 5-year survival rate for rectal cancer patients undergoing surgery is 50%. This is because even with curative resection, the risk of local recurrence or distant metastasis is high [1]. Therefore, improving survival remains an important issue, even in resectable rectal cancer. Meanwhile, in patients with rectal cancer, preoperative chemoradiotherapy (CRT) significantly improves the overall and cancer-specific survival rates compared to surgery alone. Therefore, chemoradioresistance is an important challenge in rectal cancer and a major aspect of its treatment.

Polo-like kinase 4 (PLK4) is a serine/threonine kinase located in the centriole of the chromosome throughout the cell cycle and is essential for centriole duplication [2-5]. PLK4 expression has been described in a variety of human solid tumors [6]. In particular, high levels of PLK4 mRNA have been detected in triple-negative breast cancers, which are resistant to conventional systemic therapy [7]. PLK4 expression upregulation independently

induces aneuploidy, loss of cell polarity, and hyperplasia in certain non-transformed cell lines and proliferative tissues [8,9]. In the context of p53 dysfunction, elevated PLK4 expression contributes to aneuploidy and tumorigenesis [9,10]. Contrarily, PLK4 acts as a haploinsufficient tumor suppressor in some situations. Rosario et al. pointed out that haploid levels of PLK4 interfered with RhoGTPase function during cytokinesis, leading to aneuploidy and tumorigenesis, thus suggesting that early loss of heterozygosity in PLK4 is one of the factors leading to hepatocellular carcinogenesis [11,12]. These results underscore the importance of strict regulation of PLK4 expression, activity, and function [13]. However, studies on PLK4 expression in patients with rectal cancer are limited. Thus, this study aimed to retrospectively analyze PLK4 expression in patients with rectal carcinoma treated with preoperative CRT in both preoperative biopsy specimens and postoperative surgical specimens.

MATERIALS AND METHODS

Patients and sample collection

The electronic records of rectal cancer patients treated at Keimyung University Dongsan Hospital were reviewed retrospectively. Among them, 102 cases containing both biopsy and surgical specimens were chosen. These tissue specimens along with patient clinical data (age, sex, date of surgery, recurrence, death, data on time to recurrence or death) and records of clinicopathological features (differentiation, lymphovascular invasion, pT category, pN category, pM category, microsatellite instability [MSI] status, *KRAS*, *NRAS* and *BRAF* mutations) of the rectal cancer were collected.

Among the various grading systems devised to evaluate chemoradioresistance, the Mandard system [14] was used (Mandard-TRG [tumor regression grade]). Additionally, the KSP-TRG system, newly proposed by the Gastrointestinal Pathology Research Group of the Korean Society of Pathologists (KSP), based on the 8th edition of American Joint Committee on Cancer and the College of American Pathologists cancer protocol, was also used and data collected [15]. This grade is divided into four tiers: grade 0 (no viable cancer cells, complete response), grade 1 (single cells or rare small groups of cancer cells, near-complete response), grade 2 (residual cancer with evident tumor regression, but more than single cells or rare small groups of cancer cells, partial response), grade 3 (extensive residual cancer with no evident tumor regression, poor or no response).

Overall survival (OS) was defined as the duration from the date of surgery to the date of the last follow-up visit or the date of death due to any cause, whereas disease-free survival (DFS) was defined as the duration from surgery to any type of recurrence.

Immunohistochemistry

We selected formalin-fixed paraffin-embedded (FFPE) tissue samples from rectal cancer tissues and used them for tissue microarray (TMA) construction. Of the 102 patients with rectal cancer, tissue specimens from both before CRT (biopsy specimen) and after CRT (surgery specimen) were selected for 71 patients. Only biopsy specimens were selected from 31 patients with no or few cells remaining in the surgical specimens. Representative tumor areas were identified by two pathologists (H.O. and H.W.L.) in hematoxylin and eosin-stained tissue sections. After the pathologists' review, TMAs were assembled from triplicate 5 mm cores of the FFPE tumor samples. Immunohistochemical staining was performed on the TMA sections with an antibody against PLK4 (12952-1-AP, 1:400, ProteinTech Group, Inc., Chicago, IL, USA) using the Ventana BenchMark XT Automated System following the manufacturer's protocol (Ventana Medical Systems, Tucson, AZ, USA).

Evaluation of immunohistochemistry

The histoscore (H-score) method was used to determine the immunohistochemical expression of PLK4. The H-score was calculated by multiplying the intensity score by the percentage

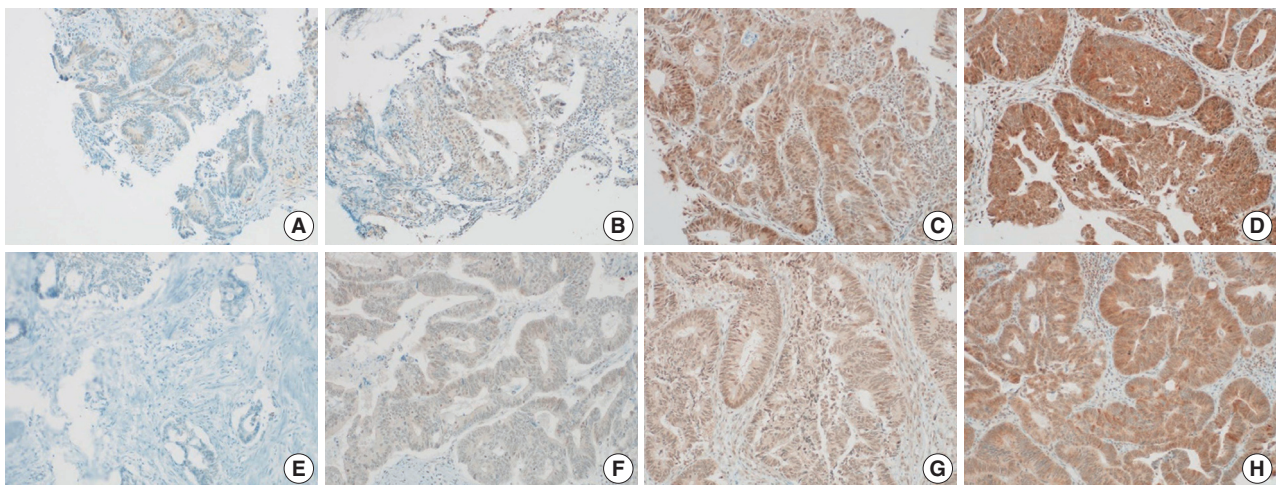


Fig. 1. Immunohistochemistry analyses of PLK4 expression in rectal cancer tissues. The expression of PLK is evaluated by H-score; intensity multiplied by percentage of positive cells. (A) Score 0 (negative staining) of PLK4 expression of pre-CRT specimen. (B) Score 1 (weak staining) of PLK4 expression of pre-CRT specimen. (C) Score 2 (medium staining) of PLK4 expression of pre-CRT specimen. (D) Score 3 (strong staining) of PLK4 expression of pre-CRT specimen. (E) Score 0 (negative staining) of PLK4 expression of post-CRT specimen. (F) Score 1 (weak staining) of PLK4 expression of post-CRT specimen. (G) Score 2 (medium staining) of PLK4 expression of post-CRT specimen. (H) Score 3 (strong staining) of PLK4 expression of post-CRT specimen. PLK4, Polo-like kinase 4; CRT, chemoradiotherapy.

of positive cells and ranges from 0 to 300 points [16]. We scored both the nucleus and cytoplasm of previously selected samples. The intensities were scored as “0” (negative staining), “1” (weak staining), “2” (medium staining), and “3” (strong staining) (Fig. 1). Based on the median H-score, two groups were formed for statistical analysis: “high expression” (H-score > median) and “low expression” (H-score ≤ median).

Statistical analysis

All analyses were performed using IBM SPSS Statistics software ver. 26.0 (IBM Corp., Armonk, NY, USA). Chi-square with Fischer’s exact tests analysis were performed. Kaplan-Meier curves were used for survival analysis. Ordinal logistic regression model was used to compare the influence of individual factors, including age, sex, pT category, pN category, MSI status, and nuclear and cytoplasmic PLK4 expression of the pre-CRT specimen, on the KSP-TRG system. A two-tailed p-value of less than .05 indicated statistical significance.

RESULTS

Cohort characteristics

The median age of the cohort was 65 years (range, 32 to 85 years). Among the 102 patients, 70 (69%) were men and 32 (31%) were women. Rectal cancer recurred in 28 patients (27%), and 11 patients (11%) died. All characteristics of the 102 patients with rectal cancer are shown in Table 1.

PLK4 expression and TRG

High nuclear PLK4 expression in pre-CRT specimens (H-score > 160) correlated with high Mandard-TRG ($p < .001$) and KSP-TRG ($p < .001$). The Mandard-TRG ($p < .001$) and KSP-TRG ($p < .001$) also showed a significant correlation in the group. Furthermore, high cytoplasmic PLK4 expression in the pre-CRT specimens (H-score > 155) correlated with high Mandard-TRG ($p = .022$) and KSP ($p = .013$) systems. Again, the Mandard-TRG ($p = .002$) and KSP-TRG ($p = .004$) were also significantly correlated within groups. There was no association between PLK4 expression in the pre-CRT specimens and other parameters. The results mentioned above are summarized in Table 2. Nuclear PLK4 expression in the post-CRT specimens was correlated with sex ($p = .015$) and mortality ($p = .035$). There was no association between PLK4 expression in the post-CRT specimens and other parameters. The results mentioned above are summarized in Table 3.

High Mandard-TRG correlated with high pT category ($p <$

Table 1. Clinicopathological parameters in 102 cases of rectal cancer patients

Characteristic	No. (%)
Age (yr)	
< 65	50 (49.0)
≥ 65	52 (51.0)
Median (range)	65 (32–85)
Sex	
Male	70 (68.6)
Female	32 (31.4)
Differentiation	
Well	5 (4.9)
Moderate	89 (87.3)
Poorly	5 (4.9)
Lymphovascular invasion	
Absent	71 (69.6)
Present	23 (22.5)
pT category	
Tx–T2	50 (49.0)
T3–T4	52 (51.0)
pN category	
N0	71 (69.6)
N1–N2	31 (30.4)
pM category	
M0	101 (99.0)
M1	1 (1.0)
TRG of Mandard (group)	
TRG1, 2	27 (26.5)
TRG3	37 (36.3)
TRG4, 5	38 (37.3)
TRG of KSP (group)	
TRG0, 1	27 (26.5)
TRG2, 3	75 (73.5)
TRG of Mandard	
TRG1	16 (15.7)
TRG2	11 (10.8)
TRG3	37 (36.3)
TRG4	28 (27.5)
TRG5	10 (9.8)
TRG of KSP	
TRG0	16 (15.7)
TRG1	11 (10.8)
TRG2	39 (38.2)
TRG3	36 (35.3)
MSI	
MSS and MSI-L	93 (91.2)
MSI-H	9 (8.8)
Recurrence	
No	74 (72.5)
Yes	28 (27.5)
Death	
No	91 (89.2)
Yes	11 (10.8)

TRG, tumor regression grade; KSP, The Korean Society for Pathologists; MSI, microsatellite instability; MSS, microsatellite stable; MSI-L, MSI-low; MSI-H, MSI-high.

Table 2. Correlation of PLK4 expression of pre-CRT specimen with clinicopathological parameters in 102 cases of rectal cancer patients

	Nuclear stain of PLK4 in pre-CRT specimen			Cytoplasmic stain of PLK4 in pre-CRT specimen		
	Low expression (H-score ≤ 160)	High expression (H-score > 160)	p-value	Low expression (H-score ≤ 155)	High expression (H-score > 155)	p-value
Age (yr)			.196			> .99
<65	18 (20.9)	24 (27.9)		21 (24.4)	21 (24.4)	
≥65	25 (29.1)	19 (22.1)		22 (25.6)	22 (25.6)	
Sex			.486			.816
Male	31 (36.0)	28 (32.6)		29 (33.7)	30 (34.9)	
Female	12 (14.0)	15 (17.4)		14 (16.3)	13 (15.1)	
Differentiation			.999			.999
Well	2 (2.4)	2 (2.4)		2 (2.4)	2 (2.4)	
Moderate	39 (45.9)	38 (44.7)		39 (45.9)	38 (44.7)	
Poorly	2 (2.4)	2 (2.4)		2 (2.4)	2 (2.4)	
Lymphovascular invasion			.118			.150
Absent	26 (32.5)	35 (43.8)		27 (33.8)	34 (42.5)	
Present	12 (15.0)	7 (8.8)		12 (15.0)	7 (8.8)	
pT category			.518			.518
Tx-T2	23 (26.7)	20 (23.3)		20 (23.3)	23 (26.7)	
T3-T4	20 (23.3)	23 (26.7)		23 (26.7)	20 (23.3)	
pN category			.323			.138
N0	30 (34.9)	34 (39.5)		29 (33.7)	35 (40.7)	
N1-N2	13 (15.1)	9 (10.5)		14 (16.3)	8 (9.3)	
pM category			> .99			.309
M0	42 (49.4)	42 (49.4)		41 (48.2)	43 (50.5)	
M1	1 (1.2)	0		1 (1.2)	0	
TRG of Mandard			< .001			.022
TRG1, 2	19 (22.1)	3 (3.5)		16 (18.6)	6 (7.0)	
TRG3	13 (15.1)	19 (22.1)		16 (18.6)	16 (18.6)	
TRG4, 5	11 (12.8)	21 (24.4)		11 (12.8)	21 (24.4)	
TRG of KSP			< .001			.013
TRG0, 1	19 (22.1)	3 (3.5)		16 (18.6)	6 (7.0)	
TRG2, 3	24 (27.9)	40 (46.5)		27 (31.4)	37 (43.0)	
MSI			> .99			> .99
MSS and MSI-L	39 (45.3)	38 (44.2)		37 (52.1)	28 (39.4)	
MSI-H	4 (4.7)	5 (5.8)		4 (5.6)	2 (2.8)	
Recurrence			.952			.357
No	32 (37.6)	33 (33.8)		31 (44.3)	19 (27.1)	
Yes	10 (23.8)	10 (11.8)		10 (14.3)	10 (14.3)	
Death			> .99			.724
No	40 (46.5)	39 (45.3)		35 (49.3)	27 (38.0)	
Yes	3 (3.5)	4 (4.7)		6 (8.5)	3 (4.2)	

Values are presented as number (%).

PLK4, Polo-like kinase 4; CRT, chemoradiotherapy; TRG, tumor regression grade; KSP, The Korean Society for Pathologists; MSI, microsatellite instability; MSS, microsatellite stable; MSI-L, MSI-low; MSI-H, MSI-high.

.001), high pN category ($p = .026$), microsatellite instability-high ($p = .049$), and high KSP-TRG ($p < .001$). There was no association between the Mandard-TRG and other parameters. The results mentioned above are summarized in Supplementary Table S1. High KSP-TRG correlated with high pT category ($p < .001$), high pN category ($p = .011$), and high Mandard-TRG ($p < .001$). There was no association between the KSP-TRG and other parameters. The results mentioned above are summarized in Sup-

plementary Table S2.

Conversely, there was no significant association between DFS and high nuclear expression of PLK4 ($p = .493$) (Fig. 2A) or high cytoplasmic expression of PLK4 ($p = .677$) (Fig. 2B) in the pre-CRT specimens. There was also no significant association between OS and high nuclear expression of PLK4 ($p = .965$) (Fig. 2C) or high cytoplasmic expression of PLK4 ($p = .434$) (Fig. 2D) in the pre-CRT specimens.

Table 3. Correlation of PLK4 expression of post-CRT specimen with clinicopathological parameters in 102 cases of rectal cancer patients

	Nuclear stain of PLK4 in post-CRT specimen			Cytoplasmic stain of PLK4 in post-CRT specimen		
	Low expression (H-score ≤160)	High expression (H-score >160)	p-value	Low expression (H-score ≤155)	High expression (H-score >155)	p-value
Age (yr)			.252			.897
<65	17 (25.4)	18 (26.9)		28 (41.8)	7 (10.4)	
≥65	20 (29.9)	12 (17.9)		26 (38.8)	6 (9.0)	
Sex			.015			.526
Male	30 (44.8)	16 (23.9)		38 (56.7)	8 (11.9)	
Female	7 (10.4)	14 (20.9)		16 (23.9)	5 (7.5)	
Differentiation			.251			.332
Well	0	2 (3.1)		1 (1.6)	1 (1.6)	
Moderate	34 (53.1)	24 (37.5)		47 (73.4)	11 (17.2)	
Poorly	2 (3.1)	2 (3.1)		4 (6.3)	0	
Lymphovascular invasion			.849			.318
Absent	26 (39.4)	21 (31.8)		36 (54.5)	11 (16.7)	
Present	11 (16.7)	8 (12.1)		17 (25.8)	2 (3.0)	
pT category			.057			.317
Tx-T2	8 (11.9)	13 (19.4)		15 (22.4)	6 (9.0)	
T3-T4	29 (43.3)	17 (25.4)		39 (58.2)	7 (10.4)	
pN category			.154			.753
N0	26 (38.8)	16 (23.9)		33 (49.3)	9 (13.4)	
N1-N2	11 (16.4)	14 (20.9)		21 (31.3)	4 (6.0)	
pM category			>.99			.197
M0	36 (54.5)	29 (43.9)		53 (80.3)	12 (18.2)	
M1	1 (1.5)	0		0	1 (1.5)	
TRG of Mandard			.918			.279
TRG1, 2	2 (3.0)	1 (1.5)		3 (4.5)	0	
TRG3	16 (23.9)	13 (19.4)		21 (31.3)	8 (11.9)	
TRG4, 5	19 (28.4)	16 (23.9)		30 (44.8)	5 (7.5)	
TRG of KSP			>.99			>.99
TRG0, 1	2 (3.0)	1 (1.5)		3 (4.5)	0	
TRG2, 3	35 (52.2)	29 (43.3)		51 (76.1)	13 (19.4)	
MSI			>.99			.574
MSS and MSI-L	34 (50.7)	28 (41.8)		49 (73.1)	13 (19.4)	
MSI-H	3 (4.5)	2 (3.0)		5 (7.5)	0	
Recurrence			.671			.314
No	25 (37.9)	21 (31.8)		35 (53.0)	11 (16.7)	
Yes	12 (18.2)	8 (12.1)		18 (27.3)	2 (3.0)	
Death			.035			.677
No	29 (43.3)	29 (43.3)		46 (68.7)	12 (17.9)	
Yes	8 (11.9)	1 (1.5)		8 (11.9)	1 (1.5)	

PLK4, Polo-like kinase 4; CRT, chemoradiotherapy; TRG, tumor regression grade; KSP, The Korean Society for Pathologists; MSI, microsatellite instability; MSS, microsatellite stable; MSI-L, MSI-low; MSI-H, MSI-high.

Multivariate analysis for the KSP-TRG

Multivariate analysis showed that pT category and nuclear and cytoplasmic PLK4 expression in the pre-CRT specimens were statistically associated with the KSP-TRG ($p < .05$). Other variables, including age, sex, pN category, and MSI status, were not associated with the KSP-TRG. In addition, pT category and nuclear and cytoplasmic PLK4 expression in the pre-CRT specimens were statistically independent of each other or other variables. The results mentioned above are summarized in Table 4.

DISCUSSION

In this study, we first distinguished the expression of immunohistochemical staining of PLK4 in samples before and after CRT by its high and low expressions and classified them according to the clinical data, including the prognosis and histopathological features. We also found that the expression of PLK4 in the pre-CRT specimens was associated with both the Mandard-TRG and KSP-TRG. This association was found in both nuclear

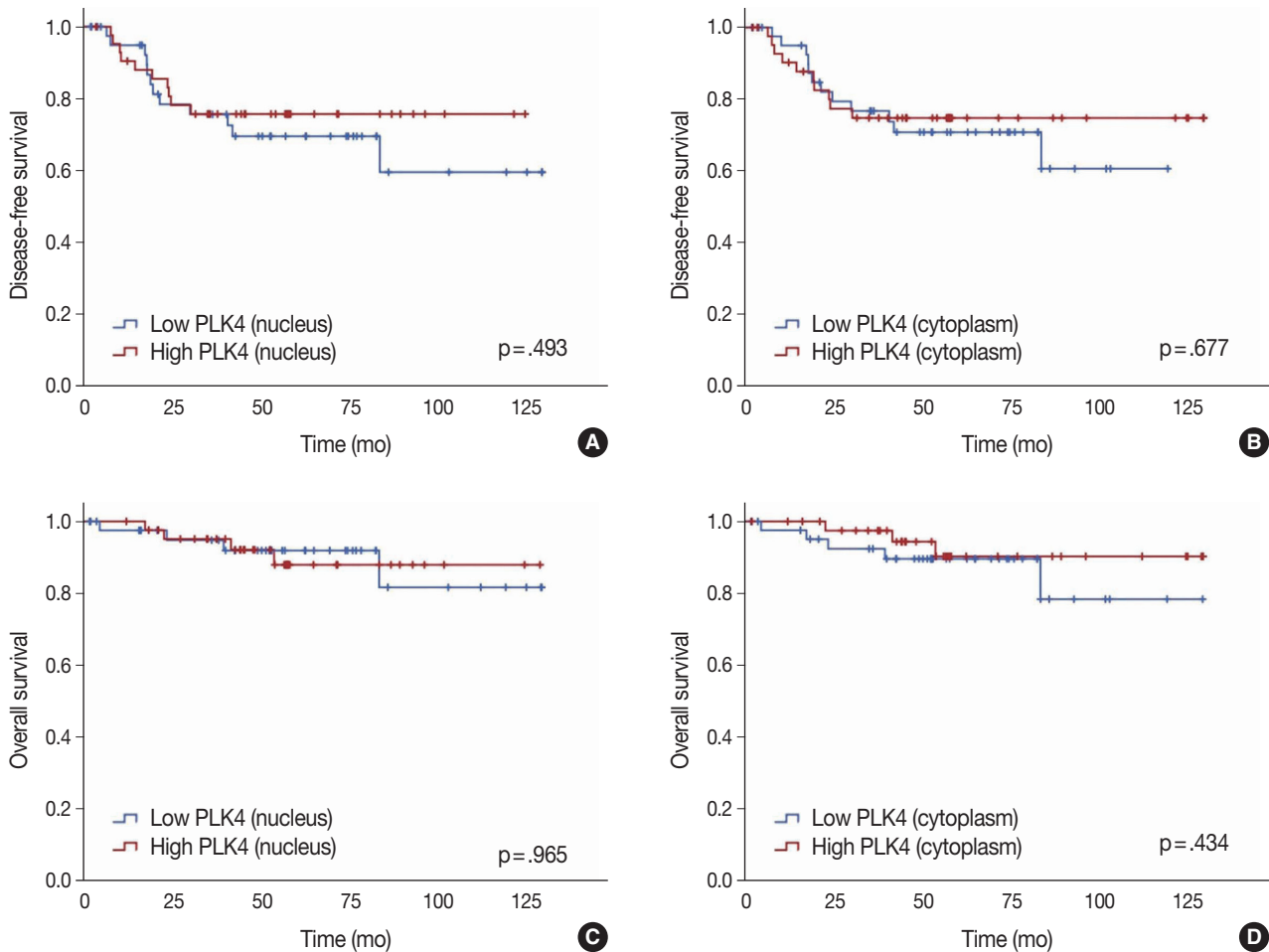


Fig. 2. (A) Kaplan-Meier curves of disease-free survival in high and low expression of nuclear expression of PLK4 of pre-CRT specimen. (B) Kaplan-Meier curves of disease-free survival in high and low expression of cytoplasmic expression of PLK4 of pre-CRT specimen. (C) Kaplan-Meier curves of overall survival in high and low nuclear expression of PLK4 of pre-CRT specimen. (D) Kaplan-Meier curves of overall survival in high and low expression of cytoplasmic expression of PLK4 of pre-CRT specimen. PLK4, Polo-like kinase 4; CRT, chemoradiotherapy.

Table 4. Multivariate analysis (ordinal logistic regression test) of TRG of KSP associated with clinicopathologic variables including nuclear and cytoplasmic PLK4 stain of pre-CRT specimen

Variable	Estimate	p-value	95% Confidence interval
Including nuclear PLK4 stain of pre-CRT specimen			
Age	-0.685	.113	-1.532 to 0.161
Sex	-0.173	.708	-1.080 to 0.734
pT category	-1.403	.003	-2.338 to -0.469
pN category	-0.520	.330	-1.567 to 0.527
MSI state	-0.578	.406	-1.939 to 0.784
Nuclear PLK4 stain of pre-CRT specimen	-1.766	<.001	-2.667 to -0.866
Including cytoplasmic PLK4 stain of pre-CRT specimen			
Age	-0.411	.329	-1.237 to 0.415
Sex	-0.351	.444	-1.250 to 0.548
pT category	-1.595	.001	-2.532 to -0.658
pN category	-0.513	.335	-1.558 to 0.531
MSI state	-0.444	.530	-1.829 to 0.940
Cytoplasmic PLK4 stain of pre-CRT specimen	-1.500	.001	-2.376 to -0.623

TRG, tumor regression grade; KSP, The Korean Society for Pathologists; PLK4, Polo-like kinase 4; CRT, chemoradiotherapy; MSI, microsatellite instability.

and cytoplasmic expression. Therefore, preoperative evaluation of PLK4 will be useful as one of the methods to predict the response of rectal cancer patients to CRT. Unfortunately, the association between PLK4 and prognosis was not revealed in this study and more robust studies are needed in the future to support this possibility.

Although radiation therapy before surgery reduces the local recurrence rate by more than 50% than surgery alone [1] and treatment for rectal cancer has greatly evolved in recent years, patients are prone to recurrence and many eventually die from the disease. Therefore, the importance of the response to preoperative CRT in rectal cancer is very important.

In a study on the correlation between preoperative CRT and PLK4 expression, PLK4 enhanced chemoradiation resistance in glioblastoma multiforme (GBM), whereas PLK4 knockdown via lentiviral transfection significantly increased the chemoradiation sensitivity of GBM cells [17]. The authors stated that PLK4 was transcriptionally regulated depending on *ATAD2* (ATPase family AAA domain containing 2), a gene involved in cell proliferation and metastasis, and that this regulation increased PLK4 radioresistance. In addition, PLK4 expression is known to be a negative predictor of response to taxane-based neoadjuvant chemotherapy [18]. The authors stated that the resistance to taxane-based chemotherapy appeared in patients with high PLK4 expression because PLK4 was involved as an upstream regulator of gamma-tubulin, which affected the treatment response to taxane. Therefore, the authors concluded that PLK4 inhibitors enhanced the effect of chemotherapy. However, reports on the possibility of prognostic effects of PLK4 expression in rectal cancer are lacking.

There are several drawbacks to our study. The most significant drawback was the limited number of cases. Despite the small sample size that could undermine the power of the study, we found a significant difference, which should be confirmed by large-scale studies in the future. Additionally, the retrospective nature of the study was a limitation to its design. It would also be necessary to design a better-validated study with no missing factors. Future research with better power should be conducted to confirm the preliminary results obtained from this study.

We reported PLK4 expression and the prognosis of rectal cancer by dividing our study into pre-CRT and post-CRT groups. Based on our human tissue study results, PLK4 expression could be a potential predictor for the response of CRT. Therefore, the clinical development of PLK4 could be an effective therapeutic strategy for the management of advanced rectal cancer.

Supplementary Information

The Data Supplement is available with this article at <https://doi.org/10.4132/jptm.2021.10.07>.

Ethics Statement

All procedures performed in the current study were approved by the Institutional Review Board (IRB) of the Keimyung University Dongsan Hospital (DSMC 2019-09-007-002) in accordance with the 1964 Helsinki declaration and its later amendments. Formal written informed consent was not required with a waiver by the IRB.

Availability of Data and Material

The datasets generated or analyzed during the study are available from the corresponding author on reasonable request.

Code Availability

Not applicable.

ORCID

Hyunseung Oh	https://orcid.org/0000-0001-9440-189X
Soon Gu Kim	https://orcid.org/0000-0002-1436-8442
Sung Uk Bae	https://orcid.org/0000-0002-7876-4196
Sang Jun Byun	https://orcid.org/0000-0002-6115-2804
Shin Kim	https://orcid.org/0000-0002-1099-5027
Jae-Ho Lee	https://orcid.org/0000-0002-5562-0720
Ilseon Hwang	https://orcid.org/0000-0002-6122-4417
Sun Young Kwon	https://orcid.org/0000-0002-8410-0185
Hye Won Lee	https://orcid.org/0000-0001-8540-524X

Author Contributions

Conceptualization: HWL. Methodology: HO, IH, SGK, HWL. Data curation: SUB, SJB, SK, JHL. Formal analysis: HO, IH, SGK. Supervision: SYK. Visualization: HO, SGK. Writing—original draft: HO, HWL. Writing—review & editing: HO, IH, SYK, HWL. Approval of final manuscript: all authors.

Conflicts of Interest

The authors declare that they have no potential conflicts of interest.

Funding Statement

This work was supported by the National Research Foundation of Korea (NRF) grant funded by the Korea government (MSIT) (No. 2017R1C1B5077166).

References

1. Camma C, Giunta M, Fiorica F, Pagliaro L, Craxi A, Cottone M. Preoperative radiotherapy for resectable rectal cancer: a meta-analysis. *JAMA* 2000; 284: 1008-15.
2. Bettencourt-Dias M, Rodrigues-Martins A, Carpenter L, et al. SAK/PLK4 is required for centriole duplication and flagella development. *Curr Biol* 2005; 15: 2199-207.
3. Habadanck R, Stierhof YD, Wilkinson CJ, Nigg EA. The Polo kinase Plk4 functions in centriole duplication. *Nat Cell Biol* 2005; 7: 1140-6.
4. Sillibourne JE, Tack F, Vloemans N, et al. Autophosphorylation of polo-like kinase 4 and its role in centriole duplication. *Mol Biol Cell* 2010; 21: 547-61.
5. Rodrigues-Martins A, Riparbelli M, Callaini G, Glover DM, Bet-

- tencourt-Dias M. Revisiting the role of the mother centriole in centriole biogenesis. *Science* 2007; 316: 1046-50.
6. Macmillan JC, Hudson JW, Bull S, Dennis JW, Swallow CJ. Comparative expression of the mitotic regulators SAK and PLK in colorectal cancer. *Ann Surg Oncol* 2001; 8: 729-40.
 7. Mason JM, Lin DC, Wei X, et al. Functional characterization of CFI-400945, a Polo-like kinase 4 inhibitor, as a potential anticancer agent. *Cancer Cell* 2014; 26: 163-76.
 8. Denu RA, Zasadil LM, Kanugh C, Laffin J, Weaver BA, Burkard ME. Centrosome amplification induces high grade features and is prognostic of worse outcomes in breast cancer. *BMC Cancer* 2016; 16: 47.
 9. Coelho PA, Bury L, Shahbazi MN, et al. Over-expression of Plk4 induces centrosome amplification, loss of primary cilia and associated tissue hyperplasia in the mouse. *Open Biol* 2015; 5: 150209.
 10. Sercin O, Larsimont JC, Karambelas AE, et al. Transient PLK4 over-expression accelerates tumorigenesis in p53-deficient epidermis. *Nat Cell Biol* 2016; 18: 100-10.
 11. Ko MA, Rosario CO, Hudson JW, et al. Plk4 haploinsufficiency causes mitotic infidelity and carcinogenesis. *Nat Genet* 2005; 37: 883-8.
 12. Rosario CO, Ko MA, Haffani YZ, et al. Plk4 is required for cytokinesis and maintenance of chromosomal stability. *Proc Natl Acad Sci U S A* 2010; 107: 6888-93.
 13. Kazazian K, Go C, Wu H, et al. Plk4 promotes cancer invasion and metastasis through Arp2/3 complex regulation of the actin cytoskeleton. *Cancer Res* 2017; 77: 434-47.
 14. Mandard AM, Dalibard F, Mandard JC, et al. Pathologic assessment of tumor regression after preoperative chemoradiotherapy of esophageal carcinoma: clinicopathologic correlations. *Cancer* 1994; 73: 2680-6.
 15. Kim BH, Kim JM, Kang GH, et al. Standardized pathology report for colorectal cancer, 2nd edition. *J Pathol Transl Med* 2020; 54: 1-19.
 16. McCarty KS Jr, Miller LS, Cox EB, Konrath J, McCarty KS Sr. Estrogen receptor analyses. Correlation of biochemical and immunohistochemical methods using monoclonal antireceptor antibodies. *Arch Pathol Lab Med* 1985; 109: 716-21.
 17. Wang J, Zuo J, Wang M, et al. Pololike kinase 4 promotes tumorigenesis and induces resistance to radiotherapy in glioblastoma. *Oncol Rep* 2019; 41: 2159-67.
 18. Li Z, Dai K, Wang C, et al. Expression of polo-like kinase 4 (PLK4) in breast cancer and its response to taxane-based neoadjuvant chemotherapy. *J Cancer* 2016; 7: 1125-32.

Chronic lymphocytic leukemia and concurrent seminoma in the same testis

Kosuke Miyai^{1,2}, Fumihisa Kumazawa¹, Kimiya Sato¹, Hitoshi Tsuda¹

¹Department of Basic Pathology, National Defense Medical College, Saitama; ²Department of Pathology, Japan Self-Defense Forces Central Hospital, Tokyo, Japan

A 59-year-old man presented with a painless testicular mass and underwent a radical orchiectomy. The resected specimen showed a 5-cm-sized, white-yellow and homogenous solid mass in the testicular parenchyma. Histologically, the central part of the tumor exhibited typical features of seminoma. The peripheral part of the tumor exhibited diffuse infiltration of small, monotonous lymphoid cells involving the tunica albuginea. The monotonous lymphoid cells were immunoreactive for CD20, CD79a, CD5, and CD23, and negative for CD3, CD10, and cyclin D1. Kappa light chain restriction was detected on flow cytometry using the resected specimen. Considering the circulating lymphoid cell count of $>5.0 \times 10^3/\mu\text{L}$, we diagnosed the peripheral component of the tumor as an infiltration of chronic lymphocytic leukemia. This extremely rare combination of seminoma and lymphoid neoplasm should be considered in the differential diagnosis of classic seminoma with extensive lymphoid reaction in tumors arising in elderly patients.

Key Words: Testis; Seminoma; Chronic lymphocytic leukemia; Concurrent tumor

Received: May 31, 2021 **Revised:** July 12, 2021 **Accepted:** September 10, 2021

Corresponding Author: Kosuke Miyai, MD, PhD, Department of Basic Pathology, National Defense Medical College, 3-2 Namiki, Tokorozawa, Saitama 359-8513, Japan
 Tel: +81-4-2995-1211, Fax: +81-4-2996-5193, E-mail: mykusu228@nifty.com

Germ cell tumors derived from germ cell neoplasia in situ (GCNIS) account for more than 90% of testicular tumors, and approximately half of these tumors are histologically determined to be pure seminomas [1]. In contrast, less than 5% of testicular neoplasms are malignant lymphomas, most of which are diffuse large B-cell lymphomas (DLBCLs) [2]. As the distribution of age at onset differs between testicular germ cell tumors (20–45 years) and lymphomas (> 50 years) [1,2], only a few reports have described the concurrent and/or synchronous presentation of testicular seminoma and lymphoid neoplasms [3-6]. Leukemia, including lymphoid and myelogenous subtypes, can also involve testis in a subset of cases [7,8]. Chronic lymphocytic leukemia (CLL) is an indolent type of lymphoid neoplasm, characterized by an increased number of peripheral monoclonal B-lymphocytes, as well as lymphadenopathy, organomegaly, and cytopenia. Extranodal involvement—including the skin, gastrointestinal tract, or central nervous system—has been reported in a small subset of the patients, and testicular involvement is relatively rare [7]. Recently, we experienced a unique case of CLL and concurrent seminoma in a single tumor of the same testis. Herein, we de-

scribe the clinicopathological features of this case.

CASE REPORT

A 59-year-old Japanese man, without any notable past or familial medical history, was admitted to our hospital because of a painless right testicular mass. Abdominal and pelvic computed tomography (CT) revealed a 4.5 cm-sized mass in the right testicular parenchyma without evidence of ascites or nodal/distant metastasis. His interleukin-2 receptor level was 613 U/mL (normal range, 122 to 496 U/mL), and the levels of lactate dehydrogenase, α -fetoprotein, and human chorionic gonadotropin were within the normal limits. His white blood cell count on admission was $12.0 \times 10^3/\mu\text{L}$ with a lymphocyte percentage of 69.3% (absolute lymphocyte count, $8.3 \times 10^3/\mu\text{L}$). No obvious anemia or thrombocytopenia was observed. Under the clinical diagnosis of a germ cell tumor or malignant lymphoma, right radical orchiectomy was performed.

The cut surface of the resected specimen showed a well-circumscribed, white-yellow and homogenous solid mass with no

hemorrhage or necrosis measuring $5.0 \times 4.0 \times 2.9$ cm in the testicular parenchyma (Fig. 1). Histologically, the tumor consisted of two components: a central multinodular component and a peripheral diffuse infiltrative component (Fig. 2A). The multinodular component was composed of large polygonal cells with clear cytoplasm and prominent nucleoli intermingled with lymphocytes (Fig. 2B). Around the nodular proliferation of polygonal tumor cells, dense infiltration of variously sized lymphocytes with multiple lymphoid follicles was observed. In contrast, the peripheral part of the tumor exhibited monotonous, diffuse infiltration of small lymphoid cells, focally involving the entire tunica albuginea (Fig. 2C). Immunohistochemically, the large polygonal cells were diffusely positive for octamer-binding transcription factor 4 (Oct-4), and scattered Oct-4-positive cells were detected in the peritumoral seminiferous tubules (Fig. 2D); these observations confirmed the diagnosis of seminoma and the corresponding GCNIS. No vascular permeation, invasion beyond the tunica albuginea, or spermatic cord invasion by the seminoma cells was observed (pathological T1).

The peripheral monotonous lymphoid cells were immunoreactive for CD20, CD79a, CD5, and CD23 and negative for CD3, CD21, CD10, and cyclin D1 (Fig. 2E, F). Kappa light chain restriction was detected during flow cytometry using the resected specimen. Considering that the patient's circulating lymphoid cell count was $> 5.0 \times 10^3/\mu\text{L}$ at admission, the peripheral component of the tumor was diagnosed as testicular involvement of CLL. Immunostaining for CD21 revealed a retained follicular dendritic-cell meshwork in the lymphoid stroma of the seminoma (Fig. 3A). The Ki67 labeling index in the lymphoid stroma of the seminoma was much higher than that in CLL (approximately

30% vs. <5%) (Fig. 3B). These findings suggested that CLL was not intermixed with the lymphoid stroma of the seminoma; these two components existed exclusively within a single tumor mass. Postoperative fluorodeoxyglucose positron emission tomography/CT showed no obvious nodal lesions or mass-forming lesions within systemic organs. The patient required no additional therapy during follow-up, and remained alive and well, with no evidence of disease progression, recurrence, or metastases after 2 years.

DISCUSSION

A vast majority of primary testicular lymphoid neoplasms (80%–95%) are DLBCLs [2]. Previously reports of other rare histological types of malignant lymphoma included mantle cell lymphoma [9], testicular follicular lymphoma [10], extranodal marginal zone lymphoma [11], natural killer/T-cell lymphoma, nasal type [12], peripheral T-cell lymphoma (PTCL) [13], and activin receptor-like kinase-1-negative anaplastic large cell lymphoma [14]. On the other hand, testicular involvement of lymphoid leukemia has been described in some previous reports [7,8]. In a previous report reviewing 13,500 autopsy and 641 surgical specimens, seven cases with lymphoid leukemia secondarily involving the testis were detected; 6 were acute lymphoblastic leukemia (without information of B- or T-cell lineage) and only one case was CLL [7]. Schniederjan and Osunkoya [8] identified 40 patients with lymphoid neoplasms of male urogenital organs. Of these, two were acute B-lymphoblastic leukemia in the testis and 4 were CLL in the prostate [8]. There have been a few reported cases of Richter syndrome, defined as the development of DLBCL in a patient with a previous or concomitant CLL/small lymphocytic lymphoma, with testicular involvement [15,16]. In the present report, we described an additional rare case of testicular involvement of CLL without progression to DLBCL.

The present case also showed the synchronous, concurrent CLL and seminoma in a single testicular tumor. There is no obvious pathophysiologic link or common risk factor between seminoma and CLL. Our literature review found a few rare examples of patients with synchronous seminoma and lymphoid neoplasms. All of these patients—including the present one—were aged more than 50 years [3–6]. Singh et al. [3] reported a case of synchronous classical Hodgkin lymphoma in the mediastinal/intra-abdominal lymph nodes and right testicular seminoma. In another case, a huge pelvic mass and partially obstructed small intestine were simultaneously, but separately, resected, and histological examination of these two lesions revealed pure seminoma and DLBCL, respectively [4]. Jacobsen et al. [5] described



Fig. 1. The cut surface of the resected specimen shows a white-yellow, solid mass measuring 5.0 cm in the right testicular parenchyma.

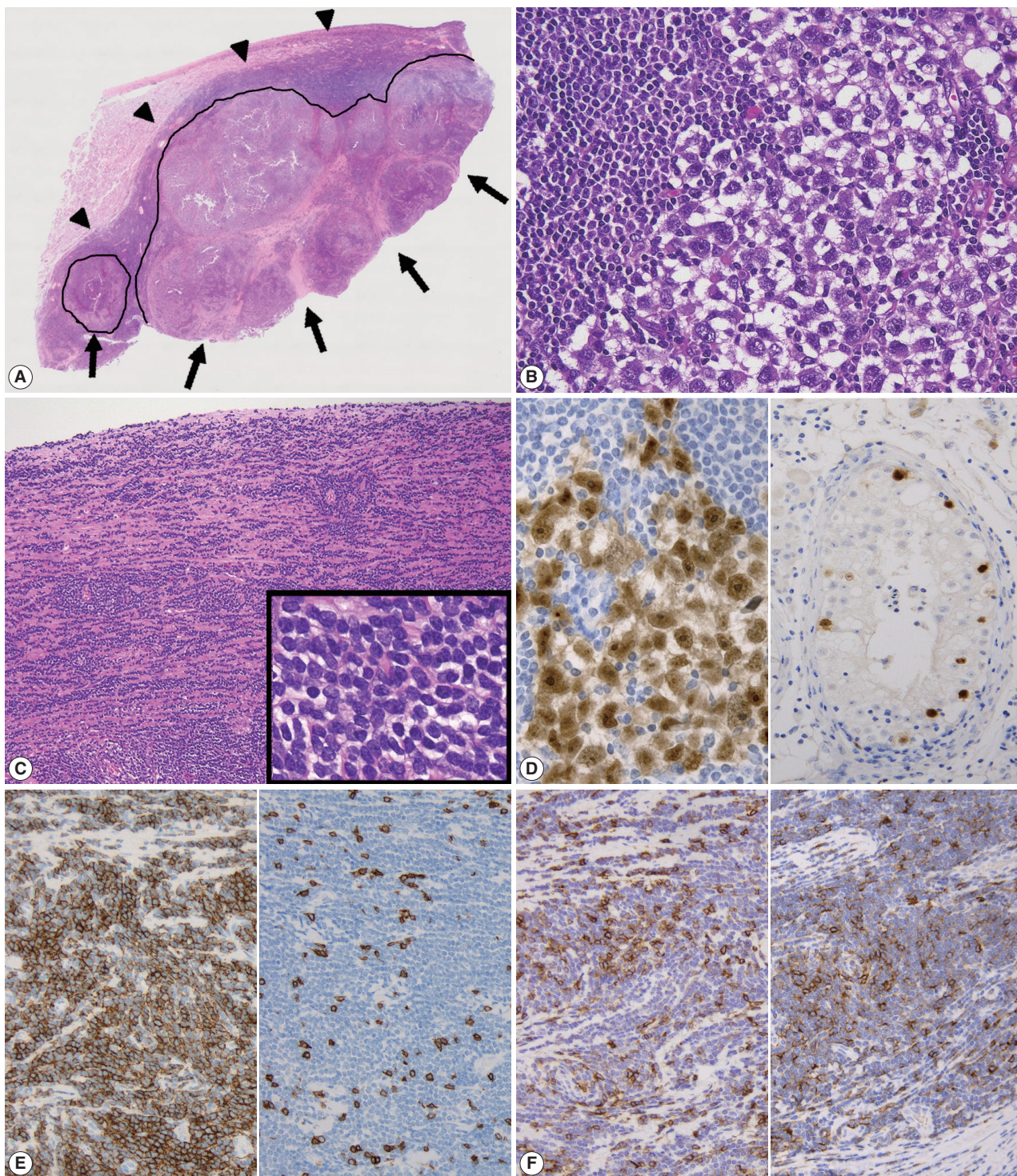


Fig. 2. (A) The scan image showing a central multinodular component (arrows) and peripheral diffuse infiltrative component (arrowheads). (B) The multinodular component comprises large polygonal cells with clear cytoplasm and prominent nucleoli intermingled with variously sized lymphocytes. (C) The peripheral component showing diffuse, dense infiltration of small lymphoid cells involving the entire tunica albuginea. Lymphoid cells with hyperchromatic and monotonous nuclei are noted (inset). (D) The large polygonal cells are diffusely positive for octamer-binding transcription factor 4 (Oct-4) (left), and scattered Oct-4-positive cells are detected in the seminiferous tubules (right). (E, F) Small, monotonous lymphoid cells are diffusely immunoreactive for CD20 (E, left), CD5 (F, left), and CD23 (F, right) and negative for CD3 (E, right).

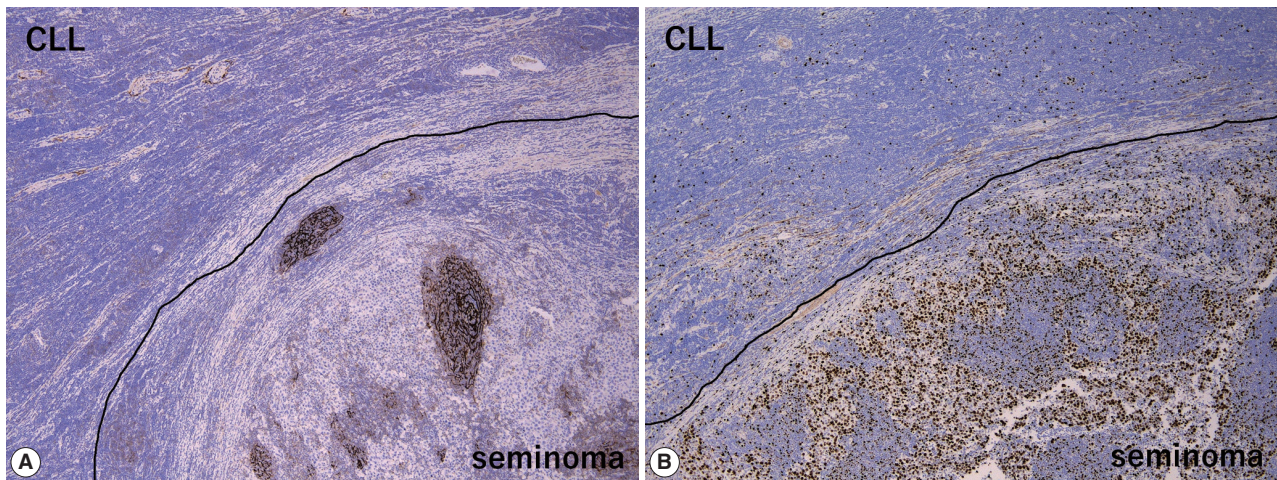


Fig. 3. (A) Meshwork of CD21+ follicular dendritic cells is retained in the lymphoid stroma of the seminoma; it is absent in the chronic lymphocytic leukemia (CLL). (B) The Ki-67 labeling indices in the lymphoid stroma of the seminoma and CLL were approximately 30% and <5%, respectively.

a case of metastatic seminoma and concurrent follicular lymphoma, grade 1 in a supraclavicular lymph node. Only one case of concurrent seminoma and PTCL, NOS in the same testis has been reported [6]. Because of indolent clinical courses of CLL and seminoma, additional/adjuvant therapy was not administered for both tumors in the present case. However, concurrent management of the two different malignancies is usually necessary in these cases. An accurate pathological diagnosis is especially important for improving the patients' clinical courses.

Concerning the large cell component of the present tumor, the presence of GCNIS and careful histological/immunohistochemical examination made it possible to distinguish the seminoma from other tumors including large cell lymphoid neoplasms (DLBCL, PTCL, and anaplastic large cell lymphoma) and solid-type non-seminomatous tumors (embryonal carcinoma and yolk sac tumor). However, when DLBCL is detected, surrounded by dense, small lymphocytic infiltration as in the present case, Richter syndrome should be considered during differential diagnosis [15,16]. On the other hand, differential diagnoses of the small cell component of the present tumor (i.e., CLL) include non-neoplastic, reactive lymphocytes and other mature small B-cell lymphomas, such as follicular lymphoma, mantle cell lymphoma, and extranodal marginal zone lymphoma. Of these, the most important differential diagnosis is small reactive lymphocytes infiltrating into the seminoma, which can be misdiagnosed as "two-cell pattern" of classic seminoma. Compared to small monotonous lymphoid tumor cells of CLL, lymphoid stroma intervening in seminoma cells is composed of various sizes of lymphocytes. In addition, reactive lymphocytes in seminoma sometimes exhibit

lymphoid follicles with CD21-positive follicular dendritic-cell meshwork (Fig. 3A) and show much higher Ki67 labeling index than CLL (Fig. 3B). Finally, because immunohistochemical detection of the monoclonality of lymphoid cells without plasmacytic differentiation is sometimes challenging, light chain restriction detected by flow cytometry is useful for ruling out non-neoplastic, reactive lymphocytic infiltration. Our patient's specific immunohistochemical findings (CD20+, CD3+, and CD23+) and a circulating lymphoid cell count of $>5.0 \times 10^3/\mu\text{L}$ supported the diagnosis of CLL rather than that of other mature small B-cell lymphomas.

In summary, we have described a case of isolated CLL with concurrent seminoma in the same testis. With respect to diagnostic and therapeutic aspects, this extremely rare combination should be kept in mind for both clinicians and pathologists.

Ethics Statement

This single case report in exempted submission to Institutional Review Board and subsequent informed consent by the National Defense Medical College, Tokorozawa, Japan.

Availability of Data and Material

Data sharing not applicable to this article as no datasets were generated or analyzed during the study.

Code Availability

Not applicable.

ORCID

Kosuke Miyai <https://orcid.org/0000-0003-1776-3541>
 Fumihisa Kumazawa <https://orcid.org/0000-0001-9019-669X>
 Kimiya Sato <https://orcid.org/0000-0002-8534-8852>

Hitoshi Tsuda <https://orcid.org/0000-0003-3457-4224>

Author Contributions

Conceptualization: KM. Data curation: KM, FK. Formal analysis: KM. Funding acquisition: KM. Investigation: KM, FK, KS. Methodology: KM, FK, KS. Resources: KS, HT. Supervision: KS, HT. Visualization: KM. Writing—original draft: KM. Writing—review & editing: FK, KS, HT. Approval of final manuscript: all authors.

Conflicts of Interest

The authors declare that they have no potential conflicts of interest.

Funding Statement

This work was supported by JSPS KAKENHI Grant Number 19K16729 (KM).

Acknowledgments

The authors deeply appreciate Drs. Shojiro Morinaga and Koichi Oshima for their advice regarding the pathological diagnosis of the present case.

References

- Ulbright TM, Amin MB, Balzer B, et al. Germ cell tumours. In: Mock H, Humphrey PA, Ulbright TM, Reuter VE, eds. WHO classification of tumours of the urinary system and male genital organs. 4th ed. Lyon: IARC Press, 2016; 189-226.
- Cheah CY, Wirth A, Seymour JF. Primary testicular lymphoma. *Blood* 2014; 123: 486-93.
- Singh P, Toom S, Shrivastava M, et al. Synchronous Hodgkin's lymphoma and seminoma: a rare coexistence and an important lesson. *Clin Case Rep* 2017; 5: 1658-9.
- White MA, Dehaan AP, Wilson JM, Zakem MH, Maatman TJ. Synchronous advanced pure seminoma and diffuse large B-cell lymphoma: a case of multiple oncologic dilemmas. *J Clin Oncol* 2009; 27: e181-3.
- Jacobsen E, Chen JH, Schurko B, Benson C, Oh WK. Metastatic seminoma and grade 1 follicular lymphoma presenting concurrently in a supraclavicular lymph node: a case report. *Cases J* 2009; 2: 7273.
- Kitagawa J, Goto N, Shibata Y, et al. Peripheral T-cell lymphoma, not otherwise specified and concurrent seminoma in testis. *J Clin Exp Hematop* 2015; 55: 169-74.
- Dutt N, Bates AW, Baithun SI. Secondary neoplasms of the male genital tract with different patterns of involvement in adults and children. *Histopathology* 2000; 37: 323-31.
- Schniederjan SD, Osunkoya AO. Lymphoid neoplasms of the urinary tract and male genital organs: a clinicopathological study of 40 cases. *Mod Pathol* 2009; 22: 1057-65.
- Epstein AS, Hedvat C, Habib F, Hamlin P. Testis-isolated mantle cell lymphoma: a unique case. *Clin Lymphoma Myeloma Leuk* 2011; 11: 439-41.
- Finn LS, Viswanatha DS, Belasco JB, et al. Primary follicular lymphoma of the testis in childhood. *Cancer* 1999; 85: 1626-35.
- Kuper-Hommel MJ, Janssen-Heijnen ML, Vreugdenhil G, et al. Clinical and pathological features of testicular diffuse large B-cell lymphoma: a heterogeneous disease. *Leuk Lymphoma* 2012; 53: 242-6.
- Liang DN, Yang ZR, Wang WY, et al. Extranodal nasal type natural killer/T-cell lymphoma of testis: report of seven cases with review of literature. *Leuk Lymphoma* 2012; 53: 1117-23.
- Jun HJ, Kim WS, Yang JH, et al. Orbital infiltration as the first site of relapse of primary testicular T-cell lymphoma. *Cancer Res Treat* 2007; 39: 40-3.
- Lagmay J, Termuhlen A, Fung B, Ranalli M. Primary testicular presentation of ALK-1-negative anaplastic large cell lymphoma in a pediatric patient. *J Pediatr Hematol Oncol* 2009; 31: 330-2.
- Jha B, Dass J, Sachdev R, Bhargava R. Testicular swelling: a rare manifestation of chronic lymphocytic leukemia presenting with Richter's syndrome. *Indian J Pathol Microbiol* 2014; 57: 133-5.
- Kawase K, Naiki T, Naiki-Ito A, et al. Rare case of Richter syndrome with testicular involvement successfully obtained good prognosis with rapid operation and immunochemotherapy. *IJU Case Rep* 2019; 2: 232-5.

TTF1-positive *SMARCA4*/BRG1 deficient lung adenocarcinoma

Anurag Mehta¹, Himanshi Diwan¹, Divya Bansal¹, Manoj Gupta²

Departments of ¹Laboratory, Molecular and Transfusion Services and ²Nuclear Medicine, Rajiv Gandhi Cancer Institute and Research Centre (RGCIRC), New Delhi, India

SMARCA4/BRG1-deficient lung adenocarcinoma (SD-LUAD) is being recognized as a distinct subtype based on subtle differences in its clinical, morphological, and immunophenotypic attributes compared to other non-small cell lung carcinomas. We present here a case of SD-LUAD with curious thyroid transcription factor 1 (TTF1) expression in a morphologically heterogenous lung adenocarcinoma. The better differentiated area showed preservation of TTF1 expression, and a poorly differentiated tumor had loss of TTF1 expression with universal BRG1 loss.

Key Words: BRG1; Lung; Non-small cell lung carcinoma; *SMARCA4*; Thyroid transcription factor 1

Received: July 4, 2021 **Revised:** August 27, 2021 **Accepted:** September 16, 2021

Corresponding Author: Himanshi Diwan, MD, Department of Laboratory, Molecular and Transfusion Services, Rajiv Gandhi Cancer Institute and Research Centre, New Delhi 110085, India

Tel: +91-9413542252, Fax: +91-11-27051037, E-mail: himanshidiwan89@gmail.com

Mammalian switch/sucrose non-fermentable (SWI/SNF) complex is a major chromatin remodeling pathway comprising of three orthologues. Of these, BRG1/BRM-associated factor (BAF) is most significant with *SMARCA4* and *SMARCA2* providing energy through their ATPase like enzymatic activity [1]. *SMARCA4* gene encodes BRG1 (Brahma related gene), which is a catalytic subunit of the SWI/SNF complex. Several *SMARCA4* mutated cancers have been described, of these small cell carcinomas of ovary, hypercalcemic-type, and thoracic tumors have been best studied. It is widely believed that *SMARCA4*/BRG1-deficient lung adenocarcinoma (SD-LUAD) is devoid of thyroid transcription factor 1 (TTF1) expression though a contrary view exists [2-5]. We report a case of morphologically heterogenous lung adenocarcinoma with heterogenous TTF1 expression and universal BRG1 loss.

CASE REPORT

A 54-year-old male, chronic smoker with a 40 pack-year history, presented with complaints of breathlessness and hemoptysis. Routine laboratory investigations were within normal limits. Chest X-ray revealed a large rounded mass in the parahilar region of the left lung with mediastinal widening. Whole-body positron

emission tomography and non-diagnostic computed tomography (PET-CT) revealed a parahilar mass in the left lung measuring 6.2×4.8 cm with bulky mediastinal lymphadenopathy and bony metastases (Fig. 1). Computed tomography (CT)-guided trucut biopsy from the left lung mass revealed a heterogeneous tumor with solid pattern (Fig. 2A). The tumor cells in the better differentiated area had bland nuclei, high nuclear to cytoplasmic ratio, and a compact morphology (Fig. 2B, C). The tumor cells in other areas had abundant pink bubbly cytoplasm, pleomorphic vesicular nuclei with prominent nucleoli, and brisk mitoses (Fig. 2D, E). Neutrophilic emperipolesis and inflamed stroma were also seen in these areas (Fig. 2D, E).

Upon immunohistochemistry (IHC) analysis, tumor cells in the better differentiated area (Fig. 3A) expressed cytokeratin (CK) (Fig. 3B), but lacked BRG1 expression (Fig. 3C). These tumor cells were positive for TTF1 (Fig. 3D) while tumor cells in lesser differentiated area (Fig. 3E) expressed weaker CK (Fig. 3F), and were devoid of BRG1 (Fig. 3G) and TTF1 (Fig. 3H). In summary, tumor cells in both the areas were devoid of BRG1 and expressed CK, CK7, epithelial membrane antigen, and BerEp4, while TTF1 expression was noted only in better differentiated component. On additional IHC, the tumor cells in the better differentiated area revealed aberrant expression of SRY-box tran-

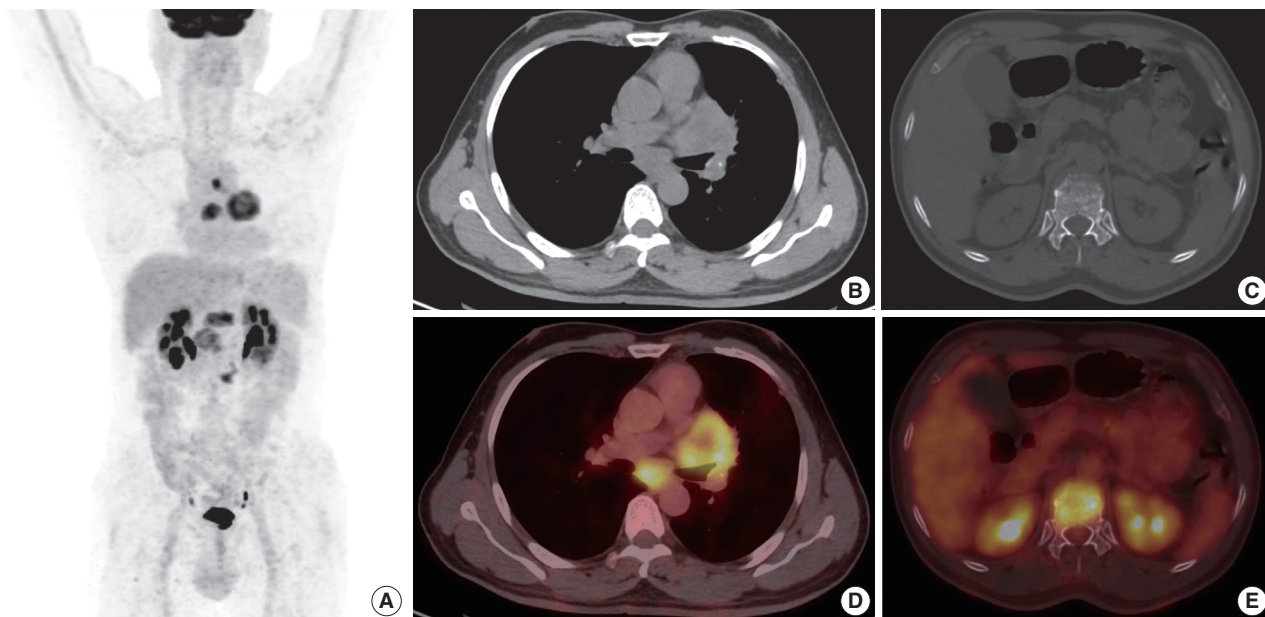


Fig. 1. Positron emission tomography computed tomography (PET-CT) image. (A) Maximum intensity projection. (B, C) Axial computed tomography. (D, E) Fused fluorodeoxyglucose PET-CT axial images showing left lung central lesion with mediastinal lymph nodes and bone lesions.

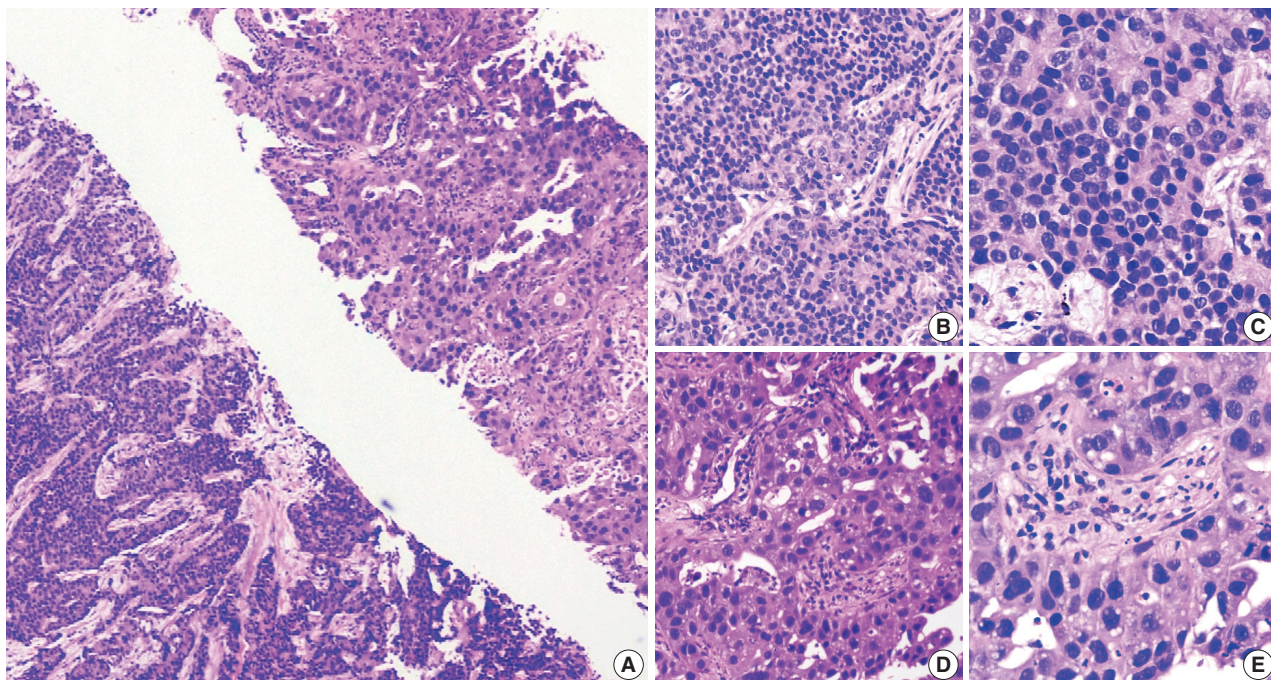


Fig. 2. Histopathological findings of the case. (A) Scanner view depicting two cores: one with compact morphology with a trabecular and abortive cribriform pattern (left) and another more loose and pink owing to abundant cytoplasm (right). (B) Low power view of better differentiated area (compact morphology) with tumor cells arranged in acinar and abortive cribriform pattern. (C) Tumor cells in a better differentiated area showing uniform tumor cells with scant eosinophilic cytoplasm and high nucleocytoplasmic ratio. (D) Low power view of lesser differentiated area (loose area) with tumor cells showing abundant bubbly cytoplasm, pleomorphic nuclei, and inflamed stroma. (E) Tumor cells of a lesser differentiated area showing abundant eosinophilic cytoplasm, vesicular pleomorphic nuclei, and neutrophilic emperipolesis with stroma rich in inflammatory cells.

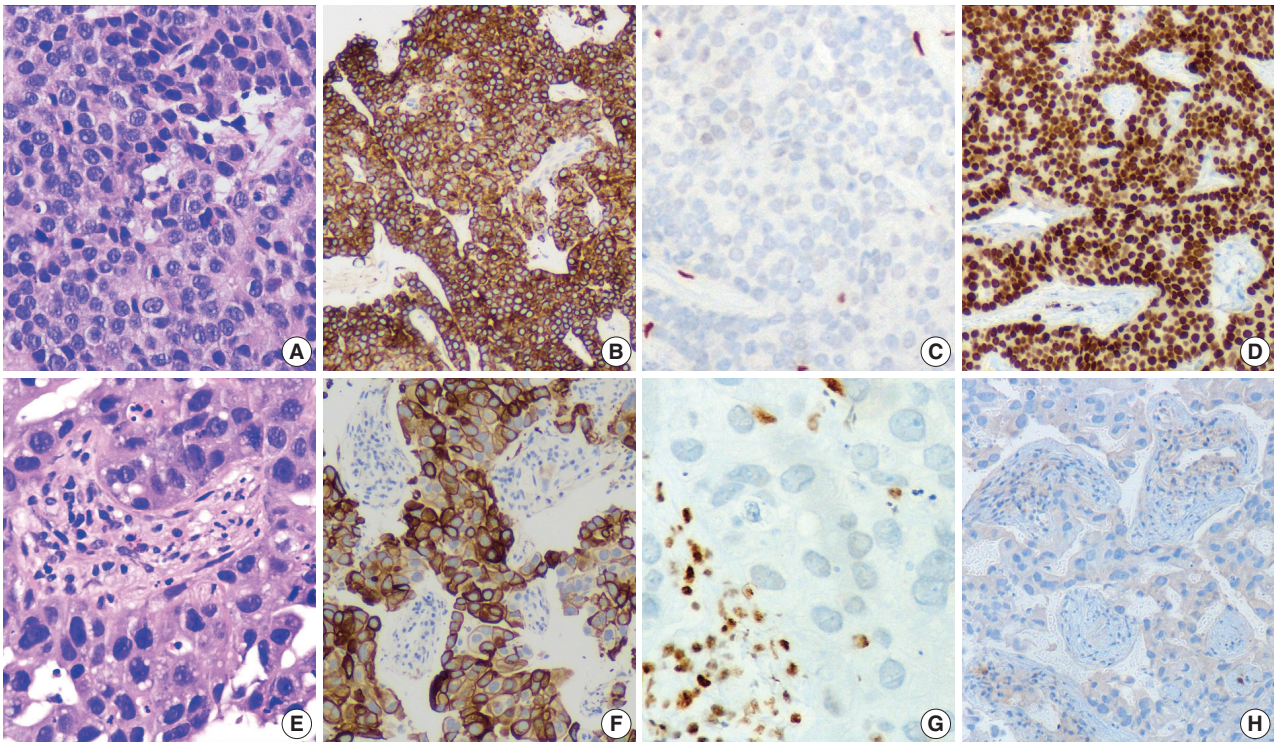


Fig. 3. Representative images of immunohistochemistry. Tumor cells in a better differentiated area (A), showing cyto­keratin (CK) expression in tumor cells (B), loss of BRG1 in tumor cells (C), thyroid transcription factor 1 (TTF1) expression by tumor cells in better differentiated area (D). Tumor cells in lesser differentiated area (E) showing weaker CK expression in tumor cells (F). Loss of BRG1 in tumor cells (G) and loss of TTF1 (H) in tumor cells showing poor differentiation.

scription factor (SOX) 2 and SOX11, and were negative for p40, Hep Par 1, spalt like transcription factor 4 (SALL4), and CD34 immunopositivity. Other areas with poor differentiation exhibited immunopositivity for SALL4 and were negative for p40, Hep Par 1, SOX2, SOX11, and CD34 expression. This contrasts with the well-defined expression of Hep Par 1 in SD-LUAD and SALL4, SOX2, and CD34 in *SMARCA4*/BRG1-deficient thoracic sarcoma (SD-TS) [4]. A final diagnosis of SD-LUAD was established on the basis of epithelial marker expression and BRG1 loss. Programmed death-ligand 1 immunopositivity showed a tumor proportion score of < 1%. No targetable driver mutation was identified for epidermal growth factor receptor (*EGFR*), reactive oxygen species 1 (*ROS1*), and anaplastic lymphoma kinase 1 (*ALK-1*).

The patient received six cycles of 5 Gy radiotherapy, but unfortunately succumbed to his illness.

DISCUSSION

The literature describes a varied morphology of SD-LUAD in the form of solid adenocarcinoma, large cell carcinoma, hepatoid, rhabdoid, spindle, and signet ring cell along with inflamed

stroma, emperipolesis, necrosis, and brisk mitosis [4-9]. There is only a handful of cases with acinar/papillary morphology [3,6]. SD-LUAD are typically negative for TTF1 as described in the literature [5,6]. Contrary observations were described by Herpel et al. [3] and Agaimy et al. [4] with intact TTF1 expression in 20% and 10% of their cases, respectively. The present case is unique with heterogeneous tumor morphology and heterogeneous TTF1 expression, but with diffuse loss of BRG1. Despite having a typical morphology of adenocarcinoma in one core, BRG1 immunopositivity was studied in view of the morphological telltale signs of SD-LUAD in other areas.

SD-LUAD can variably express Hep Par 1 and stem cell markers are more often expressed in SD-TS [4]. Our case unfolds the dynamic and evolving genetic events of lung adenocarcinoma. TTF1 was expressed only by the better differentiated component and BRG1 loss was exhibited by both areas in the present case. The loss of BRG1 in the better differentiated component is germane to our hypothesis that BRG1 loss was the primary event, which eventually had downregulated the transcription of TTF1 and was reflected as loss of TTF1 in poorly differentiated area and suggested that *SMARCA4* mutation was the driver mutation. The observation of SALL4 expression in lesser differentiated area

with aberrant SOX2 and SOX11 expression in better differentiated area is difficult to explain in the present case. However, it clearly unravels the evolutionary pathway of oncogenesis with SMARCA4 protein loss being the primary oncogenic event. There is continuous remodeling of chromatin responsible for gain and loss of many genes and protein expression, which is reflected as aberrant and heterogenous expression of SALL4, SOX2, and SOX11 in the present case. Rekhtman et al. also proposed that *SMARCA4*-deficient thoracic sarcomas are indeed undifferentiated or dedifferentiated lung carcinoma associated with smoking [10]. The IHC in the present case imitates the ongoing continuous remodeling, thereby leaving a probability of possible dedifferentiation of adenocarcinoma into sarcoma over time.

Given an almost indistinctive morphology, a need to minimize IHC, the unique biology propelling a rapid progression, and lack of actionable driver mutation, this entity needs separation from other lung adenocarcinoma, so that it can be studied more exhaustively to develop a genome-directed therapy. This task however, is rendered more difficult by the fact that some of the SD-LUAD may express TTF1, and this finding opens up the question whether all non-small cell lung carcinomas should be assessed for *SMARCA4*/BRG1 protein expression.

Ethics Statement

All procedures performed in the study were approved by the Institutional Review Board (IRB) (vide letter no: Nos. RGCIRC/IRB-BHR/61/2021 dated 3rd July 2021) in accordance with the 1964 Helsinki declaration and its latest amendments. Informed consent was obtained from each of the individuals included in the study.

Availability of Data and Material

The datasets generated or analyzed during the study are available from the corresponding author on reasonable request.

Code Availability

Not applicable.

ORCID

Anurag Mehta <https://orcid.org/0000-0001-6517-3664>
 Himanshi Diwan <https://orcid.org/0000-0002-4305-0951>
 Divya Bansal <https://orcid.org/0000-0001-9445-4086>
 Manoj Gupta <https://orcid.org/0000-0002-6401-815X>

Author Contributions

Conceptualization: AM. Data curation: HD. Formal analysis: AM, HD. Investigation: AM, HD, DB, MG. Methodology: AM. Project administration:

AM, DB. Resources: MG. Supervision: AM. Visualization: HD. Writing—original draft: HD. Writing—review & editing: AM, DB. Approval of final manuscript: all authors.

Conflicts of Interest

The authors declare that they have no potential conflicts of interest.

Funding Statement

No funding to declare.

References

1. Kadoch C, Hargreaves DC, Hodges C, et al. Proteomic and bioinformatic analysis of mammalian SWI/SNF complexes identifies extensive roles in human malignancy. *Nat Genet* 2013; 45: 592-601.
2. Errichiello E, Mustafa N, Vetro A, et al. SMARCA4 inactivating mutations cause concomitant Coffin-Siris syndrome, microphthalmia and small-cell carcinoma of the ovary hypercalcaemic type. *J Pathol* 2017; 243: 9-15.
3. Herpel E, Rieker RJ, Dienemann H, et al. SMARCA4 and SMARCA2 deficiency in non-small cell lung cancer: immunohistochemical survey of 316 consecutive specimens. *Ann Diagn Pathol* 2017; 26: 47-51.
4. Agaimy A, Fuchs F, Moskalev EA, Sirbu H, Hartmann A, Haller F. SMARCA4-deficient pulmonary adenocarcinoma: clinicopathological, immunohistochemical, and molecular characteristics of a novel aggressive neoplasm with a consistent TTF1(neg)/CK7(pos)/HepPar-1(pos) immunophenotype. *Virchows Arch* 2017; 471: 599-609.
5. Mehta A, Bansal D, Tripathi R, Jajodia A. SMARCA4/BRG1 protein-deficient thoracic tumors dictate re-examination of small biopsy reporting in non-small cell lung cancer. *J Pathol Transl Med* 2021; 55: 307-16.
6. Nambirajan A, Singh V, Bhardwaj N, Mittal S, Kumar S, Jain D. SMARCA4/BRG1-deficient non-small cell lung carcinomas: a case series and review of the literature. *Arch Pathol Lab Med* 2021; 145: 90-8.
7. Naito T, Udagawa H, Umemura S, et al. Non-small cell lung cancer with loss of expression of the SWI/SNF complex is associated with aggressive clinicopathological features, PD-L1-positive status, and high tumor mutation burden. *Lung Cancer* 2019; 138: 35-42.
8. Oike T, Ogiwara H, Tominaga Y, et al. A synthetic lethality-based strategy to treat cancers harboring a genetic deficiency in the chromatin remodeling factor BRG1. *Cancer Res* 2013; 73: 5508-18.
9. Yoshida A, Kobayashi E, Kubo T, et al. Clinicopathological and molecular characterization of SMARCA4-deficient thoracic sarcomas with comparison to potentially related entities. *Mod Pathol* 2017; 30: 797-809.
10. Rekhtman N, Montecalvo J, Chang JC, et al. SMARCA4-deficient thoracic sarcomatoid tumors represent primarily smoking-related undifferentiated carcinomas rather than primary thoracic sarcomas. *J Thorac Oncol* 2020; 15: 231-47.

Composite follicular lymphoma and classic Hodgkin lymphoma

Han-Na Kim¹, Min Ji Jeon², Eun Sang Yu², Dae Sik Kim², Chul-Won Choi², Young Hye Ko¹

¹Department of Pathology, ²Division of Hematology-Oncology, Department of Internal Medicine, Korea University Guro Hospital, Seoul, Korea

Composite lymphoma is very rare and a combination of Hodgkin lymphoma and non-Hodgkin lymphoma and even histiocytic tumors can occur. Because of the unfamiliarity, not only can this cause diagnostic problems, but can also affect treatment plan. We report a case of composite lymphoma in a 40-year-old male. Initial biopsy showed a composite lymphoma of follicular lymphoma grade 1 and classic Hodgkin lymphoma. After chemotherapy, another lymph node was taken because of disease progression, which revealed follicular lymphoma, grade 3a without Hodgkin lymphoma component.

Key Words: Composite lymphoma; Follicular lymphoma; Hodgkin lymphoma

Received: September 14, 2021 **Revised:** September 28, 2021 **Accepted:** October 9, 2021

Corresponding Author: Young Hye Ko, MD, PhD, Department of Pathology, Korea University Guro Hospital, 148 Gurodong-ro, Guro-gu, Seoul 08308, Korea
 Tel: +82-2-2626-1482, Fax: +82-2-2626-1486, E-mail: yhko310@skku.edu

Composite lymphoma was initially recognized by Custer [1] as two or more distinct lymphomas that occur in the same patient. This definition was later refined by Kim et al. [2] as simultaneous occurrence of more than one type of lymphoma in the same organ or tissue site of the same patient. Composite lymphoma is rare and may consist of non-Hodgkin lymphoma (NHL) with Hodgkin lymphoma (HL) [3,4], B-cell NHL with T-cell NHL [5-8], T-cell or B-cell NHL with other histologic type(s) of the same lineage [9], or NHL with histiocytic or dendritic cell tumors [10]. Excluding follicular lymphoma (FL) associated with diffuse large B-cell lymphoma, the most common composite lymphoma is FL of low grade associated with classic HL [3,4,11] followed by FL associated with mantle cell lymphoma [9,12]. Histologically, composite lymphomas display a mixed pattern, or less commonly, distinct zonal distribution of each lymphoma component [3,5]. Composite lymphoma may pose a diagnostic challenge, especially when two lymphoma components are mixed in the same lymph node. Herein we report a case of composite HL and FL of mixed histologic pattern.

CASE REPORT

Clinical findings

A 40-year-old man was diagnosed with HL at an outside hos-

pital and was referred for treatment. He showed a neck mass and weight loss. Laboratory tests were within normal limits except for a positive hepatitis B antigen test. A positron emission tomography (PET)-computed tomography (CT) scan revealed multiple right level I, II, and V hypermetabolic lymph nodes of the neck, both axillae, and retropancreatic regions. Abdominal CT scan revealed no organomegaly, but mild irregular hypermetabolism was noted in the spleen and along the marrow space by PET-CT. Under the diagnosis of classic HL, nodular sclerosis, stage IV, the patient was treated with doxorubicin, bleomycin, vinblastine, and dacarbazine (ABVD) chemotherapy, and an antiviral agent for hepatitis B was administered. A few months later, abdominal CT scan revealed slightly increased sizes of multiple lymph nodes at the portocaval, aortocaval, left paraaortic, and small bowel mesentery. Lymph node biopsy from a level IV node was diagnosed as FL, grade 3a. Bone marrow biopsy was negative. Six cycles of rituximab with bendamustine were planned.

Pathologic findings

All the lymph node biopsies were reviewed. The biopsy was evaluated with immunohistochemical stains including staining for CD20, CD3, CD30, CD15, PAX5, BCL2, CD10, and Ki-67 (Leica Biosystems, Newcastle upon Tyne, UK). Immunohistochemistry was performed using a Leica BOND-III automated

stainer (Leica Biosystems, Melbourne, Australia). Epstein-Barr virus was detected by in situ hybridization (ISH) using a Bond Ready-to-Use ISH Epstein-Barr virus (EBV)-encoded RNA probe (Leica Biosystems, Newcastle upon Tyne, UK).

The initial biopsy that was diagnosed as HL at outside clinic was reviewed. Enlarged follicles were found at the peripheral part of the node but the center showed diffuse area. Large neoplastic Hodgkin Reed-Sternberg cells were easily recognizable in the diffuse area but also found in the peripheral area between the neoplastic follicles. Histiocytes were mixed but eosinophils were not prominent. Reed-Sternberg cells were positive for CD30, CD15, and PAX5, but negative for CD20 and CD3. PAX5 staining was relatively weak in comparison with the neighboring non-neoplastic B cells. Neoplastic follicles were positive for CD20, CD10, and BCL2, but negative for CD30 and CD15. Therefore, we concluded that it was a composite lymphoma of FL grade 1 and clas-

sic HL (Figs. 1A–I, 2A–C). EBV was negative in both HL and FL cells. The second biopsy performed in our hospital showed only FL without HL component but this time the grade of FL was 3a because of centroblastic proliferation (Fig. 2D–F).

DISCUSSION

Composite FL and HL is extremely rare and only 25 cases have been reported in the literature written in English to date [3,4,11–16]. While composite lymphoma usually is indicated histopathologically by at least two morphologically distinct lymphomatous proliferations, the proof that these proliferations are separate and distinct neoplasms requires immunologic analysis. The true incidence of composite lymphoma may be underestimated because as in this case, separate tumor components can be easily overlooked on initial microscopic examination.

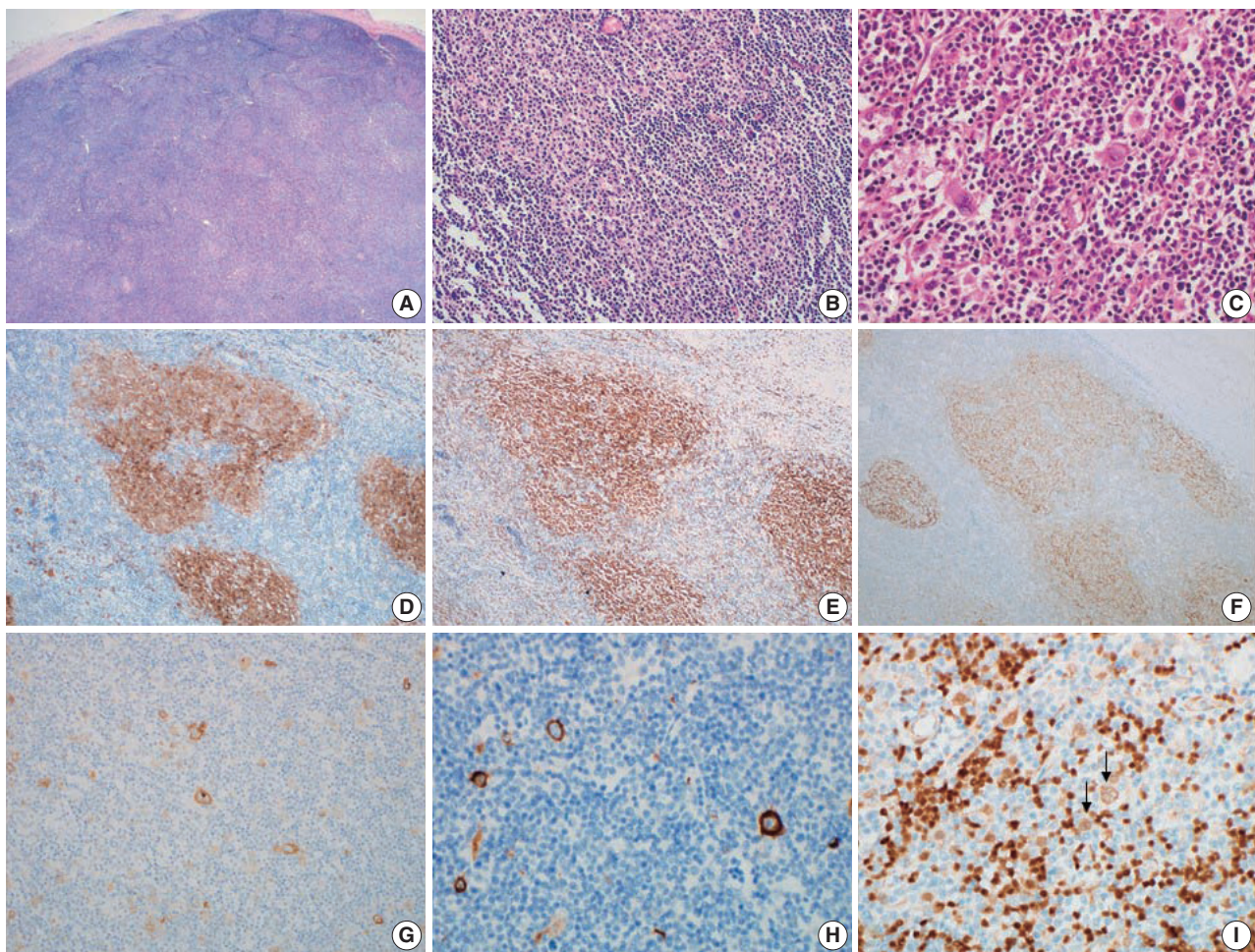


Fig. 1. Composite follicular lymphoma and Hodgkin lymphoma of initial biopsy. (A) Lymph node shows nodular area representing follicular lymphoma and diffuse area containing Hodgkin lymphoma. (B) Follicular lymphoma, grade 1. (C) Reed-Sternberg cells of Hodgkin lymphoma. (D) CD10-positive cells of follicular lymphoma. (E) BCL2-positive follicular lymphoma. (F) CD21-positive follicular dendritic cell meshwork of follicular lymphoma. (G) CD30 in Reed-Sternberg cells. (H) CD15 in Reed-Sternberg cells. (I) PAX5 weak positive in Reed-Sternberg cells (arrows).

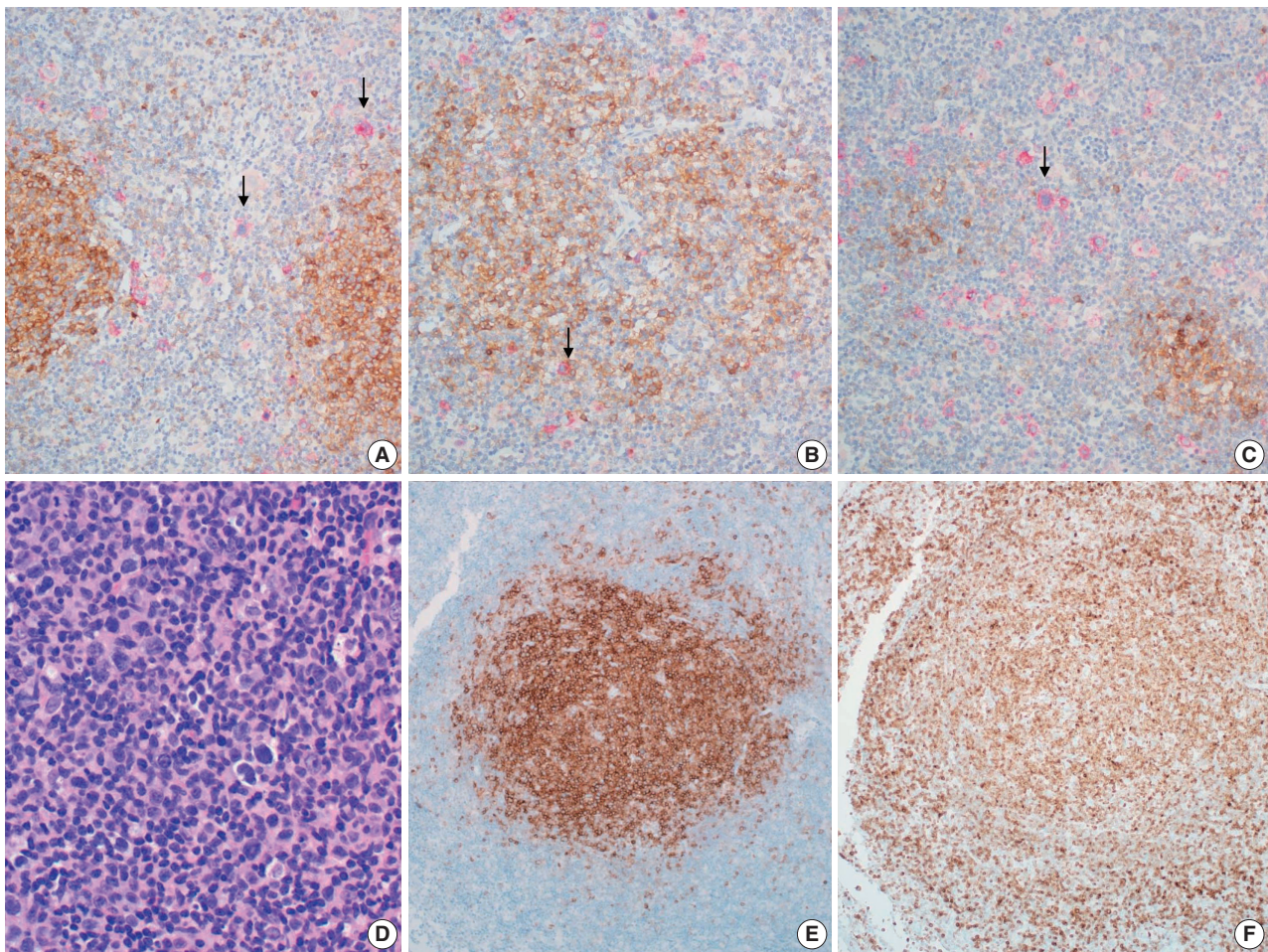


Fig. 2. (A–C) Composite follicular lymphoma and Hodgkin lymphoma of initial biopsy. Double stain for CD10 to show follicular lymphoma (brown) and CD30 to identify Hodgkin lymphoma (red). (A) CD30-positive Reed-Sternberg cells (arrows) are scattered in between follicular lymphoma. (B) A few CD30-positive Reed-Sternberg cells (arrow) within neoplastic follicles of follicular lymphoma. (C) Diffuse permeation of Hodgkin lymphoma to follicular lymphoma area. Reed-Sternberg cells (arrow) are scattered in diffuse area and small nodular remnant of neoplastic follicles. (D–F) Follicular lymphoma of recurrent lesion: (D) follicular lymphoma, grade 3a, (E) CD10, (F) BCL2.

In the initial biopsy of the present case, neoplastic follicles in the periphery of the lymph node were misinterpreted as a component of HL because the cellular atypia of the follicle was not recognized, and HL frequently has a vague follicular pattern.

While distinct clonal origin of separate tumor component of composite lymphoma has been reported in one study [12], it is well known that separate tumor components share a common clonal relationship, including a BCL2 translocation [3,11,13]. Recent next generation sequencing study revealed both components also share the same mutational variants but have pathogenic variants that are specific for each component as well [3]. These findings indicate that two distinct lymphomas sharing a common cytogenetic abnormality derived from the same precursor, overlaid with a subtype-specific mutation occurring in each subclone, can lead to composite HL and FL. In addition, EBV

infection observed in HL cells, but not FL cells of the composite lymphoma [3] emphasizes the role of EBV infection in the pathogenesis of HL [17] and suggests that EBV infection also contributes to the formation of composite lymphoma. Composite lymphoma may pose both a diagnostic and managerial challenge [3]. A previous report demonstrated that the HL component in composite lymphoma pursues an indolent clinical course compared with de novo HL. No recurrence of the HL component was reported even without ABVD treatment for HL. In contrast, patients treated with ABVD only or who were untreated, experienced recurrence of FL like the present case [3]. Although the number of cases is too small to provide definitive information for treatment or to establish concrete guidelines for management [18], the above report may give a hint on how best to treat composite FL and HL.

Ethics Statement

All procedures performed in the current study were approved by the Institutional Review Board (2021GR0492) in accordance with the 1964 Helsinki declaration and its later amendments. Informed consent was waived.

Availability of Data and Material

The datasets generated or analyzed during the study are available from the corresponding author on reasonable request.

Code Availability

Not applicable.

ORCID

Young Hyeon Ko <https://orcid.org/0000-0002-4383-0579>
 Han-Na Kim <https://orcid.org/0000-0001-5171-3658>
 Min Ji Jeon <https://orcid.org/0000-0003-4044-5314>
 Eun Sang Yu <https://orcid.org/0000-0003-2196-0732>
 Dae Sik Kim <https://orcid.org/0000-0001-8424-8561>
 Chul-Won Choi <https://orcid.org/0000-0002-3032-4239>

Author Contributions

Conceptualization: MJJ, YHK. Review of data: HNK, ESY, DSK, CWC. Writing—original draft: HNK, YHK. Writing—review & editing: MJJ, CWC, YHK.

Conflicts of Interest

The authors declare that they have no potential conflicts of interest.

Funding Statement

No funding to declare.

References

- Custer R. Pitfalls in the diagnosis of lymphoma and leukemia from the pathologist's point of view. In: Proceedings of Second National Cancer Conference; 1952 Mar 3-5; Comcoinnati, OH, USA. New York: New York American Cancer Society, 1954; 554-7.
- Kim H, Hendrickson R, Dorfman RF. Composite lymphoma. *Cancer* 1977; 40: 959-76.
- Trecourt A, Mauduit C, Szablewski V, et al. Plasticity of mature B cells between follicular and classic Hodgkin lymphomas: a series of 22 cases expanding the spectrum of transdifferentiation. *Am J Surg Pathol* 2021 Jul 15 [Epub]. <https://doi.org/10.1097/PAS.0000000000001780>.
- Vasudevan JA, Nair RA, Sukumaran R, Nair SG. Composite lymphomas: Experience from a tertiary cancer center in Kerala, South India. *Indian J Cancer* 2017; 54: 358-61.
- Tanaka J, Su P, Luedke C, et al. Composite lymphoma of follicular B-cell and peripheral T-cell types with distinct zone distribution in a 75-year-old male patient: a case study. *Hum Pathol* 2018; 76: 110-6.
- Suefuji N, Niino D, Arakawa F, et al. Clinicopathological analysis of a composite lymphoma containing both T- and B-cell lymphomas. *Pathol Int* 2012; 62: 690-8.
- Sun T, Susin M, Koduru P, et al. Phenotyping and genotyping of composite lymphoma with Ki-1 component. *Hematol Pathol* 1992; 6: 179-92.
- York JC 2nd, Cousar JB, Glick AD, Flexner JM, Stein R, Collins RD. Morphologic and immunologic evidence of composite B- and T-cell lymphomas: a report of three cases developing in follicular center cell lymphomas. *Am J Clin Pathol* 1985; 84: 35-43.
- Miyazawa Y, Yokohama A, Ishizaki T, et al. Pathological and molecular analysis of a composite lymphoma of mantle cell lymphoma and Epstein-Barr virus-positive follicular lymphoma. *Int J Hematol* 2021; 113: 592-9.
- Almanaseer IY, Kosova L, Pelletiere EV. Composite lymphoma with immunoblastic features and Langerhans' cell granulomatosis (histiocytosis X). *Am J Clin Pathol* 1986; 85: 111-4.
- Schmitz R, Renne C, Rosenquist R, et al. Insights into the multistep transformation process of lymphomas: IgH-associated translocations and tumor suppressor gene mutations in clonally related composite Hodgkin's and non-Hodgkin's lymphomas. *Leukemia* 2005; 19: 1452-8.
- Fend F, Quintanilla-Martinez L, Kumar S, et al. Composite low grade B-cell lymphomas with two immunophenotypically distinct cell populations are true biclonal lymphomas: a molecular analysis using laser capture microdissection. *Am J Pathol* 1999; 154: 1857-66.
- Kuppers R, Sousa AB, Baur AS, Strickler JG, Rajewsky K, Hansmann ML. Common germinal-center B-cell origin of the malignant cells in two composite lymphomas, involving classical Hodgkin's disease and either follicular lymphoma or B-CLL. *Mol Med* 2001; 7: 285-92.
- Thirumala S, Esposito M, Fuchs A. An unusual variant of composite lymphoma: a short case report and review of the literature. *Arch Pathol Lab Med* 2000; 124: 1376-8.
- Brauninger A, Hansmann ML, Strickler JG, et al. Identification of common germinal-center B-cell precursors in two patients with both Hodgkin's disease and non-Hodgkin's lymphoma. *N Engl J Med* 1999; 340: 1239-47.
- Gonzalez CL, Medeiros LJ, Jaffe ES. Composite lymphoma. A clinicopathologic analysis of nine patients with Hodgkin's disease and B-cell non-Hodgkin's lymphoma. *Am J Clin Pathol* 1991; 96: 81-9.
- Mancao C, Altmann M, Jungnickel B, Hammerschmidt W. Rescue of "crippled" germinal 18.center B cells from apoptosis by Epstein-Barr virus. *Blood* 2005; 106: 4339-44.
- Linck D, Lentini G, Tiemann M, Fauser AA, Parwaresch R, Basara N. Sequential application of chemotherapy and monoclonal CD 20 antibody: successful treatment of advanced composite-lymphoma. *Leuk Lymphoma* 2005; 46: 285-8.

